CHAPTER 3

NATURAL CONDITION

Chapter 3 Natural Condition

3.1 Topographic Condition

The port city of Beira is located in Sofala Province, central Mozambique.

The administrative area of the city is bounded in the east by the Indian Ocean. In the north, the boundary runs in the east-west direction along the Madzidze River from the coast to its source, turning in the northeast - southwest direction until it reaches the left shore of the Pungue River, along which the boundary runs from there to the Mozambique Channel.

Beira Port is located on the left bank of the Pungue River near the Macuti Beach at the southern part of the city, facing the Mozambique Channel.

The urban area of Beira is flat with its average altitude of 8 m.

3.2 Meteorological Condition

The meteorological elements are shown below.

Table 3.2- 1 Meteorological Records, 1987-1996

	Jan	Feb	Mar	Apr	May	Jun	Jul	Aug	Sep	Oct	Nov	Dec	Mean
TX	28.6	28.8	28.1	26.8	25.0	22.8	21.8	22.3	24.4	26.3	27.3	28.8	25.9
TN	27.2	27.2	27.0	24.6	23.1	20.8	20.1	21.0	22.4	24.0	25.0	25.8	24.0
TM	27.8	27.9	27.2	25.7	23.9	21.7	20.9	21.8	23.5	25.0	26.5	27.3	24.9
UU	71.8	73.1	72.8	72.8	74.4	73.2	74.4	73.9	70.8	69.2	69.1	70.1	72.1
RR	254.6	233.4	229.5	*113.5	80.2	47.7	40.4	39.1	11.6	40.0	81.3	166.7	** 1337.9

Source : Instituto Nacional de Meteorologia, Beira Meteorological Station
Note: TX ; Maximum Temperature (℃)
TN ; Minimum Temperature (℃)
TM ; Mean Temperature (℃)
UU ; Relative Humidity (%)
RR ; Rainfall (mm), *N/A in 1993, **Annual Total

General meteorological characteristics in the vicinity of Beira are described below. Mozambique extends between latitudes 10° S and 27° S. The whole territory is considered climatically to be of tropical zone type which is characterized by the wet season (November to April) and the dry season (May to October). Due to the nature of the meteorological phenomena which affect the weather conditions, Mozambique can be divided into 2 distinct zones, the first being to the north from latitude 20° S and the other being to the south from the

same latitude. Beira is situated at latitude 19° 49' S and longitude 34° 50' E, therefore some climate phenomena of Beira is considered to have the characteristics of the first zone.

For instance, the annual rainfall in Beira ranges from 1,200 mm to 2,000 mm, which is considerably high compared to the southern region. The mean temperature in the wet season is approximately 27℃, which is slightly higher than the southern region. Meteorological data, from 1987 to 1996, such as temperature, relative humidity, rainfall and wind were obtained from the meteorological station at Beira Airport.

Severe floods occurred in the wet season from the end of 1996 to March 1997 in the upstream area of the Pungue and Buzi River. Therefore the assessment of rainfalls, winds and river flows will be necessary to carry out an accurate analysis of the structure of sedimentation in the Access Channel.

Meteorological conditions in Beira are characterized in the following.

3.2.1 Temperature

Temperature varies between 20 ℃ and 29 ℃. The mean annual temperature is 24.5 ℃. The maximum and minimum monthly mean temperatures are 25.9℃ and 24.0℃, respectively, which indicates that there is little variation in temperature throughout the year.

3.2.2 Relative Humidity

The mean annual relative humidity is 72.1 % with small difference between the wet season and the dry season.

3.2.3 Rainfall

As shown in Table 3.2.3-1, the variation in rainfall by year is remarkable like the variation within a year. In the last decade, the maximum and minimum annual rainfalls were 1,952.6 mm in 1988 and 932.5 mm in 1992.

The mean annual rainfall is approximately 1,400 mm and the monthly variation is also high. For example, it varies from 11.6 mm (in September) to 254.6 mm (in January). According to the monthly rainfall records in the last decade, the monthly rainfall of less than 50 mm occurred in some months during the dry season every year and the monthly rainfall more than 400 mm occurred in 1988, 1990, 1991 and 1996.

Table 3.2.3-1 Monthly Rainfall, 1986-1997

	1986	1987	1988	1989	1990	1991	1992	1993	1994	1995	1996	Average	1997
January	347.4	250.1	305.0	155.4	649.0	93.8	127.2	60.2	318.8	118.2	468.0	263.0	208.1
February	148.7	72.8	209.3	329.2	190.6	355.2	152.8	249.0	199.5	127.5	448.0	225.7	292.0
March	366.6	127.2	509.8	132.2	232.1	415.6	126.5	213.6	150.9	179.4	207.6	242.0	208.1
April	220.4	70.6	121.2	166.8	314.9	22.9	159.8	N/A	67.2	85.0	126.1	135.5	202.5
May	37.3	115.0	247.7	88.5	110.9	15.6	38.6	31.4	41.3	83.7	28.9	76.3	7.6
Jun	19.0	90.8	66.5	11.0	58.3	26.5	41.4	61.7	22.4	17.0	81.3	45.1	6.8
July	25.3	4.4	20.8	24.6	11.5	31.9	3.4	150.6	21.8	47.4	87.8	39.0	39.9
August	1.5	33.9	46.5	1.8	53.6	7.6	29.3	49.3	36.8	59.1	72.8	35.7	1.7
September	14.4	15.6	0.5	9.3	27.6	25.4	0.6	0.4	32.5	1.5	2.5		
October	70.1	23.4	115.7	148.2	12.9	1.3	19.5	5.9	18.3	27.0	28.0		
November	48.6	12.6	91.4	36.3	166.0	86.5	75.3	259.2	4.5	58.1	23.5		
December	289.8	465.6	218.2	145.2	34.9	90.4	158.1	113.3	138.8	260.3	42.2		
Total	1589.1	1282.0	1952.6	1248.5	1862.3	1172.7	932.5	1194.6	1052.8	1064.2	1616.7		

Source : Beira Meteorological Station
Unit : mm

Table 3.2.3-2 Maximum Rainfall During 24 Hours, 1986-1997

	1986	1987	1988	1989	1990	1991	1992	1993	1994	1995	Average	1997
January	95.1	109.1	116.6	61.5	230.0	23.3	54.8	17.4	163.6	33.8	90.5	32.5
February	43.5	40.0	93.6	64.4	61.1	104.1	99.5	152.1	66.1	34.5	75.9	116.6
March	347.3	48.0	135.2	44.0	71.4	161.1	34.5	N/A	39.0	19.5	100.0	32.5
April	74.2	21.1	28.1	107.6	90.9	12.1	78.9	6.1	49.9	39.1	50.8	41.2
May	16.9	36.4	58.5	35.3	30.3	10.0	21.1	10.6	11.3	11.1	24.2	4.8
Jun	5.4	20.7	53.2	5.4	20.2	9.6	13.7	33.3	11.1	15.6	18.8	6.0
July	11.8	2.3	9.2	22.5	7.4	16.6	1.7	33.8	13.5	25.1	14.4	13.0
August	0.9	27.4	40.5	1.3	21.6	4.2	11.8	13.6	21.8	34.2	17.7	0.3
September	4.9	13.3	0.3	4.4	21.1	13.3	0.3	0.1	31.8	1.1		
October	55.5	13.9	49.6	49.0	4.2	0.7	N/A	2.7	5.1	21.3		
November	32.9	6.4	67.3	24.0	65.6	45.7	30.5	59.9	2.7	42.3		
December	134.0	180.7	67.6	36.3	19.7	31.6	N/A	51.2	69.6	102.5		

Source : Beira Meteorological Station
Unit : mm

Maximum rainfall in Beira during 24 hours from January to August in 1997 and the maximum rainfall in Beira in the last decade are described in Table 3.2.3-2.

Comparing the rainfall in Beira between the first three months of 1997 and the last decade, the rainfall in February 1997 was heavier. For example, the rainfall in February 1997 was 292.0 mm and the average of February in the last decade is 225.7 mm. Also the maximum rainfall during 24 hours in Beira in February 1997 was 116.6 mm and the average in the last decade was 75.9 mm.

3.2.4 Winds

The wind data from 1966 to 1995 which were recorded at the meteorological station at Beira Airport are shown in Table 3.2.4-1, Figure 3.2.4-1 and 3.2.4-2. Monthly wind frequencies in 1997 in comparison with the average wind occurence is shown in Table 3.2.4-2.

According to the statistics of the last 25 years, the frequency of occurrence of moderate wind less than 5 m/s ranges between 70 % and 79 % from April to July, between 60 % and 69 % in March and August, between 50 % and 59 % from September to February with 44 % in October. The frequency of wind more than 10 m/s is very low, being less than 1 % from February to August and 1 % to 2 % from September to January with 2.4 % in October. The most predominant direction of wind is from ENE to SE.

Monthly wind frequency of the last decade and that in wet season in 1997 at Beira is shown in Table 3.2.4-2. According to this table, wind more than 10 m/sec was recorded 14 times which seems to be caused by the cyclone "Lisette" across Mozambique Channel in March 1997.

3.2.5 Cyclones

According to the statistics from the Institute Nacional de Meteorologia in the last thirty years, there have been 23 cyclones which strongly affected Mozambique as shown in Table 3.2.5-1.

Cyclones are generated in the South-Western Indian Ocean from November to April. An average of 15 to 20 cyclones are generated annually during this season. Cyclones affect Mozambique, especially, in February and March.

Table 3.2.4-1 Monthly Frequencies of Occurrence of Winds by Direction and Intensity,25years

Month	Intensity / Direction	S	SSW	SW	WSW	W	WNW	NW	NNW	N	NNE	NE	ENE	E	ESE	SE	SSE	CALM	SUM
January	1-4.9 (m/s)	3.4	1.8	1.9	2.2	3.4	2.0	1.4	2.1	4.3	4.0	4.0	6.0	5.8	6.4	4.2	3.3		56.2
	5-9.9	3.3	1.5	1.1	0.7	0.9	0.2	0.1	0.2	0.5	0.5	1.5	4.0	5.4	6.0	5.1	3.7		34.7
	10-	0.2	0.1	0.1	0.1	0.2	0.0	0.0	0.0	0.0	0.0	0.0	0.0	0.0	0.1	0.1	0.1		1.0
	SUM	6.9	3.4	3.1	3.0	4.5	2.2	1.5	2.3	4.8	4.5	5.5	10.0	11.2	12.5	9.4	7.1	8.1	100.0
February	1-4.9	6.1	4.4	3.2	2.8	3.4	1.7	1.0	1.4	2.8	2.2	2.8	5.2	5.8	6.7	4.6	5.1		59.2
	5-9.9	4.4	2.3	1.0	1.5	0.6	0.1	0.1	0.1	0.2	0.5	1.0	2.7	3.5	5.7	4.8	4.0		32.5
	10-	0.0	0.0	0.1	0.0	0.0	0.0	0.0	0.0	0.0	0.0	0.0	0.0	0.1	0.2	0.2	0.0		0.6
	SUM	10.6	6.7	4.3	4.3	4.0	1.8	1.1	1.5	3.0	2.7	3.8	7.9	9.4	12.6	9.6	9.1	7.7	100.0
March	1-4.9	6.1	3.0	2.8	3.6	4.2	2.1	1.2	1.6	3.9	2.7	2.7	5.8	6.1	8.4	6.0	5.5		65.6
	5-9.9	5.0	2.2	1.2	0.4	0.2	0.1	0.1	0.1	0.2	0.4	0.8	1.9	2.6	4.5	4.6	4.3		28.6
	10-	0.1	0.0	0.0	0.0	0.0	0.0	0.0	0.0	0.0	0.0	0.0	0.0	0.0	0.2	0.2	0.2		0.7
	SUM	11.2	5.2	4.0	4.0	4.4	2.2	1.3	1.6	4.1	3.1	3.5	7.7	8.7	13.1	10.8	10.0	5.1	100.0
April	1-4.9	8.9	4.6	3.9	4.5	4.2	2.9	2.1	1.8	4.0	2.4	2.8	5.6	5.8	8.0	7.7	6.5		78.7
	5-9.9	3.2	2.2	1.0	0.5	0.1	0.0	0.0	0.1	0.1	0.1	0.1	0.4	1.0	1.8	2.1	3.3		16.0
	10-	0.0	0.0	0.0	0.0	0.0	0.0	0.0	0.0	0.0	0.0	0.0	0.0	0.0	0.0	0.0	0.0		0.0
	SUM	12.1	6.8	4.9	5.0	4.3	2.9	2.1	1.9	4.1	2.5	2.9	6.0	6.8	9.8	9.8	9.8	8.3	100.0
May	1-4.9	8.6	5.0	3.7	4.6	5.2	3.8	2.1	2.4	4.3	3.8	3.6	6.0	6.2	7.1	5.4	5.9		77.7
	5-9.9	2.6	2.3	1.3	0.8	0.2	0.1	0.0	0.1	0.2	0.1	0.2	0.3	0.7	1.2	1.0	1.4		12.5
	10-	0.1	0.0	0.0	0.0	0.0	0.0	0.0	0.0	0.0	0.0	0.0	0.0	0.0	0.0	0.0	0.0		0.1
	SUM	11.3	7.3	5.0	5.4	5.4	3.9	2.1	2.5	4.5	3.9	3.8	6.3	6.9	8.3	6.4	7.3	9.7	100.0
June	1-4.9	7.7	4.4	4.6	5.8	7.2	4.1	2.4	2.0	3.8	2.9	2.6	4.5	4.0	6.0	5.5	6.0		73.5
	5-9.9	4.8	2.9	1.6	1.1	0.4	0.1	0.1	0.1	0.2	0.1	0.2	0.2	0.5	0.9	1.3	0.2		14.7
	10-	0.1	0.1	0.0	0.0	0.0	0.0	0.0	0.0	0.0	0.0	0.0	0.0	0.0	0.0	0.0	0.0		0.2
	SUM	12.6	7.4	6.2	6.9	7.6	4.2	2.5	2.1	4.0	3.0	2.8	4.7	4.5	6.9	6.8	6.2	11.6	100.0
July	1-4.9	7.4	5.0	4.4	5.7	6.7	4.1	2.0	1.9	3.3	2.8	2.8	5.4	5.1	5.4	5.2	4.9		72.1
	5-9.9	4.8	2.0	1.4	0.9	0.1	0.0	0.0	0.1	0.1	0.1	0.4	0.8	1.2	2.0	2.3	2.8		19.0
	10-	0.0	0.0	0.0	0.0	0.0	0.0	0.0	0.0	0.0	0.0	0.0	0.0	0.0	0.0	0.0	0.0		0.0
	SUM	12.2	7.0	5.8	6.6	6.8	4.1	2.0	2.0	3.4	2.9	3.2	6.2	6.3	7.4	7.5	7.7	8.9	100.0
August	1-4.9	4.5	2.4	2.2	2.9	4.3	2.8	2.1	2.0	4.8	3.9	4.2	6.8	5.6	6.7	5.3	5.1		65.6
	5-9.9	3.7	2.1	0.6	0.7	0.1	0.1	0.1	0.1	0.4	0.6	0.9	2.3	3.2	5.1	4.7	4.2		28.9
	10-	0.1	0.1	0.1	0.0	0.0	0.0	0.0	0.0	0.0	0.0	0.0	0.0	0.0	0.0	0.0	0.2		0.5
	SUM	8.3	4.6	2.9	3.6	4.4	2.9	2.2	2.1	5.2	4.5	5.1	9.1	8.8	11.8	10.0	9.5	5.0	100.0
September	1-4.9	3.1	1.6	1.2	1.5	2.1	2.3	1.4	3.5	3.7	3.6	5.3	7.1	6.5	7.3	5.2	3.2		58.6
	5-9.9	2.3	0.9	0.3	0.2	0.0	0.0	0.1	0.2	0.7	1.0	2.6	5.1	5.6	6.4	4.2	4.3		33.9
	10-	0.3	0.0	0.0	0.0	0.0	0.0	0.0	0.0	0.0	0.0	0.1	0.1	0.1	0.1	0.1	0.2		1.0
	SUM	5.7	2.5	1.5	1.7	2.1	2.3	1.5	3.7	4.4	4.6	8.0	12.3	12.2	13.8	9.5	7.7	6.5	100.0
October	1-4.9	2.5	0.9	0.9	1.3	2.6	2.1	1.3	1.3	3.5	2.6	3.2	5.0	4.6	5.1	4.2	3.0		44.1
	5-9.9	3.5	0.8	0.7	0.4	0.1	0.1	0.0	0.1	0.4	1.0	1.9	6.4	8.6	10.7	8.4	5.2		48.3
	10-	0.7	0.1	0.0	0.0	0.0	0.0	0.0	0.0	0.0	0.0	0.1	0.1	0.4	0.3	0.3	0.4		2.4
	SUM	6.7	1.8	1.6	1.7	2.7	2.2	1.3	1.4	3.9	3.6	5.2	11.5	13.6	16.1	12.9	8.6	5.2	100.0
November	1-4.9	2.1	0.7	0.9	1.0	1.8	1.6	1.1	1.8	3.7	3.2	4.0	7.8	8.0	7.8	4.5	3.2		53.2
	5-9.9	3.1	0.6	0.3	0.1	0.0	0.0	0.0	0.1	0.5	0.9	1.6	4.3	7.2	8.2	7.0	4.4		38.3
	10-	0.3	0.1	0.0	0.0	0.0	0.0	0.0	0.0	0.0	0.0	0.1	0.1	0.2	0.2	0.1	0.2		1.3
	SUM	5.5	1.4	1.2	1.1	1.8	1.6	1.1	1.9	4.2	4.1	5.7	12.2	15.4	16.2	11.6	7.8	7.2	100.0
December	1-4.9	2.4	0.9	1.0	1.2	2.1	2.1	1.4	2.0	4.7	3.8	4.5	7.1	6.5	6.3	4.0	3.7		53.7
	5-9.9	2.6	1.0	0.6	0.3	0.3	0.2	0.2	0.1	0.5	0.8	1.9	4.9	6.0	7.4	5.9	3.3		36.0
	10-	0.3	0.1	0.0	0.0	0.2	0.1	0.0	0.0	0.0	0.0	0.0	0.1	0.5	0.2	0.1	0.1		1.7
	SUM	5.3	2.0	1.6	1.5	2.6	2.4	1.6	2.1	5.2	4.6	6.4	12.1	13.0	13.9	10.0	7.1	8.6	100.0

Source : Beira Meteorological Station
Unit : %

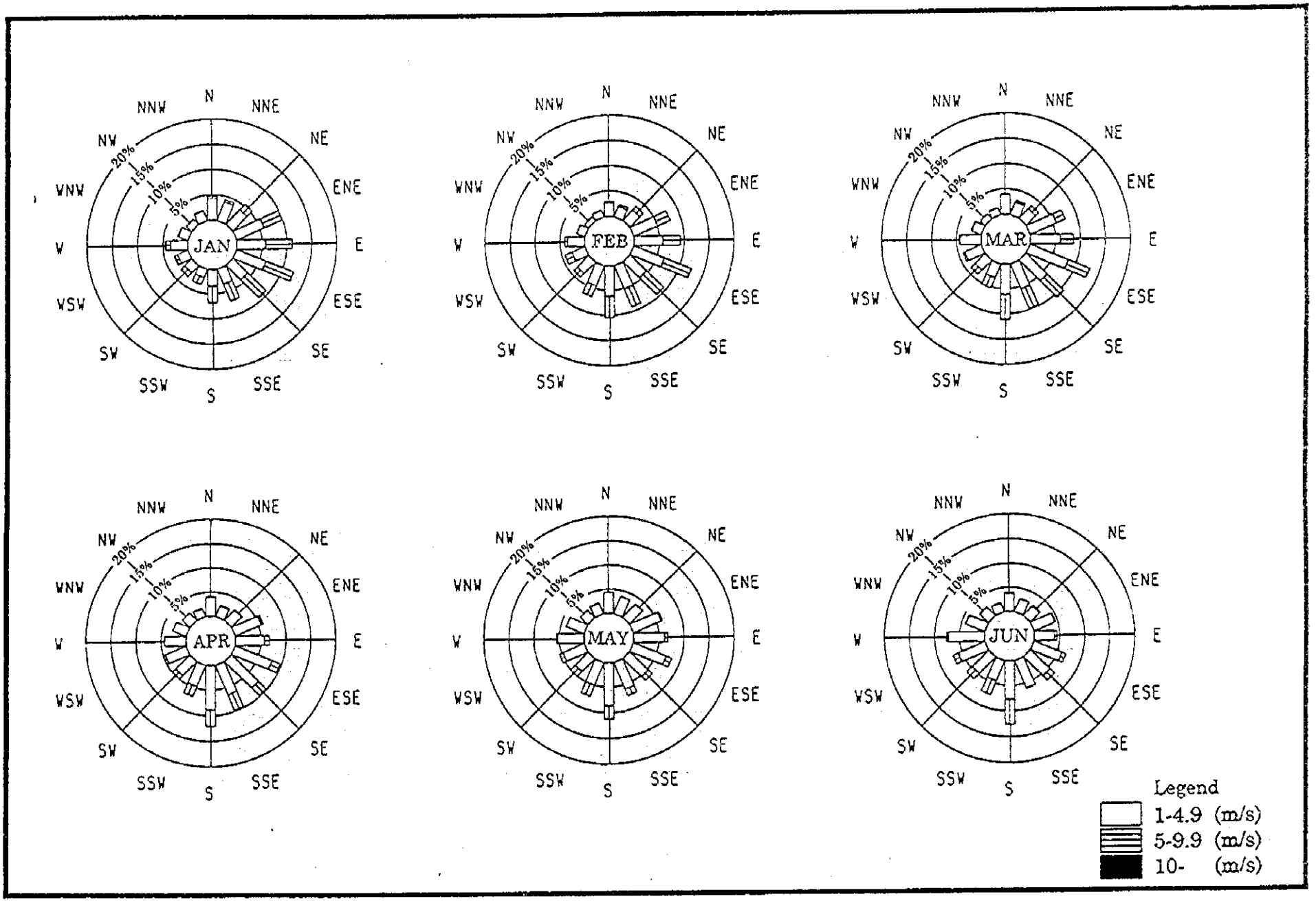

Figure 3.2.4-1 Wind Rose, 25 Years, from January to June

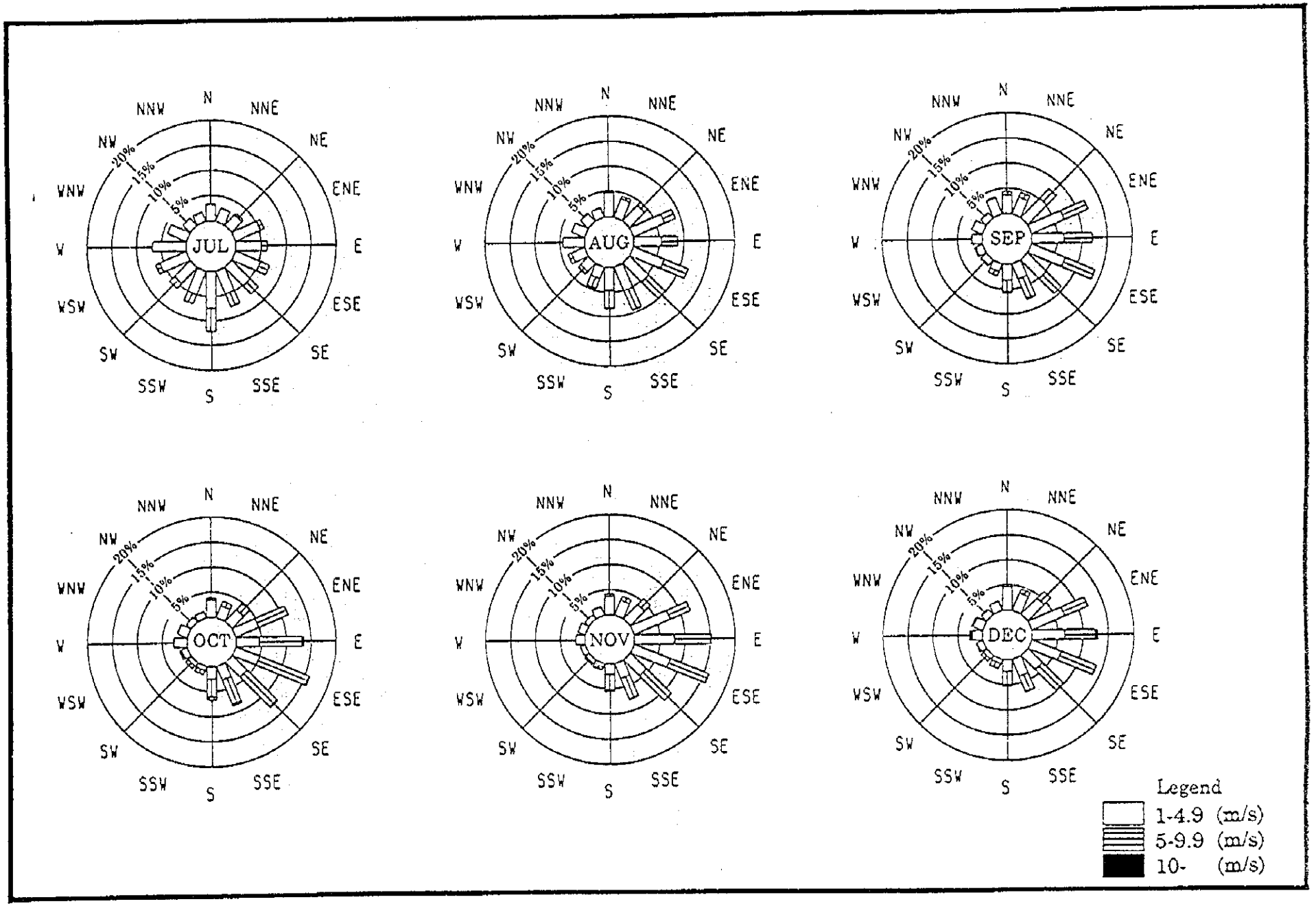

Figure 3.2.4-2 Wind Rose, 25 Years, from July to December

Table 3.2.4-2 Comparison of Monthly Frequencies of Occurrence of Winds by Direction and Intensity

	January						February					
Speed (m/s)	1-4.9		5-9.9		10-		1-4.9		5-9.9		10-	
Direction	Ave.	1997	Ave.	1997	Ave.	1997	Ave.	1997	Ave.	1997	Ave.	1997
N	29.8	56	3.2	4	0.1	0	16.9	8	1.4	0	0.0	0
NNE	27.4	36	3.5	0	0.1	0	13.6	11	2.9	0	0.3	0
NE	27.1	48	10.0	1	0.0	0	17.2	7	5.7	2	0.2	0
ENE	41.2	36	27.4	6	0.3	0	31.3	13	16.4	9	0.1	0
E	40.1	19	36.9	12	0.3	0	35.2	39	21.3	7	0.8	0
ESE	43.7	54	41.2	42	0.5	0	40.2	61	34.7	45	1.0	0
SE	28.6	53	34.7	32	0.6	0	27.9	70	28.9	80	1.3	0
SSE	22.6	23	25.4	16	0.4	0	30.7	53	23.9	43	0.3	0
S	23.6	26	22.4	8	1.7	0	37.0	51	26.3	39	0.2	0
SSW	12.6	17	10.3	4	0.4	0	26.3	25	13.9	4	0.3	0
SW	12.9	26	7.6	2	0.7	0	19.4	13	6.0	1	0.8	0
WSW	14.9	41	4.5	4	1.0	0	16.9	10	9.1	0	0.0	0
W	25.1	65	6.2	4	1.3	0	20.6	33	3.9	1	0.0	0
WNW	13.6	32	1.1	1	0.0	0	10.2	14	0.4	0	0.0	0
NW	9.8	8	0.9	0	0.0	0	6.1	5	0.7	0	0.0	0
NNW	14.5	21	1.1	6	0.0	0	8.3	7	0.7	1	0.0	0
CALM	54.4	31					44.6	19				
	March						April					
Speed (m/s)	1-4.9		5-9.9		10-		1-4.9		5-9.9		10-	
Direction	Ave.	1997	Ave.	1997	Ave.	1997	Ave.	1997	Ave.	1997	Ave.	1997
N	25.2	50	1.3	3	0.0	0	21.7	8	0.4	0	0.0	0
NNE	17.2	43	2.6	1	0.0	0	13.1	2	0.4	0	0.0	0
NE	17.4	30	4.8	0	0.0	0	15.0	7	0.8	0	0.0	0
ENE	37.2	58	11.8	10	0.3	3	30.2	7	2.3	0	0.0	0
E	38.9	48	16.5	26	0.5	0	31.1	5	5.5	1	0.0	0
ESE	53.8	89	28.9	24	1.2	5	43.0	20	10.0	10	0.0	0
SE	38.5	61	29.3	42	1.4	0	41.6	18	11.1	18	0.1	0
SSE	34.9	28	27.7	22	1.3	4	34.9	29	17.8	8	0.3	0
S	38.9	26	32.0	16	0.7	2	48.4	20	17.2	10	0.3	0
SSW	18.9	20	14.4	13	0.0	0	24.7	15	11.8	1	0.1	0
SW	17.6	14	7.8	6	0.0	0	21.1	15	5.2	0	0.0	0
WSW	23.3	16	2.9	6	0.0	0	24.2	9	2.6	0	0.0	0
W	27.0	16	1.4	0	0.0	0	22.8	8	0.4	0	0.0	0
WNW	13.6	8	0.8	0	0.0	0	15.4	3	0.1	0	0.0	0
NW	7.9	7	0.4	0	0.0	0	11.3	2	0.1	0	0.0	0
NNW	9.5	16	0.7	0	0.0	0	9.5	6	0.3	0	0.0	0
CALM	30.5	30					46.1	18				

Ave. : Average of Monthly Frequencies of Occurrence of Winds by Direction and Intensity,25years
Sourse : Beira Meteorological Station

Table 3.2.5-1 List of Major Cyclones

Year	Cyclone Name			Year	Cyclone Name		
1956/4-1957/3				1977/4-1978/3			
1957/4-1958/3				1978/4-1979/3	Angele		
1958/4-1959/3				1979/4-1980/3			
1959/4-1960/3				1980/4-1981/3	Edwige		
1960/4-1961/3				1981/4-1982/3			
1961/4-1962/3	Daisy	Kate	Gina	1982/4-1983/3	Benedite	Elinah	
1962/4-1963/3				1983/4-1984/3			
1963/4-1964/3	Christine			1984/4-1985/3			
1964/4-1965/3				1985/4-1986/3	Berobia		
1965/4-1966/3	Germaine			1986/4-1987/3			
1966/4-1967/3	Daphne	Irma		1987/4-1988/3	Hely	Filao	
1967/4-1968/3	Flossie			1988/4-1989/3			
1968/4-1969/3				1989/4-1990/3			
1969/4-1970/3				1990/4-1991/3			
1970/4-1971/3	Delphine			1991/4-1992/3			
1971/4-1972/3				1992/4-1993/3			
1972/4-1973/3	Dorothee			1993/4-1994/3	Nadia		
1973/4-1974/3				1994/4-1995/3			
1974/4-1975/3	Honorine	Elsa		1995/4-1996/3	Bonita		
1975/4-1976/3				1996/4-1997/3	Lisette		
1976/4-1977/3	Emilie						

3.2.6 River Flow

Comparison of river flow of the last 26 years and wet season in 1997 in the Pungue River is shown in Figure 3.2.6-1. The quantities of river flow from January to March in 1997 were observed larger comparing last 26 years.

3.2.7 Climatic Condition during Field Survey

During our natural condition surveys, rain and wind conditions were affected by cyclone. And river flow increased by the flood in the upstream of the Pungue and Buzi Rivers. The results of bathymetric survey, current observation, turbidity observation and wave observation were affected by such abnormal meteorological conditions.

3.3 Sea Condition

3.3.1 General

In addition to collection and analysis of the existing data and the information related to the sea conditions, the following surveys have been carried out in Beira Port, the Access Channel, dumping areas and offshore.

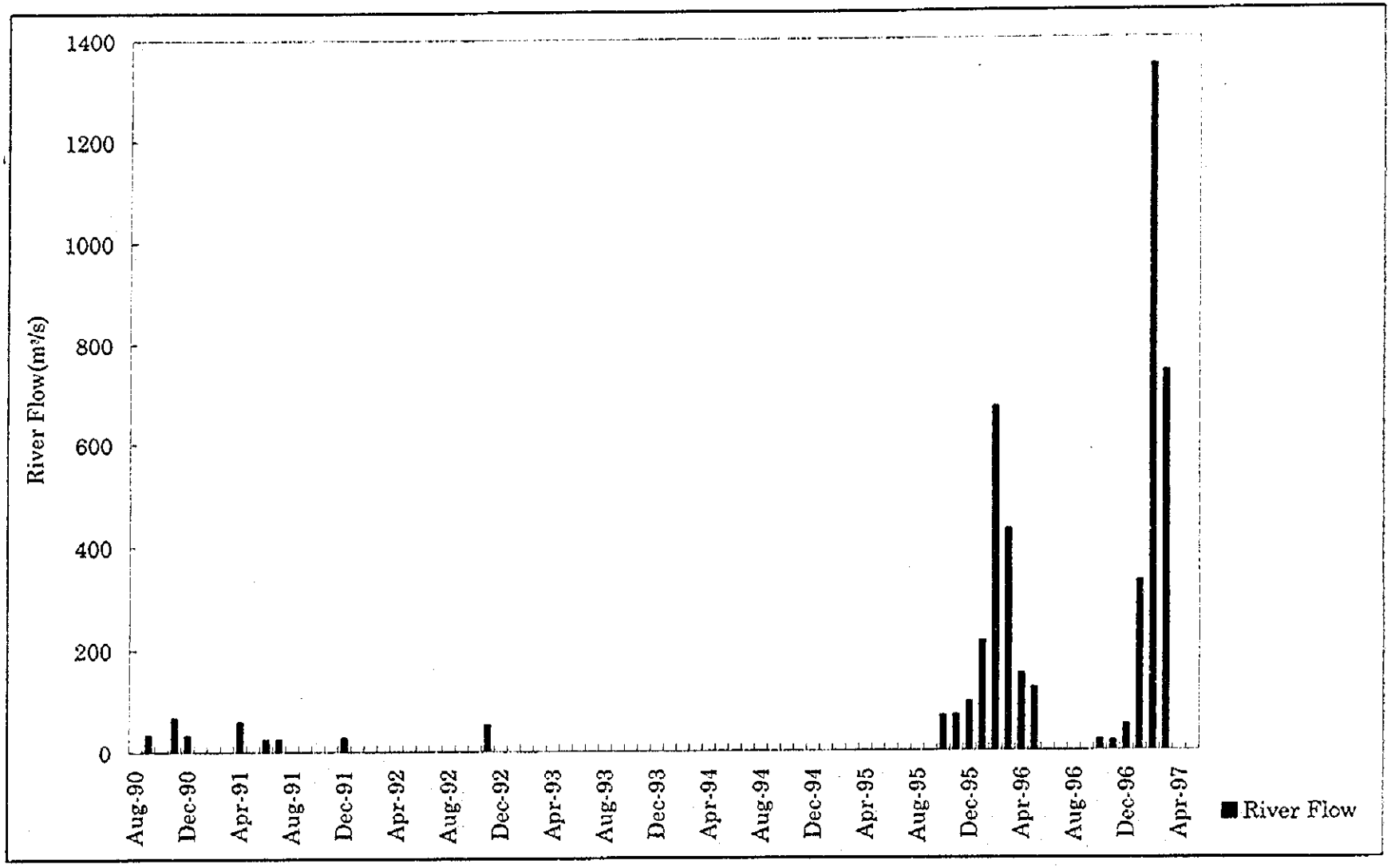

Note : The data of no indications are lacked.

Figure 3.2.6-1 River Flow of Pungue River

- Bathymetric Survey in the wet and dry seasons
- Bank Configuration Survey in the wet and dry seasons
- Tide Observation Survey in the wet and dry seasons
- Wave Observation Survey in the wet season
- Current and Turbidity Survey in the wet and dry seasons
- Turbidity Observation Survey in the wet and dry seasons

(1) Installation of Survey Station and Area

As shown in Figures 3.3.1-1 to 3.3.1-4, 3 stations of tide observation, 2 stations of wave measurement, 13 stations for the current measurement by a current meter and the turbidity measurement and 3 stations for the current measurement by float tracking were selected.

(2) Vessels Arrangement

Three small fishing boats of 20 feet long with a 15 HP engine were arranged during this field survey. Counterparts from EMODRAGA worked on board for technical transfer on how to manage the field survey using each survey equipment. Also a survey boat, 33 foot long with two high power engines, was arranged for the bathymetric survey and a tug boat used for setting up two wave measuring buoys.

(3) Positioning System

During these field surveys, the global positioning system (GPS) has been operated quite satisfactorily. Especially, the global positioning system in differential mode (DGPS) was used in the bathymetric survey for accurate positioning.

(4) Equipment

The equipment used for this field survey consists of the following devices.

- Echo Sounder for Depth Measurement : Krupp Atlas Deso 11 operated with 210 kHz and with DGPS navigation computer
- Water Level Recorder for Tide Observation : MC Systems Mod 510, 24 hours recording
- Wave Buoy for Wave Monitoring : 2 sets of Wave Measuring Buoy, 24 hours monitoring
- Current Meter for Current Measurement : DCM-II (observation item: current velocity and direction)

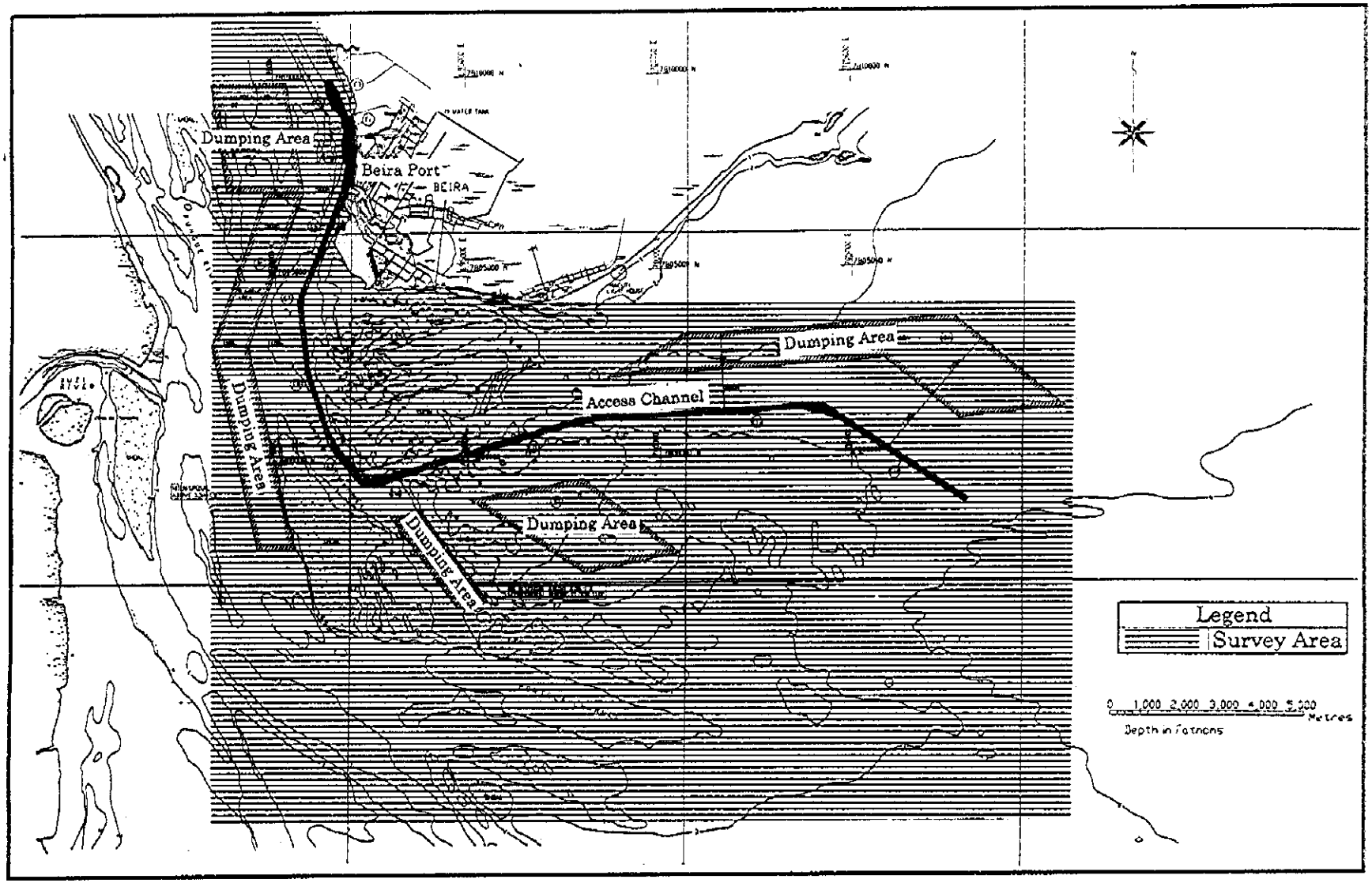

Figure 3.3.1-1 Location of Bathymetric Survey Area

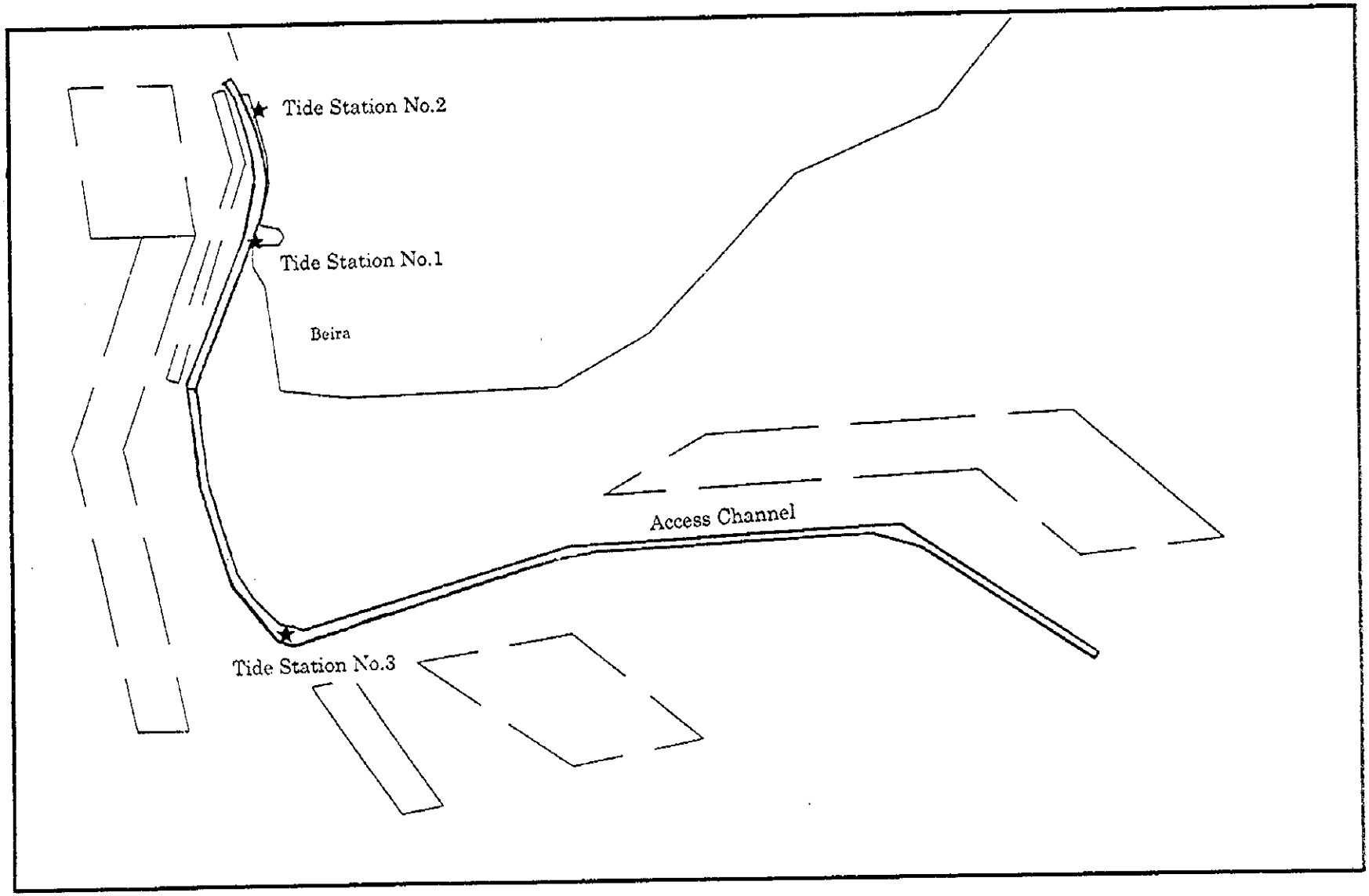

Figure 3.3.1-2 Location of Tide Observatory Stations

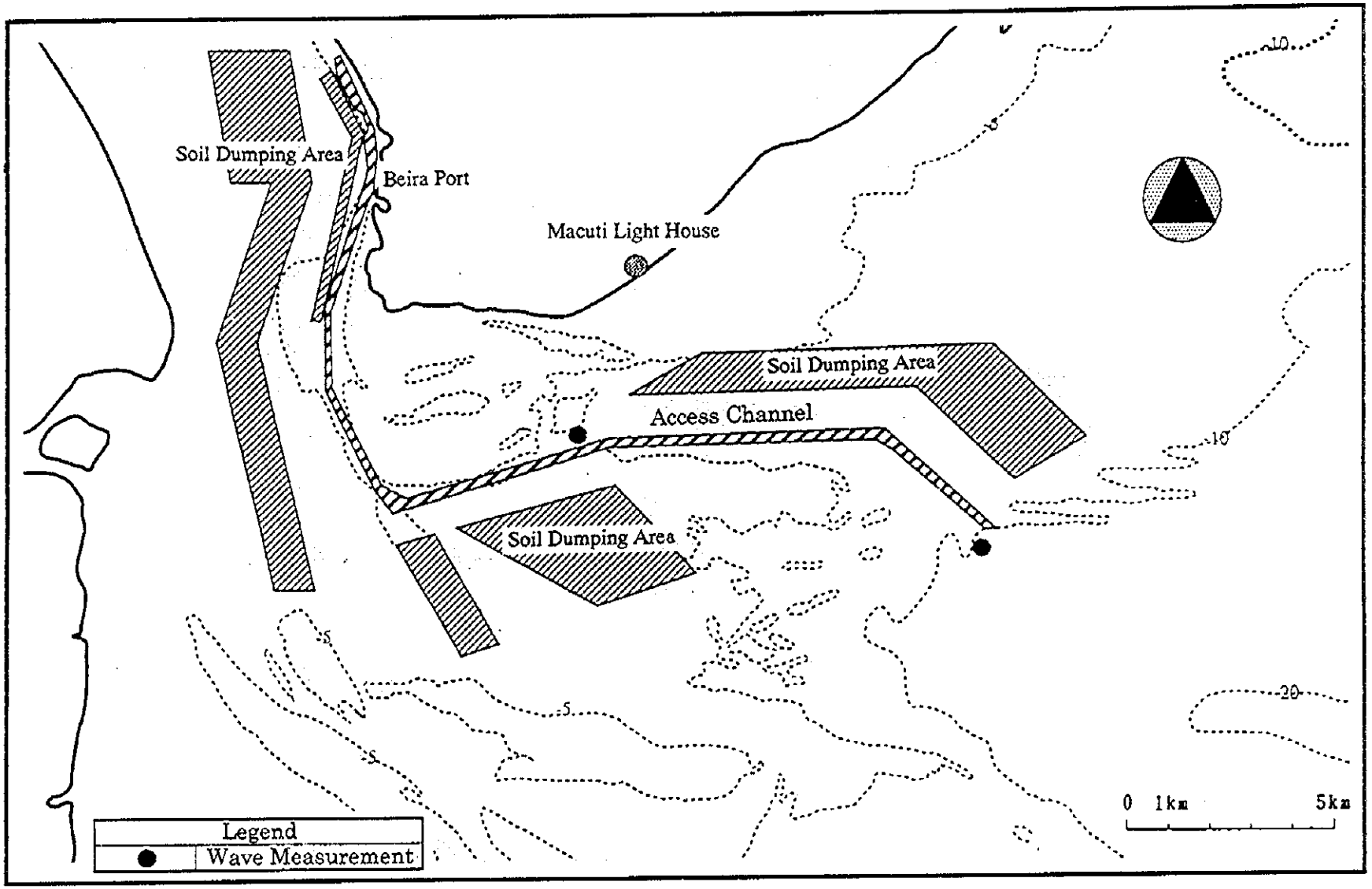

Figure 3.3.1-3 Location of Wave Observatory Stations

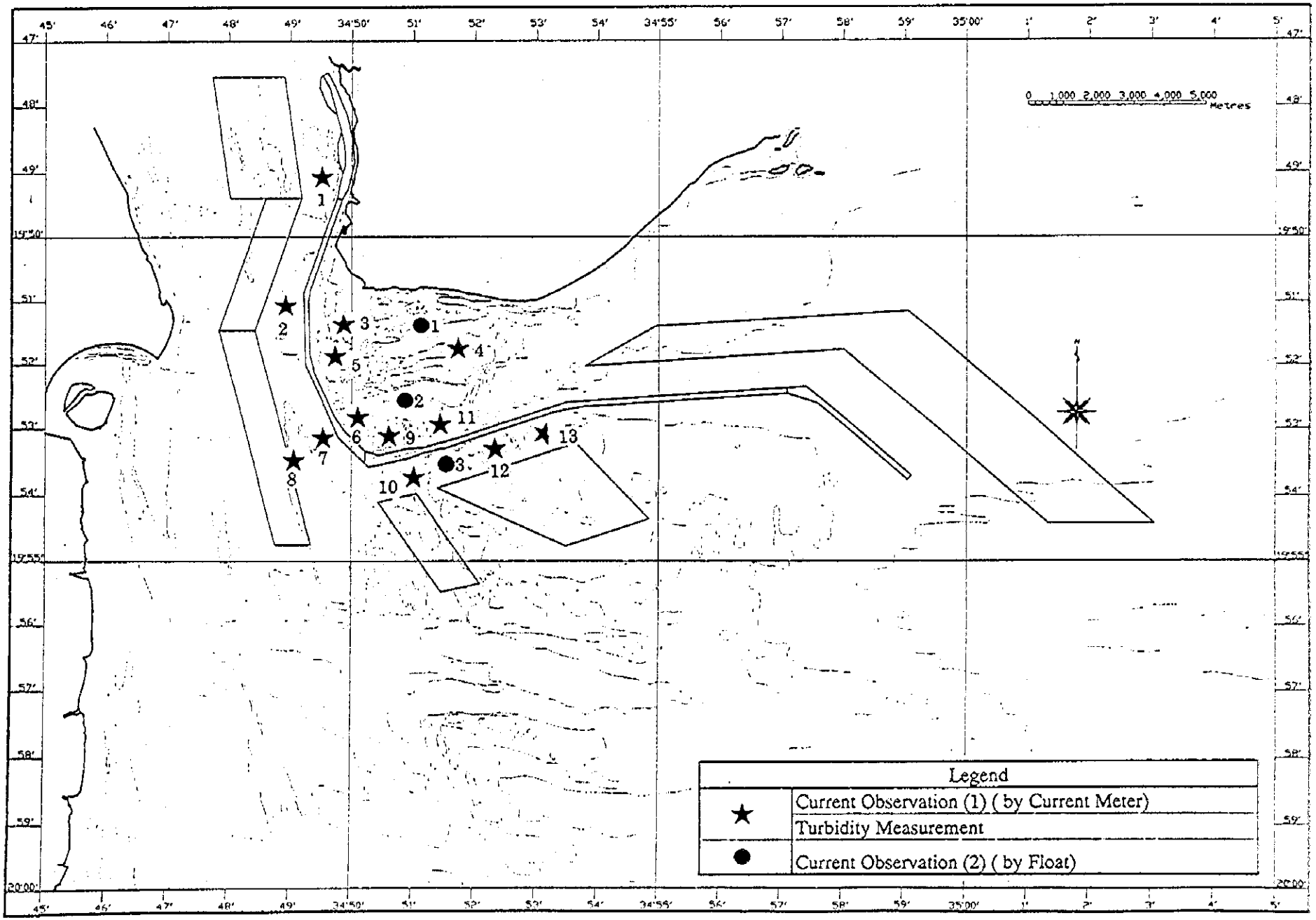

Figure 3.3.1-4 Location of Current and Turbidity Observatory Stations

- Float for Current Measurement : Length: 1.5 m, Diameter: 5 cm, Depth of observation layer: -1 m
- Turbidity Meter of Sea Water : ATU1-D, 2 types with ranges of 200 ppm and 2,000 ppm turbidity

3.3.2 Bathymetry

In order to clarify the oceanographic phenomena and siltation mechanism of the Access Channel and its surroundings, the bathymetric survey was carried out at coastal and offshore areas around Beira Port in the wet and dry seasons.

(1) Methodology

The bathymetric surveys area in the Access Channel and the dumping areas are shown in Figure 3.3.1-1. A digital echo-sounder combined with Global Positioning System in Differential Mode (DGPS) was used for the measurements of the water depth. The total area was 173 km^2 including Beira Port, the Access Channel, Dumping Areas, estuary of the Pungue and Buzi Rivers. Water level were recorded during the survey period by a water level digital recorder installed at the tug boat jetty as tide observation station No.1.

(2) Results of Bathymetric Survey

The results of survey are shown in Figures 3.3.2-1 to 3.3.2-9. According to the contour map of the large grid shown in Figure 3.3.2-1, some major shoal areas can be distinguished alongside the Access Channel, one in west to E5 in front of Beira Port, one in north to the bending corner of the Access Channel and others in south to the bending corner.

4 cross sections of the Access Channel are shown in Figure 3.3.2-3. In almost all the cross sections, the water depth in July 1997 is shallower by 0.5 to 2 m than March 1997. The other cross sections are shown in Appendix A-2. Soft sediment was observed predominant in the estuary of the Pungue River and E14 section in the Access Channel.

The cross sections of the dumping area are shown in Figure 3.3.2-10. The water depth in July 1997 is shallower than May 1997. The water depth of D5 is less than 2 m in the most part. Depth of D1 ranges from 2.0 to 4.0 m and D2 is from 3.0 to 4.0 m. Depth of D3 ranges from 1.0 to 4.0 m and D4 is from 4.0 to 8.0 m.

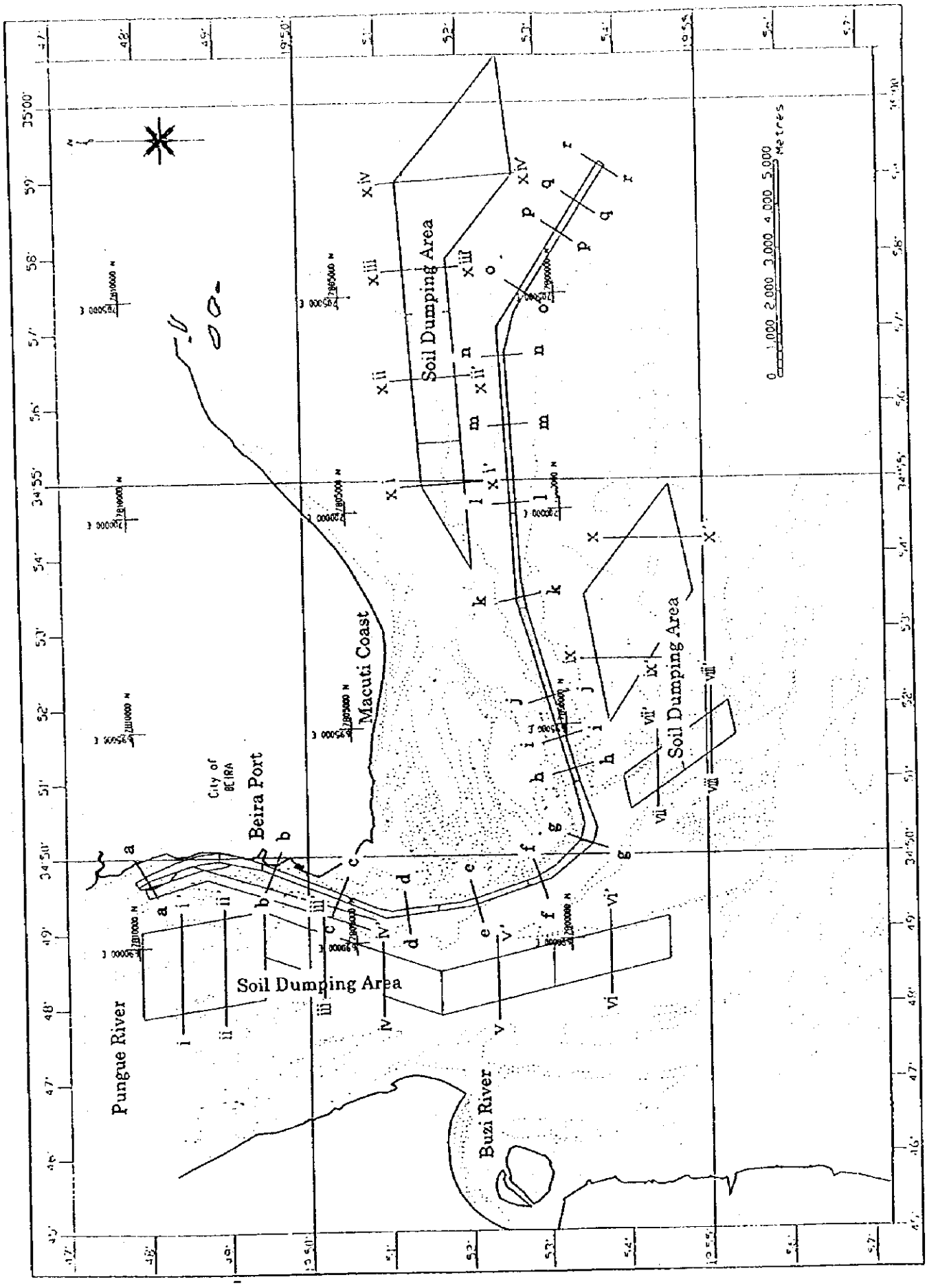

Figure 3.3.2-1 Cross Section of Bathymetric Survey Results in Wet and Dry Seasons

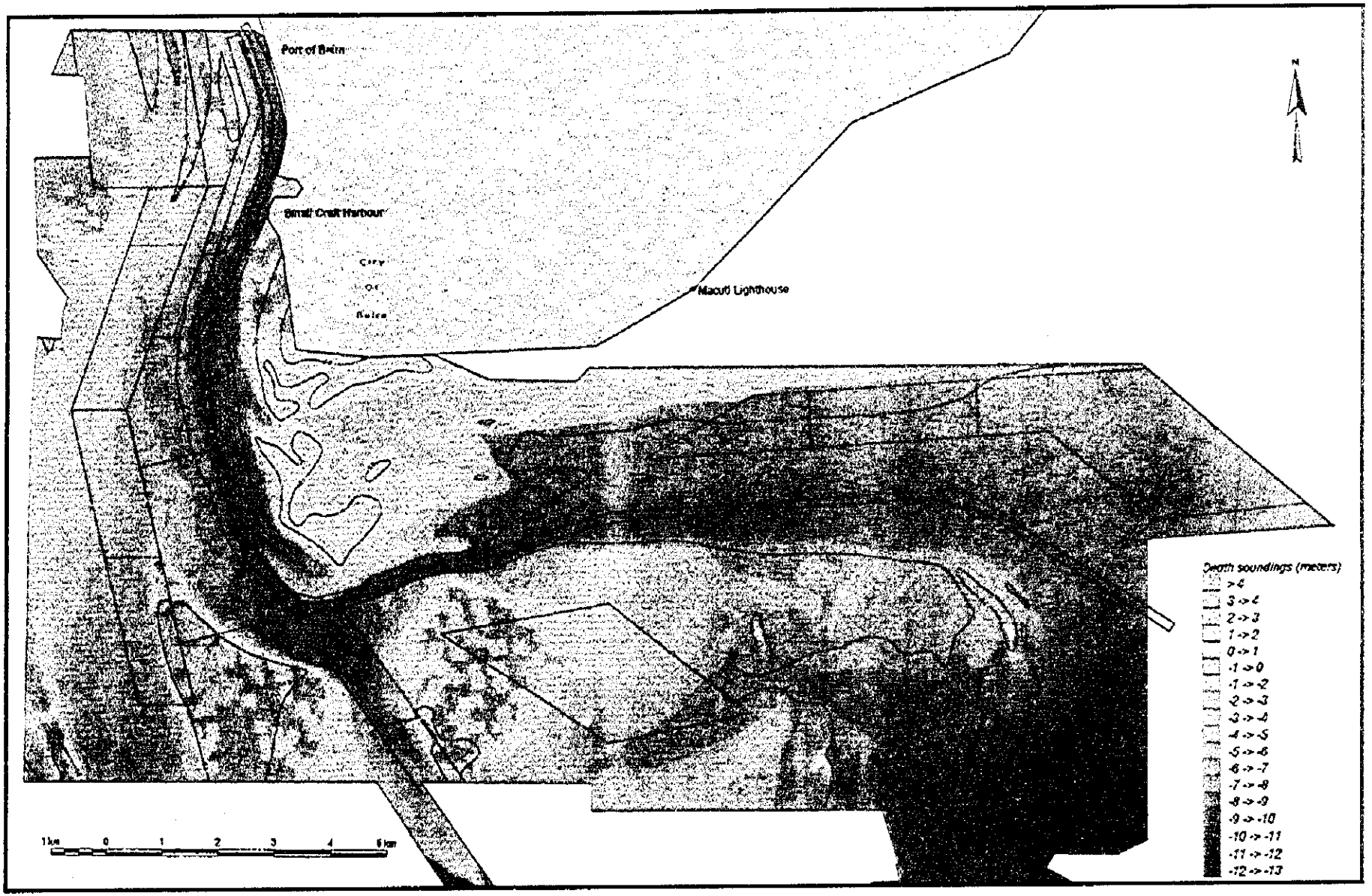

Figure 3.3.2-2 Bathymetric Chart in Dry Season

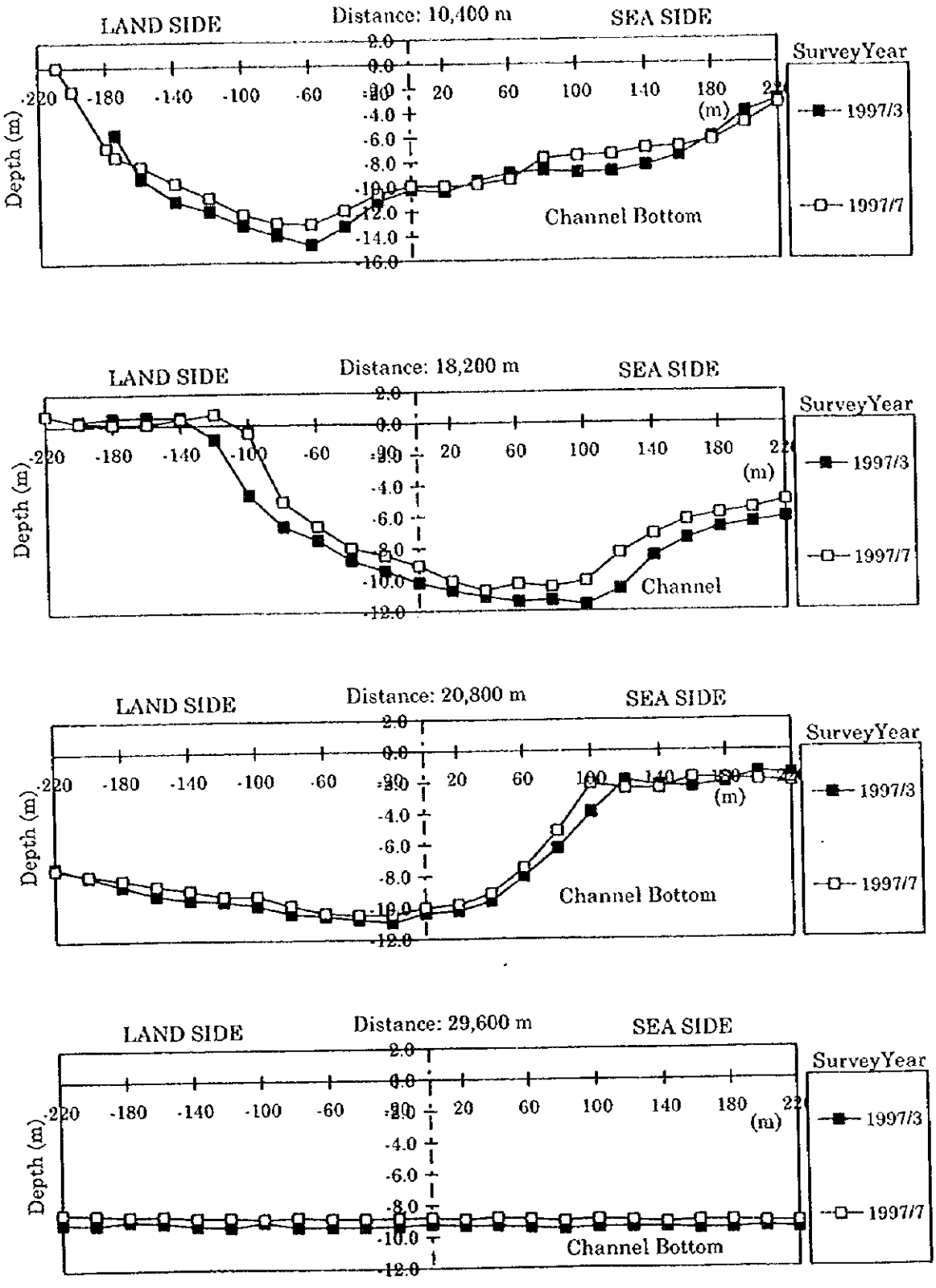

Figure 3.3.2-3 Result of Bathymetric Survey, the Access Channel

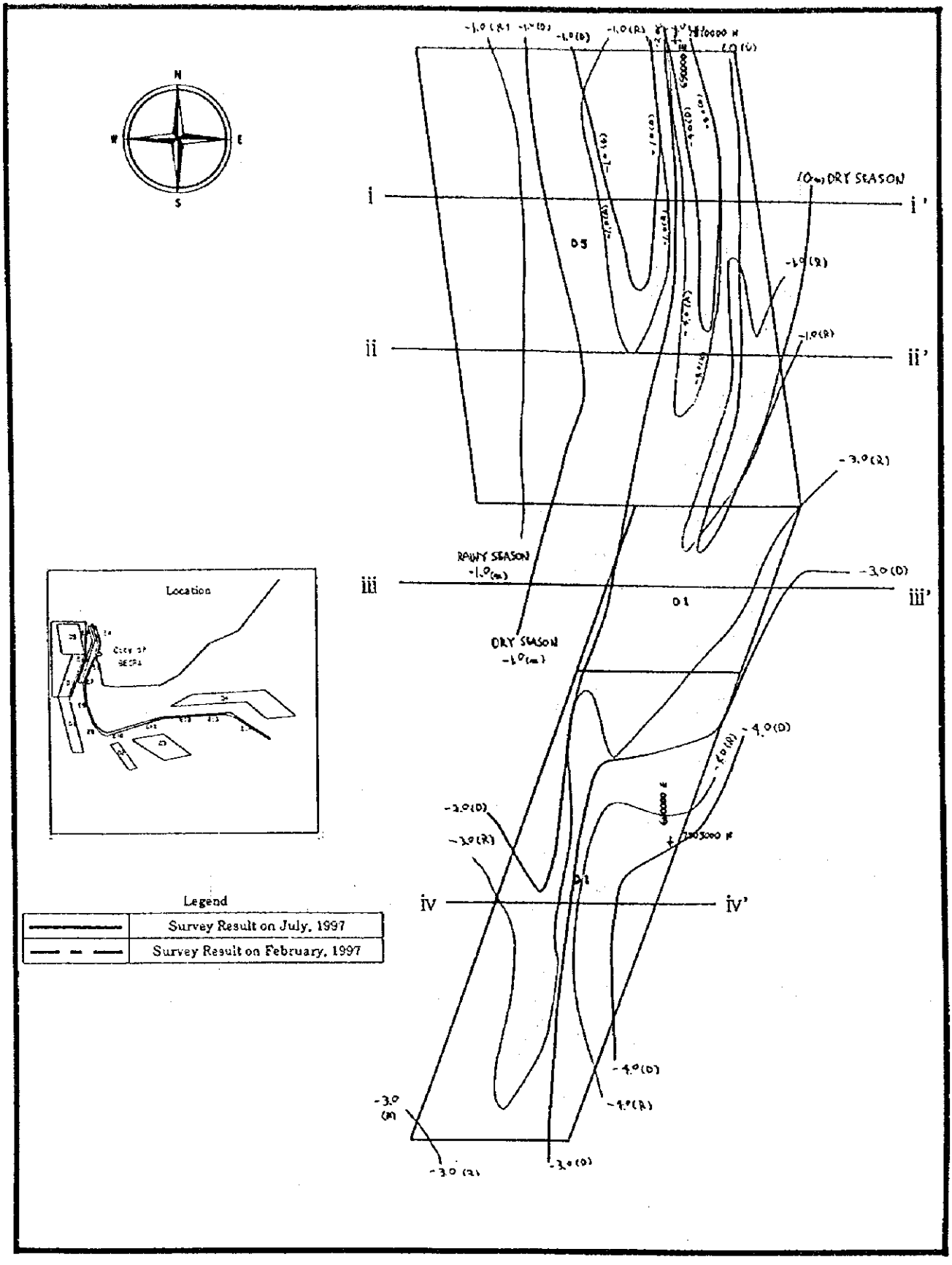

Figure 3.3.2-4 Results of Bathymetric Survey, Dumping Area D5 and D1 (1)

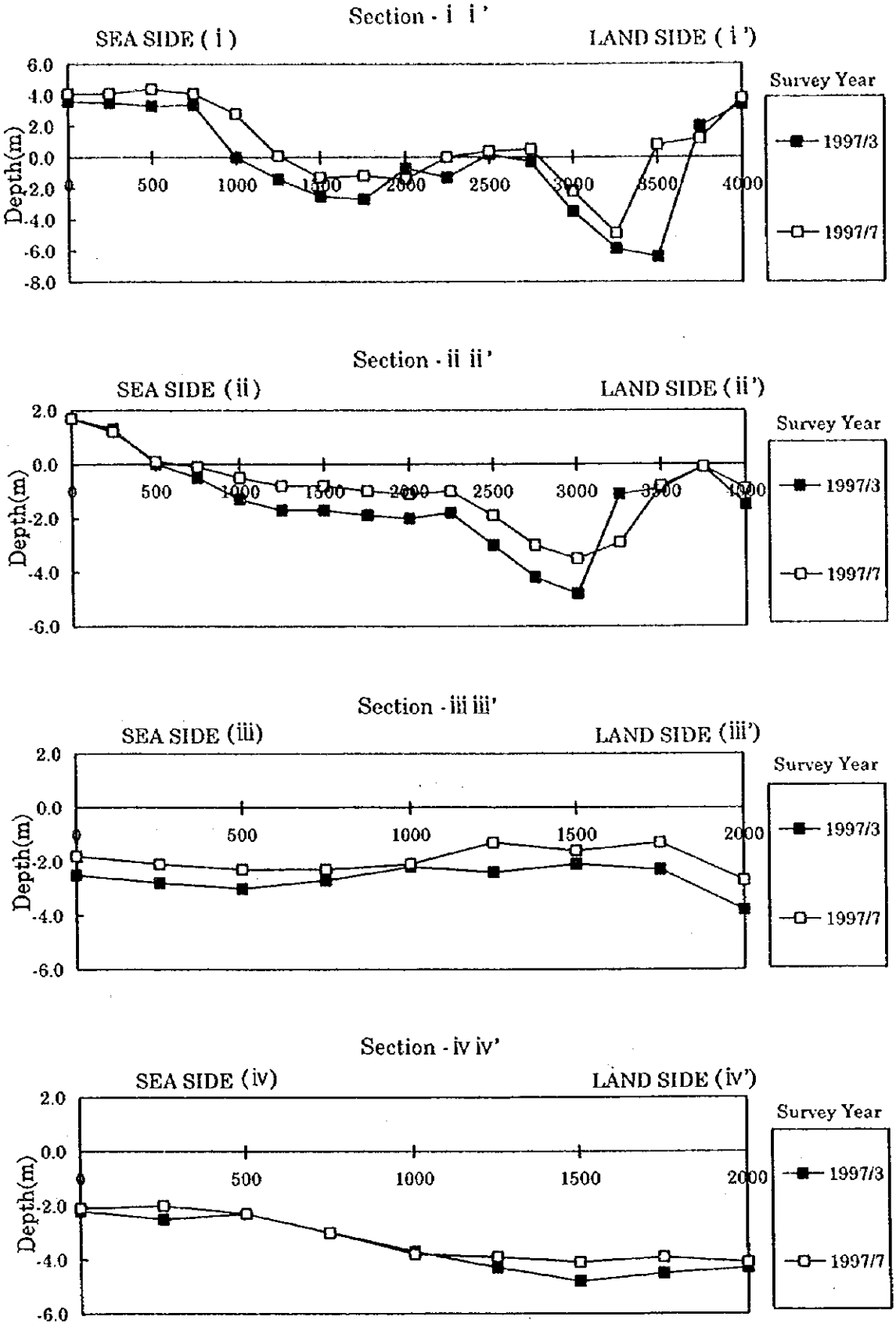

Figure 3.3.2-5 Results of Bathymetric Survey, Dumping Area D5 and D1 (2)

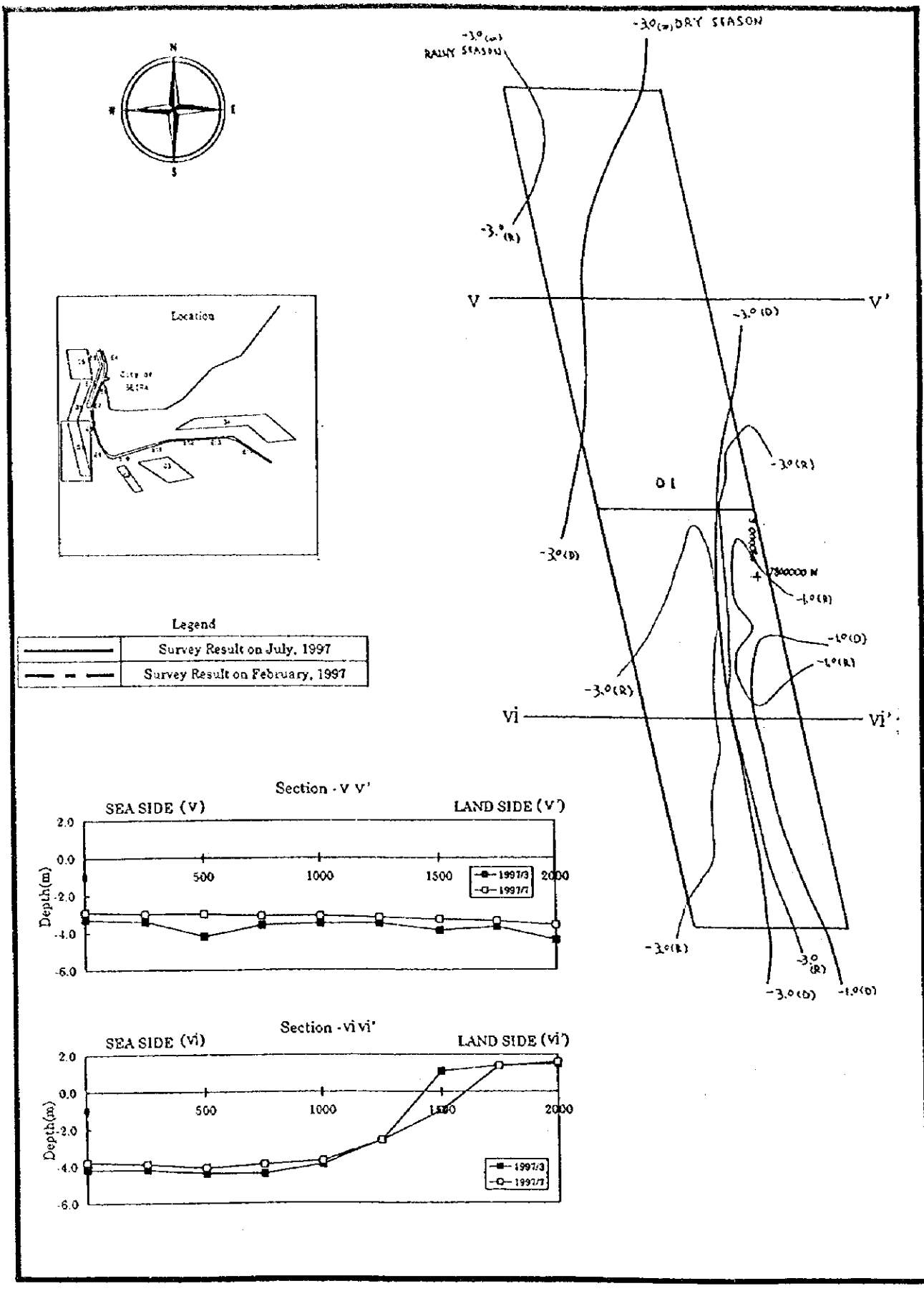

Figure 3.3.2-6 Results of Bathymetric Survey, Dumping Area D1

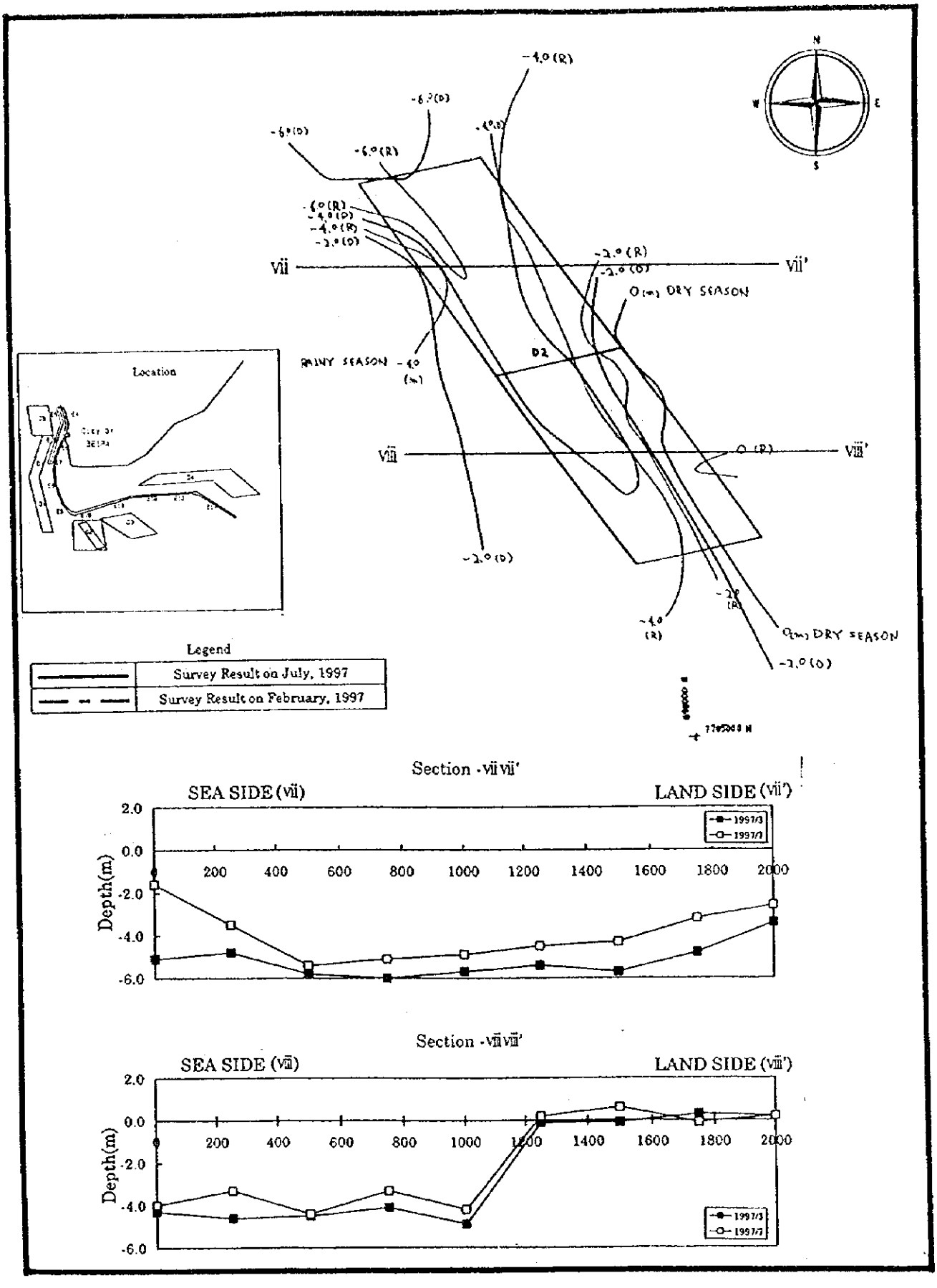

Figure 3.3.2-7 Results of Bathymetric Survey, Dumping Area D2

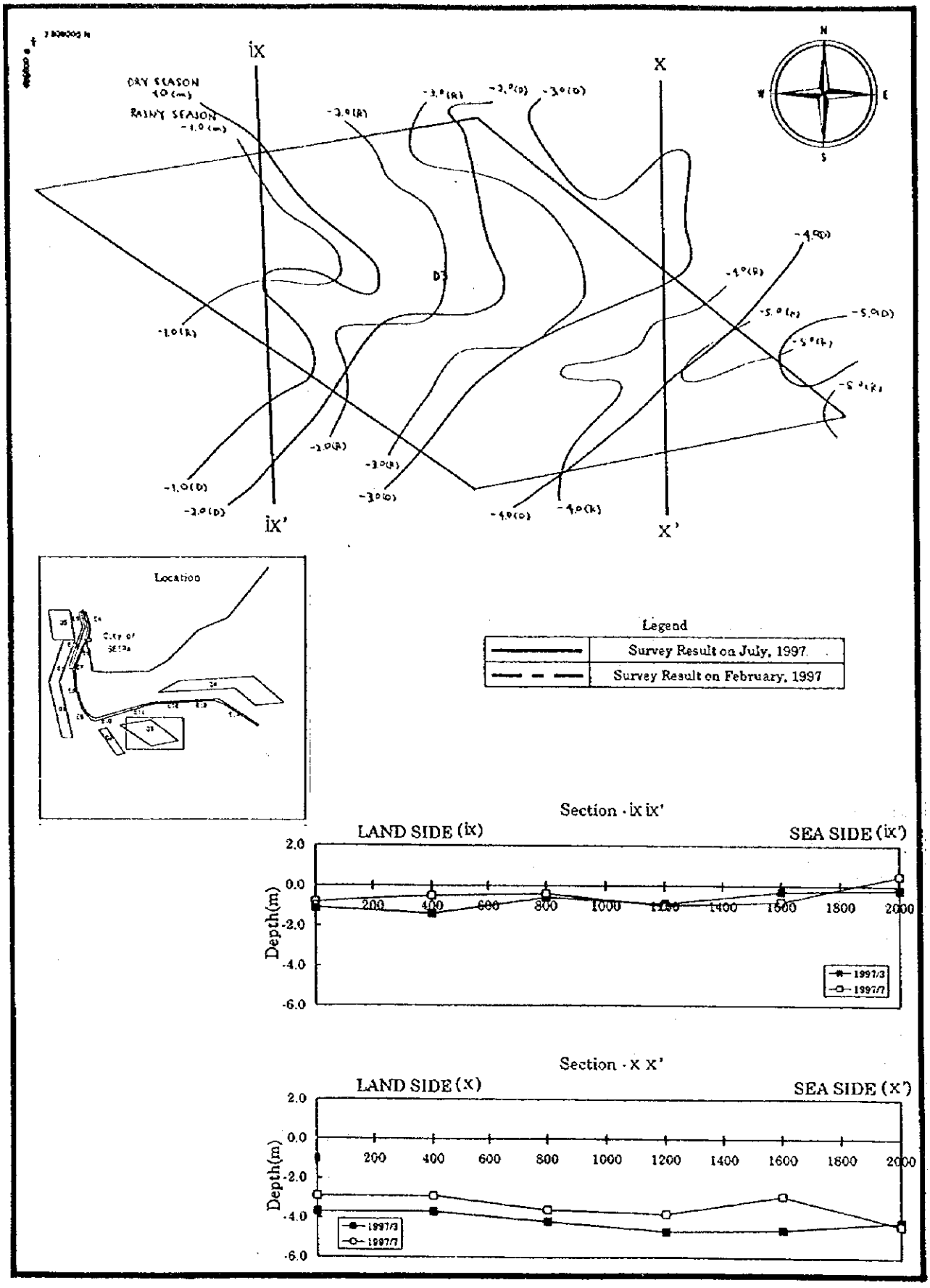

Figure 3.3.2-8 Results of Bathymetric Survey, Dumping Area D3

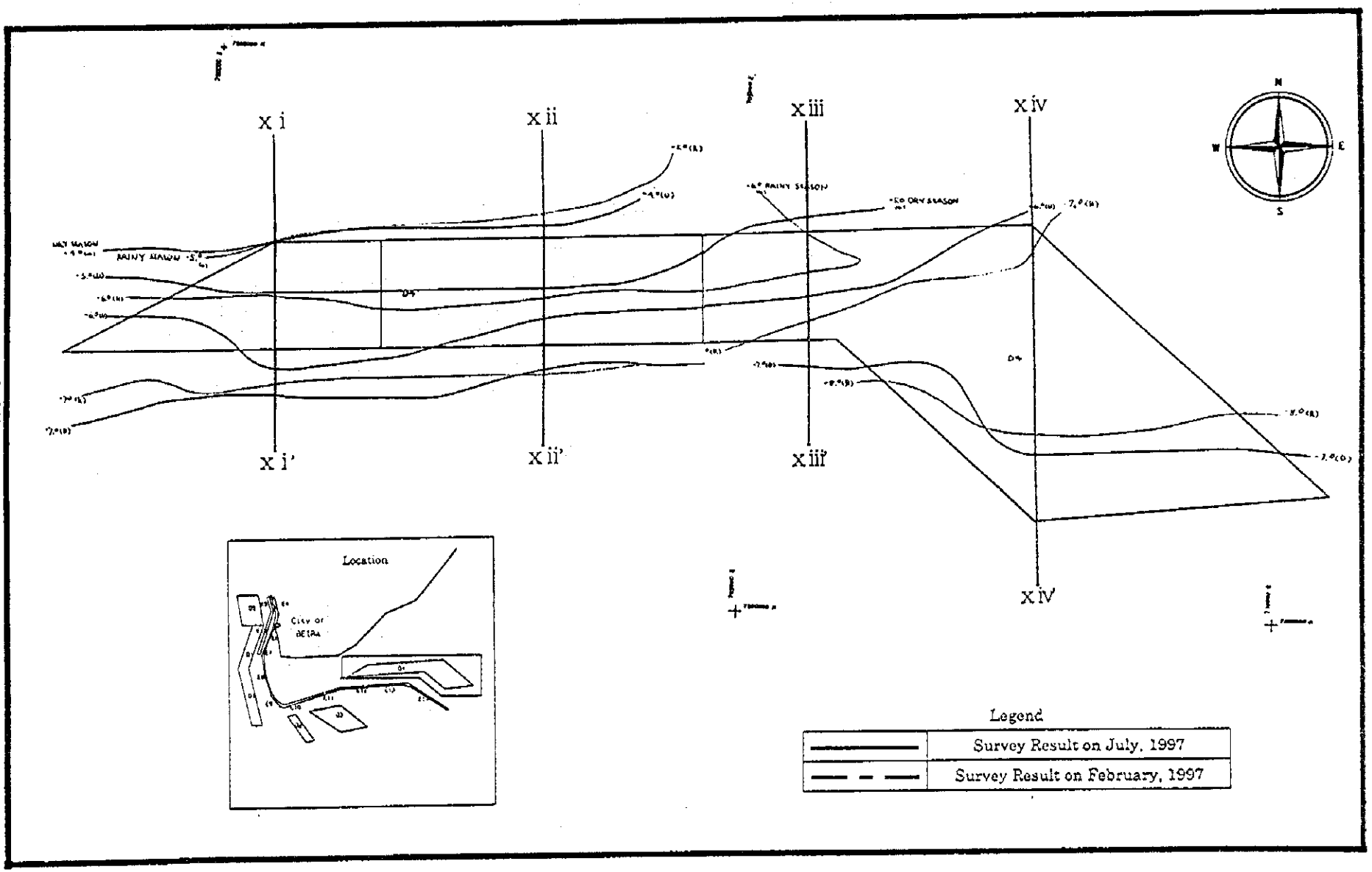

Figure 3.3.2-9 Results of Bathymetric Survey, Dumping Area D4 (1)

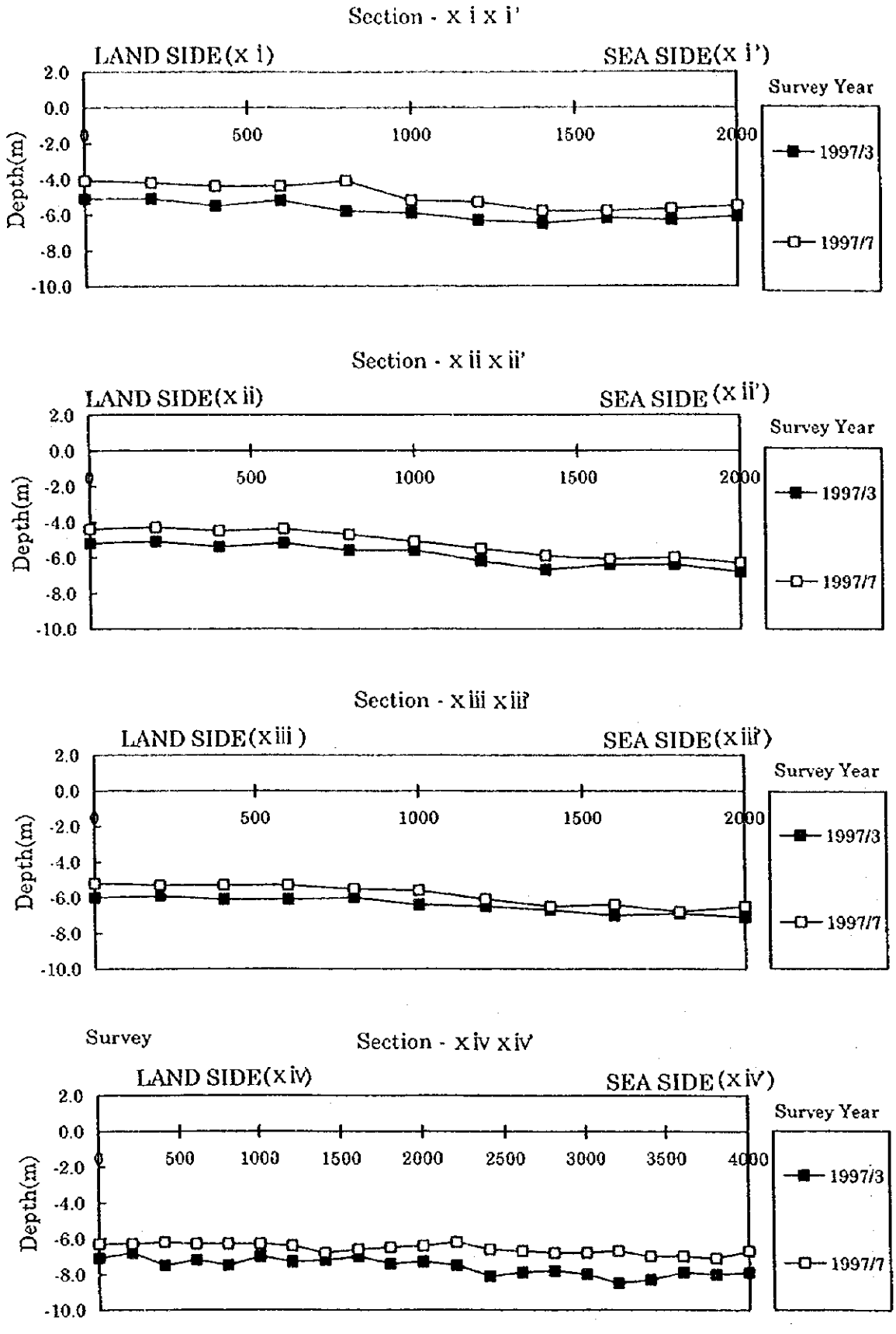

Figure 3.3.2-10 Results of Bathymetric Survey, Dumping Area D4 (2)

3.3.3 Bank Observation

A sketch of the area of banks in the wet season is illustrated in Figure 3.3.3-1. The configuration and distribution of banks and shoals existing around the estuary of the Pungue River were observed by aircraft and boat. The banks along the Access Channel from Beira Port to Macuti Light House were observed frequently at spring low tide.

3.3.4 Tide Observation

The location of tide observation stations is indicated in Figure 3.3.1-2 and tidal level in Beira Port derived from the Admiralty Tide Table is indicated in Figure 3.3.4-1. Also the actual hourly tide records are shown in Figures 3.3.4-2 and 3.3.4-3. The actual tidal level data were collected from the tide observation station at Mozambique Ports and Railways Center (CFM-C) at Beira Port and tide observation during our bathymetric surveys were carried out.

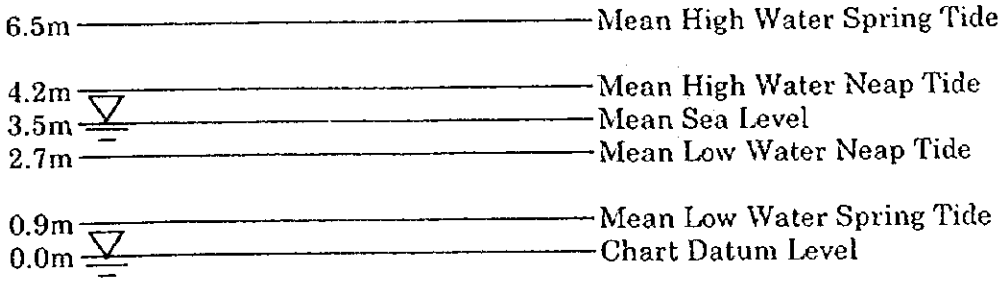

Figure 3.3.4-1 Tide Level Chart

It is typical semi-diurnal tide in the vicinity of Beira.

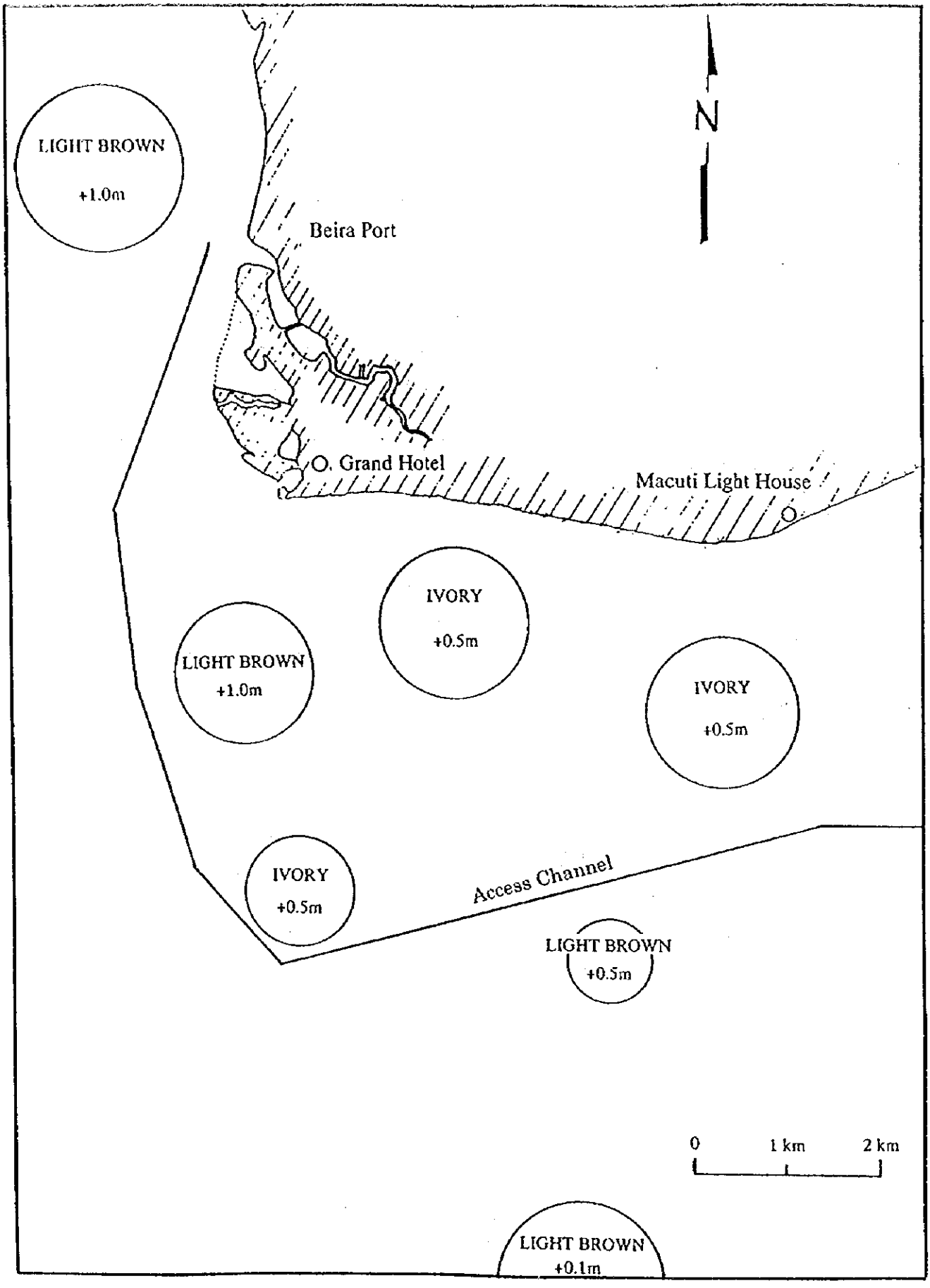

Figure 3.3.3-1 Location of Major Banks

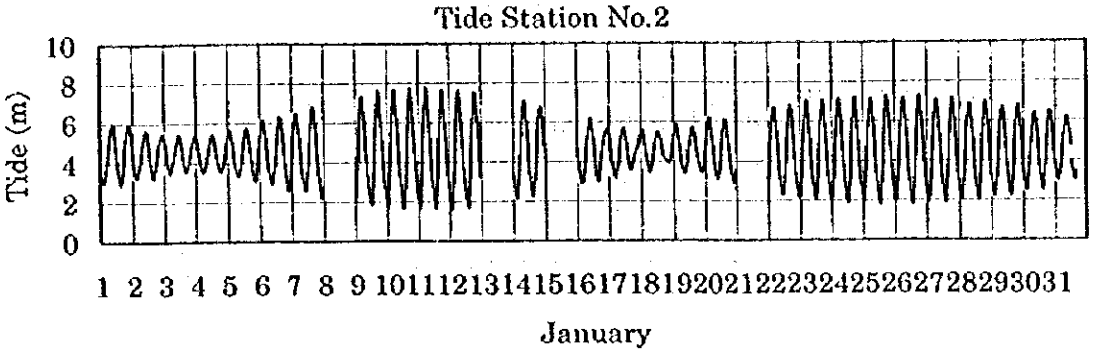

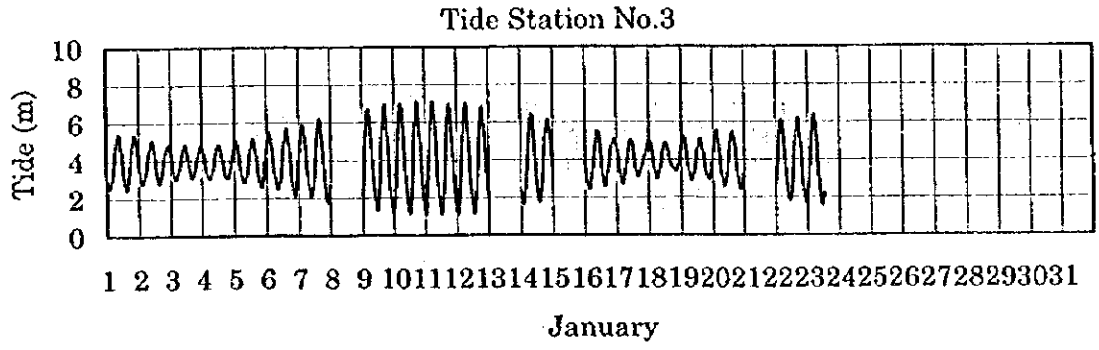

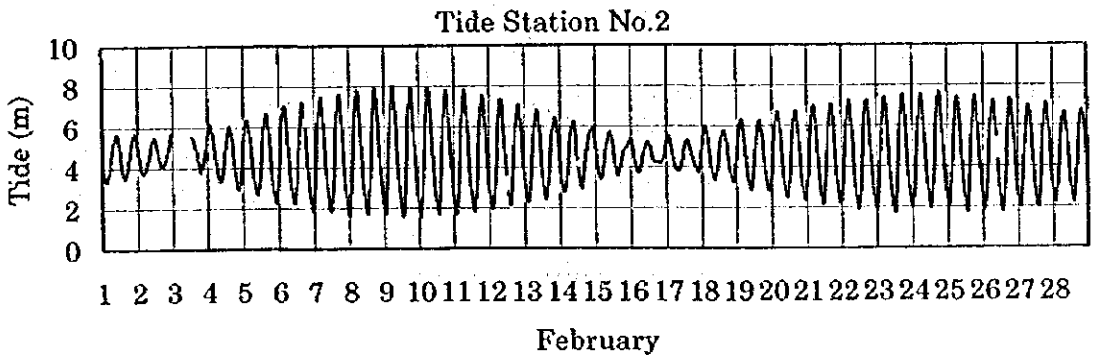

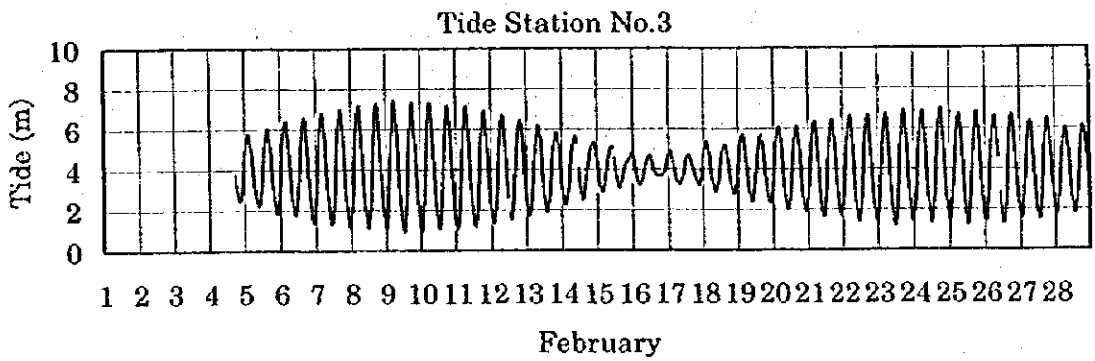

Figure 3.3.4-2 Tide Record of January and February in 1997

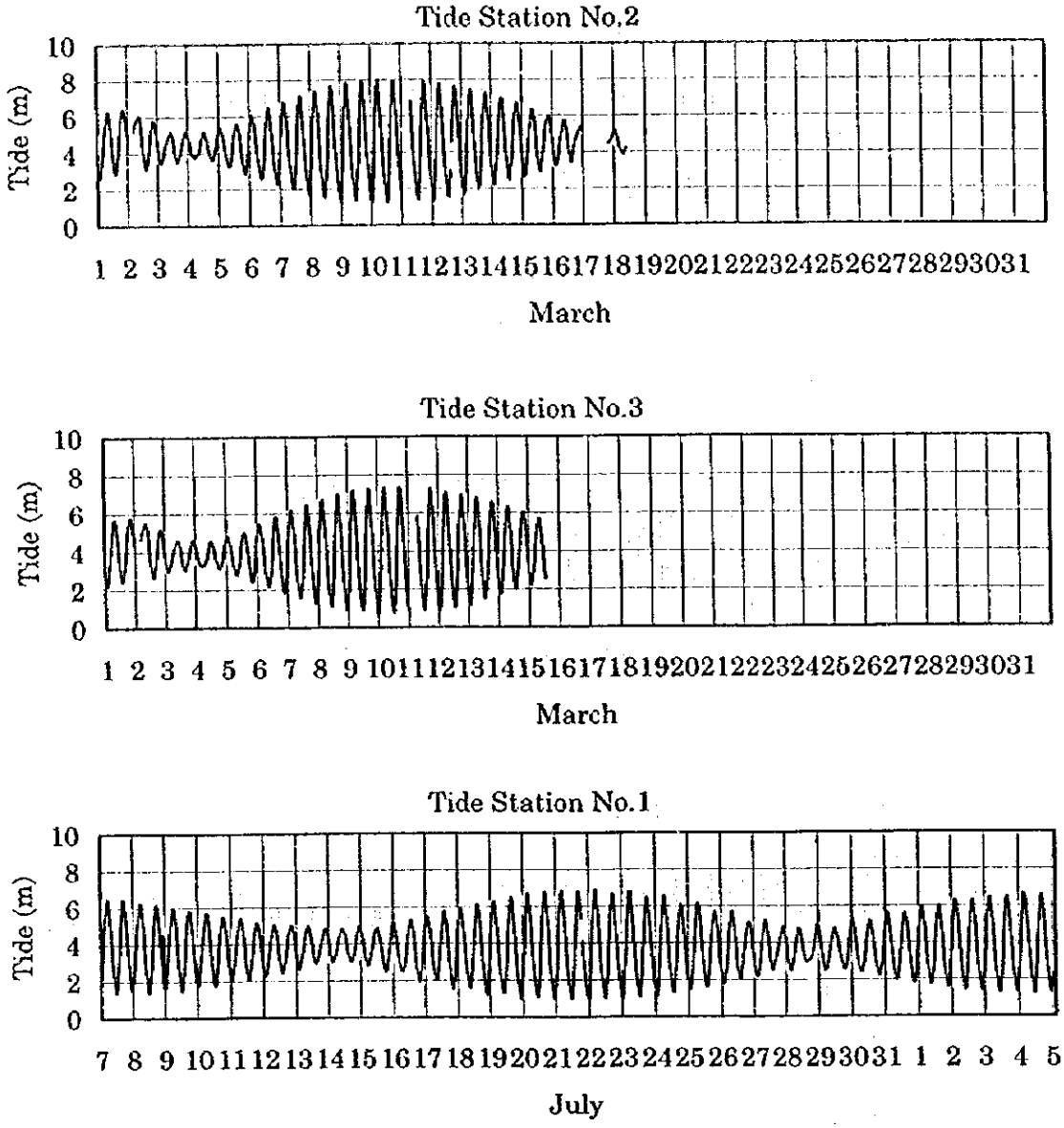

Figure 3.3.4-3 Tide Record of March and July in 1997

3.3.5 Wave Observation

The wave observation was carried out to analyze the waves along the coast and offshore area in the vicinity of the Access Channel in the wet season.

(1) Methodology

The wave observation survey was carried out for two months to find out the characteristics of induced waves at two points as shown in Figure 3.3.1-3. Wave buoy 1 was installed at 19° 55.04' S and 35° 1.57' E (13 m water depth) and wave buoy 2 was at 19° 52.64' S and 34° 52.65' E (5 m water depth). The data of these buoys were transmitted by radio transfer to the recorder located at the on-land base station.

(2) Results of Wave Observation

The results of the wave observation survey are shown in Figures 3.3.5-1 to 3.3.5-5 and Tables 3.3.5-1 to 3.3.5-3.

At the wave buoy 1, the significant wave height of 4.2 m with period of 10.7 seconds was recorded which reduced to 2.2 m and 8.8 seconds at the wave buoy 2. These waves were caused by cyclone "Lisette" which was the biggest cyclone attacking Beira Port in past ten years.

The data on the wave measurement mentioned above recorded by the wave buoys are shown in Figures 3.3.5-1 to 3.3.5-3. Wave occurrence by direction is shown in Table 3.3.5-1. Wave occurrence by height and tide is shown in Figures 3.3.5-4 and 3.3.5-5. Relations between wave spectrum and spectral density are shown in Figures 3.3.5-6 and 3.3.5-7.

The relationship between wave heights at two buoys and tide shows a particular trend as shown in the figures. At tide level from 5.0 m to 6.0 m, waves up to 3.25 m in height were recorded at Buoy 1 and waves up to 1.8 m were recorded at Buoy 2.

In Figure 3.3.5-6, the peak density is found at 0.15 - 0.20 Hz at Buoy 1, as well as at Buoy 2. In Figure 3.3.5-7, the peak density is found in 0.10 - 0.20 Hz at Buoy 1, while the peak density is not clear at Buoy 2.

Significant wave height of 1.0 m to 2.0 m at Buoy 1 and less than 1.0 m at Buoy 2 are predominant except during stormy periods.

Table 3.3.5-1 Wave Occurrence by Direction in Wet Season at Buoy1

WAVE HEIGHT(m)	S	SE	E	NE	TOTAL
4.0-	0.0%	0.6%	0.0%	0.0%	0.6%
3.5-4.0	0.0%	0.0%	0.0%	0.0%	0.0%
3.0-3.5	0.0%	1.1%	0.0%	0.0%	1.1%
2.5-3.0	0.0%	0.9%	0.0%	0.0%	0.9%
2.0-2.5	0.3%	0.9%	0.1%	0.0%	1.3%
1.5-2.0	1.0%	7.1%	0.7%	0.0%	8.8%
1.0-1.5	0.6%	26.5%	7.7%	0.7%	35.5%
0.5-1.0	1.0%	31.5%	16.2%	2.8%	51.6%
0.0-0.5	0.0%	0.0%	0.3%	0.0%	0.3%
TOTAL	2.8%	68.5%	25.1%	3.6%	100.0%

Table 3.3.5-2 Wave Occurrence by Wave Period in Wet Season at Buoy1

WAVE PERIOD(s)/ WAVE HEIGHT(m)	-6.0	6.0-8.0	8.0-10.0	10.0-12.0	12.0-14.0	14.0-	TOTAL
4.0-	0.0%	0.0%	0.1%	0.1%	0.0%	0.0%	0.3%
3.5-4.0	0.0%	0.0%	0.0%	0.0%	0.0%	0.0%	0.0%
3.0-3.5	0.0%	0.1%	0.3%	0.1%	0.0%	0.0%	0.6%
2.5-3.0	0.1%	0.1%	0.1%	0.0%	0.0%	0.0%	0.4%
2.0-2.5	0.3%	1.0%	0.0%	0.0%	0.0%	0.0%	1.3%
1.5-2.0	3.7%	4.1%	0.1%	0.6%	0.0%	0.0%	8.6%
1.0-1.5	22.4%	9.6%	5.1%	0.7%	0.6%	0.0%	38.4%
0.5-1.0	18.1%	9.3%	14.1%	6.7%	2.0%	0.1%	50.4%
0.0-0.5	0.1%	0.0%	0.0%	0.0%	0.0%	0.0%	0.1%
TOTAL	44.8%	24.3%	20.0%	8.3%	2.6%	0.1%	100.0%

Table 3.3.5-3 Wave Occurrence by Wave Period in Wet Season at Buoy2

WAVE PERIOD(s)/ WAVE HEIGHT(m)	-6.0	6.0-8.0	8.0-10.0	10.0-12.0	12.0-14.0	14.0-	TOTAL
4.0-	0.0%	0.0%	0.0%	0.0%	0.0%	0.0%	0.0%
3.5-4.0	0.0%	0.0%	0.0%	0.0%	0.0%	0.0%	0.0%
3.0-3.5	0.0%	0.0%	0.0%	0.0%	0.0%	0.0%	0.0%
2.5-3.0	0.0%	0.0%	0.0%	0.0%	0.0%	0.0%	0.0%
2.0-2.5	0.1%	0.0%	0.4%	0.0%	0.0%	0.0%	0.6%
1.5-2.0	0.9%	0.4%	0.1%	0.0%	0.0%	0.0%	1.5%
1.0-1.5	7.2%	1.0%	0.0%	0.6%	0.0%	0.0%	8.8%
0.5-1.0	50.7%	4.6%	4.9%	3.1%	0.4%	0.0%	63.9%
0.0-0.5	20.2%	1.3%	1.3%	1.8%	0.4%	0.0%	25.1%
TOTAL	79.2%	7.5%	6.9%	5.5%	0.9%	0.0%	100.0%

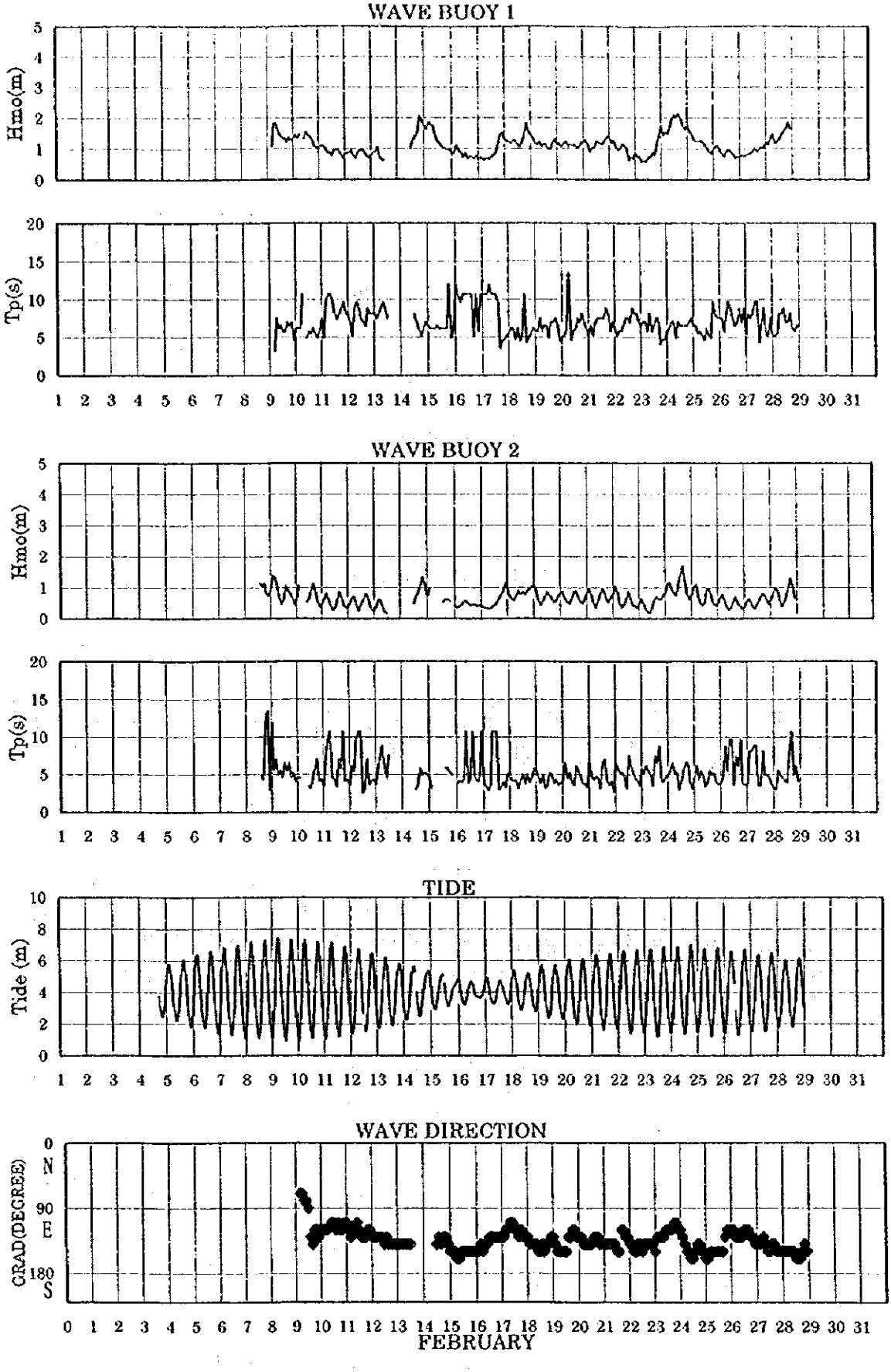

Figure 3.3.5-1 Wave Observatory Result in February

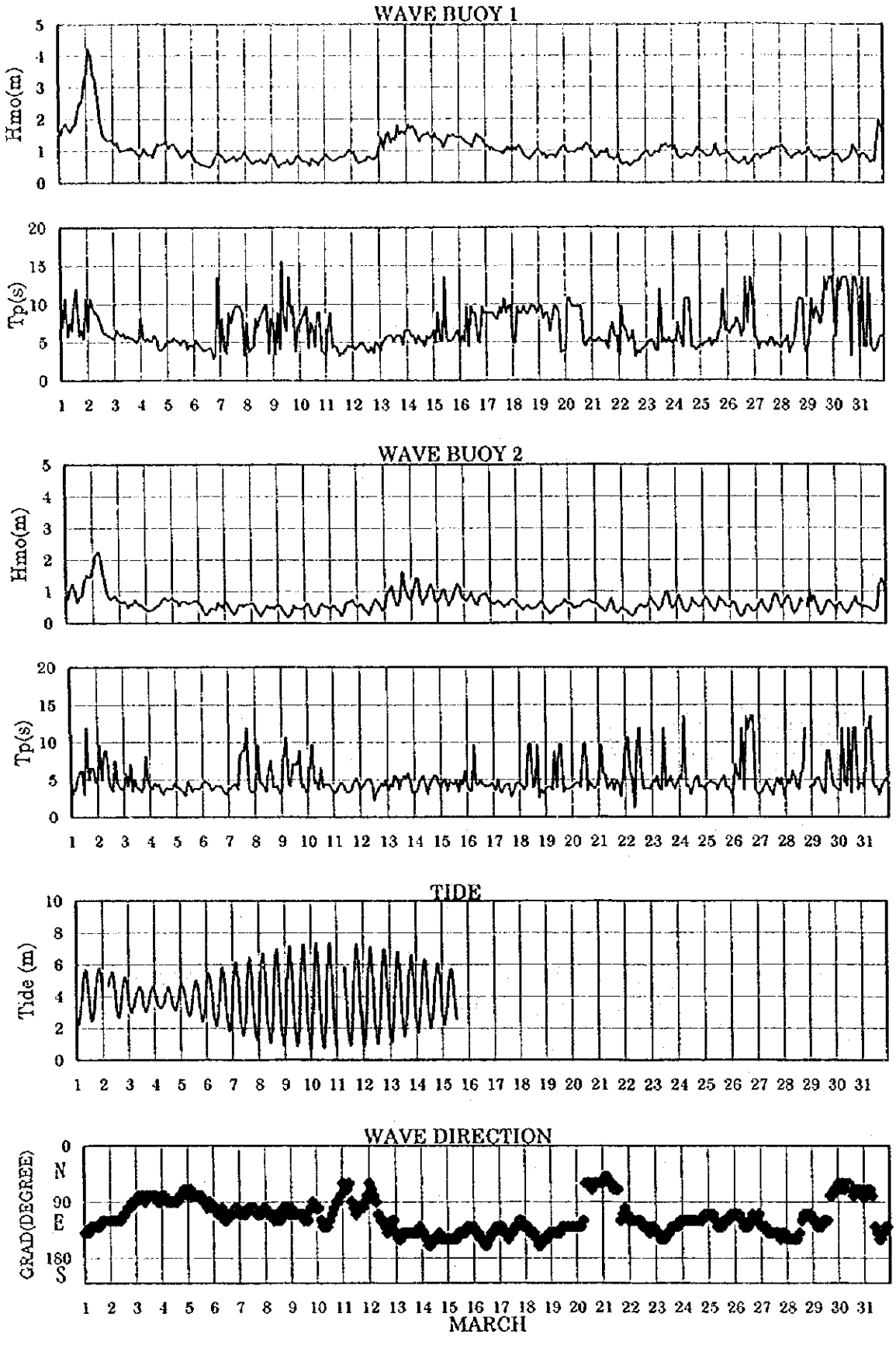

Figure 3.3.5-2 Wave Observatory Result in March

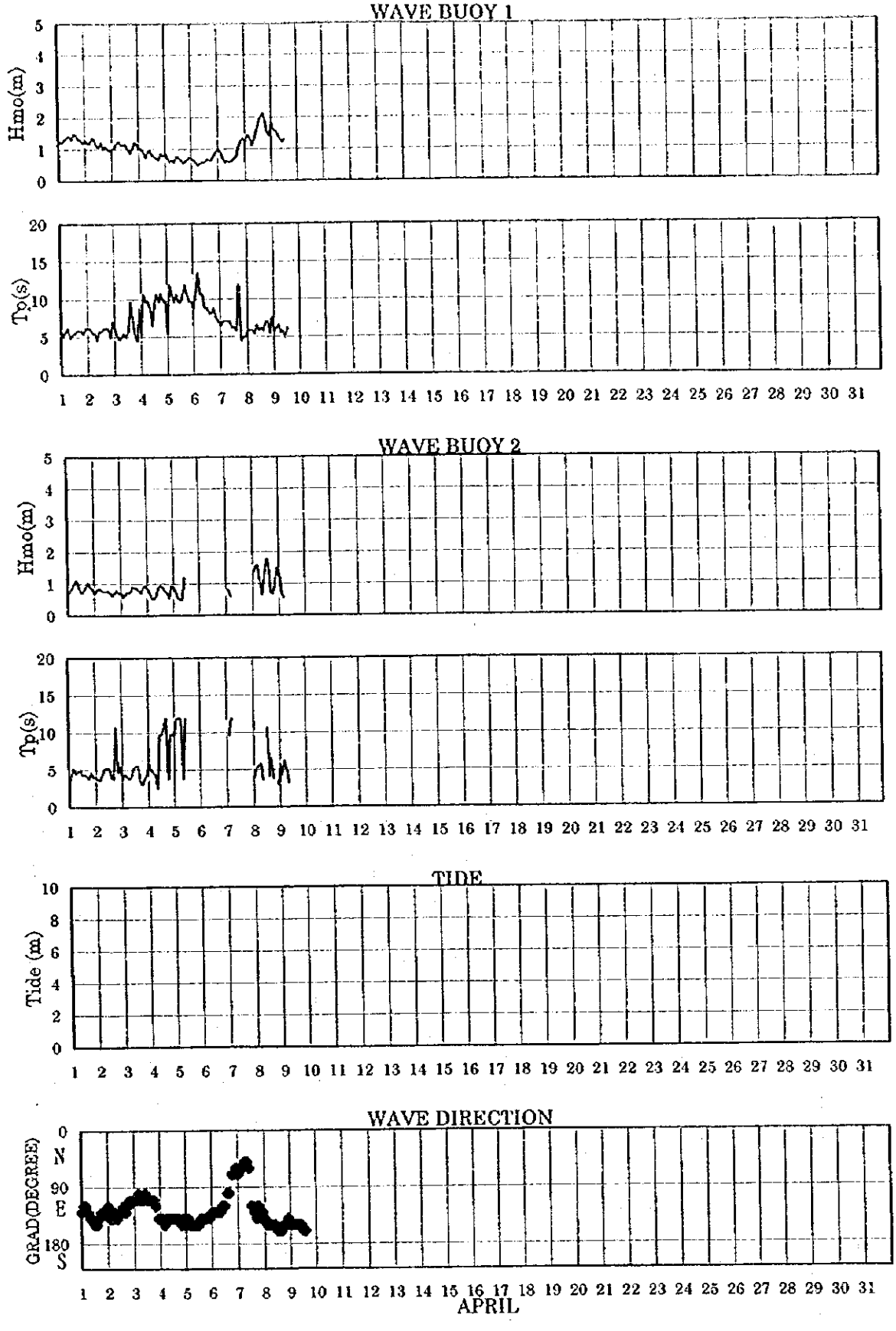

Figure 3.3.5-3 Wave Observatory Result in April

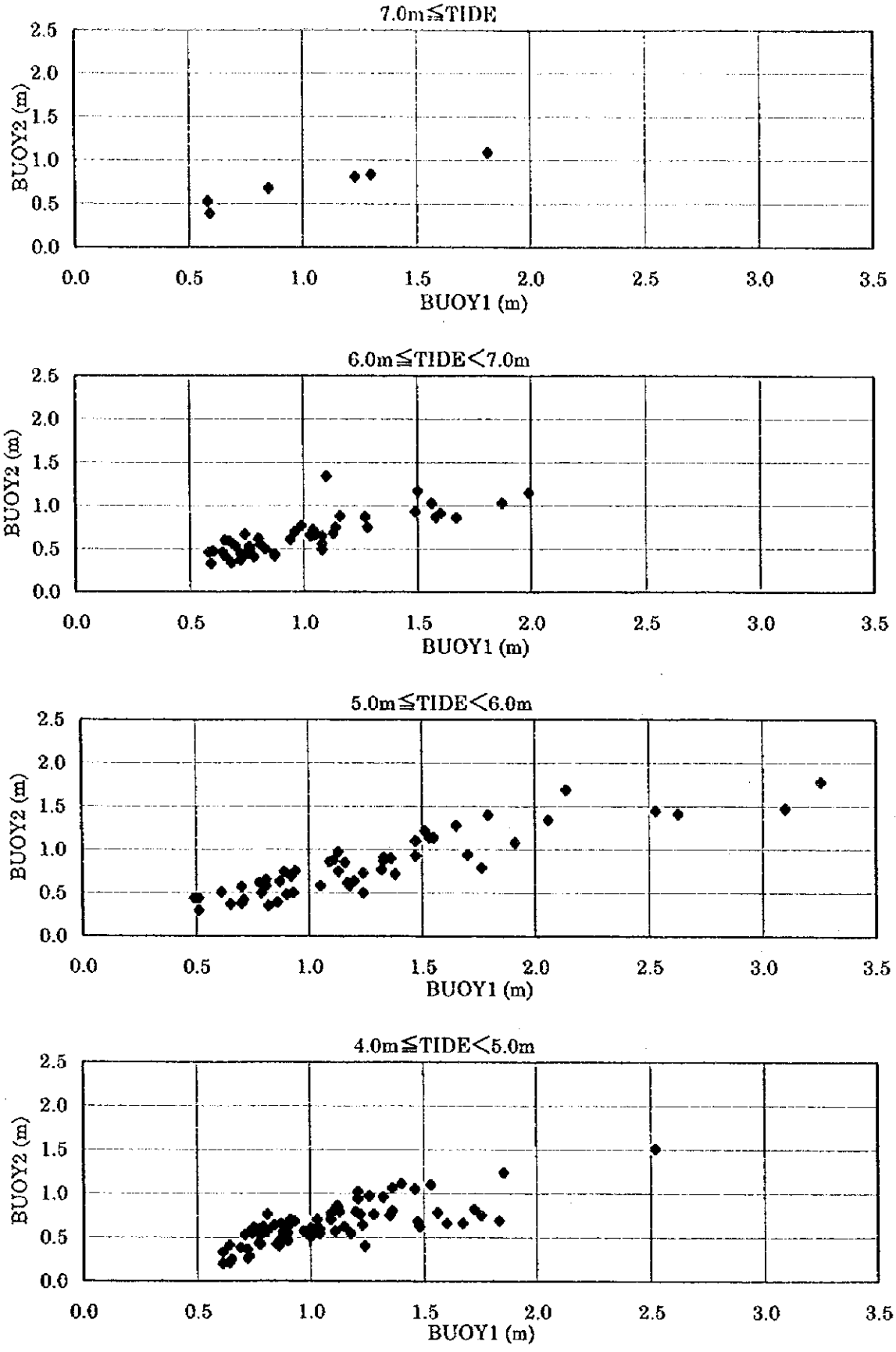

Figure 3.3.5-4 Wave Occurrence by Height and Tide in Wet Season(1)

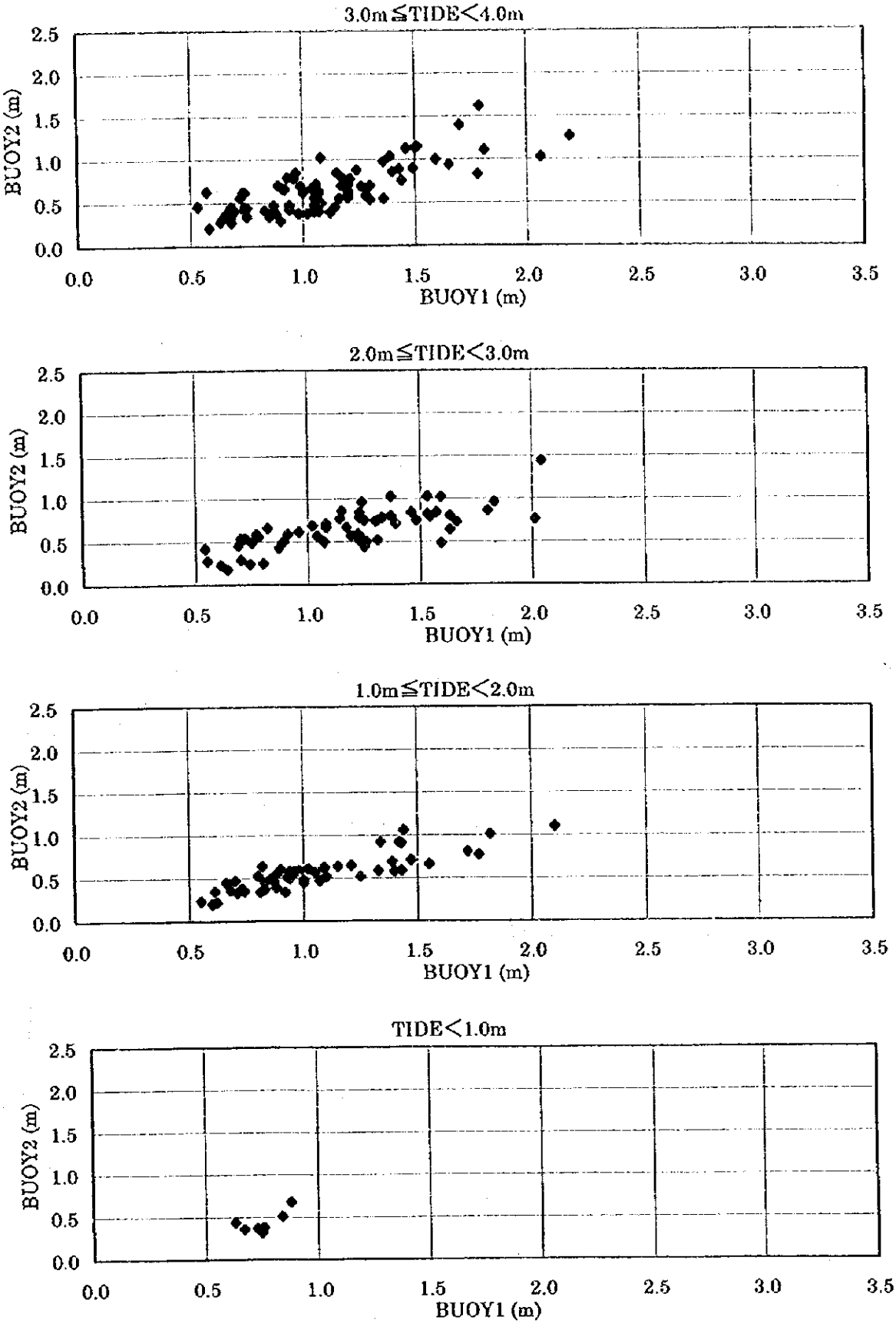

Figure 3.3.5-5 Wave Occurrence by Height and Tide in Wet Season(2)

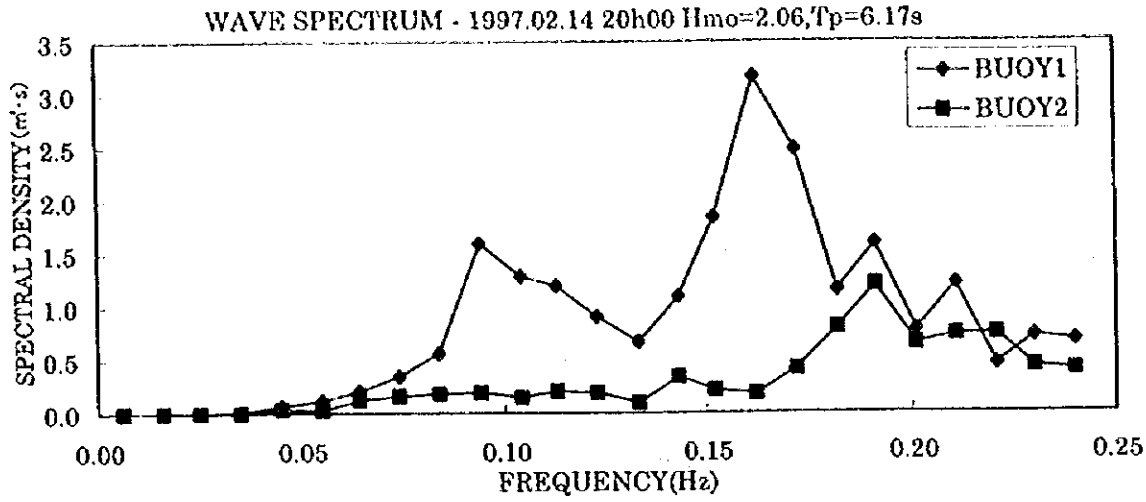

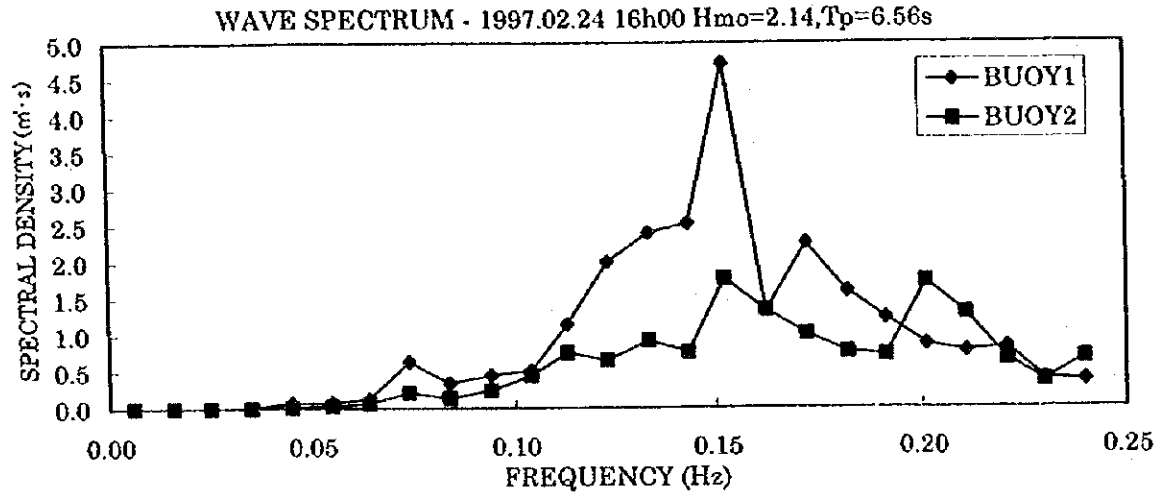

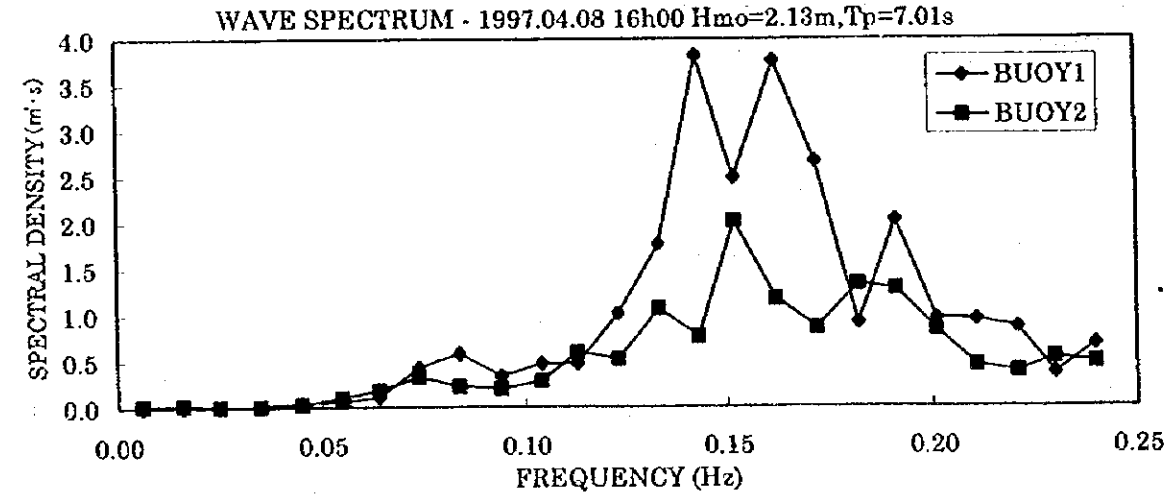

Figure 3.3.5-6 Wave Spectrum in Wet Season(1)

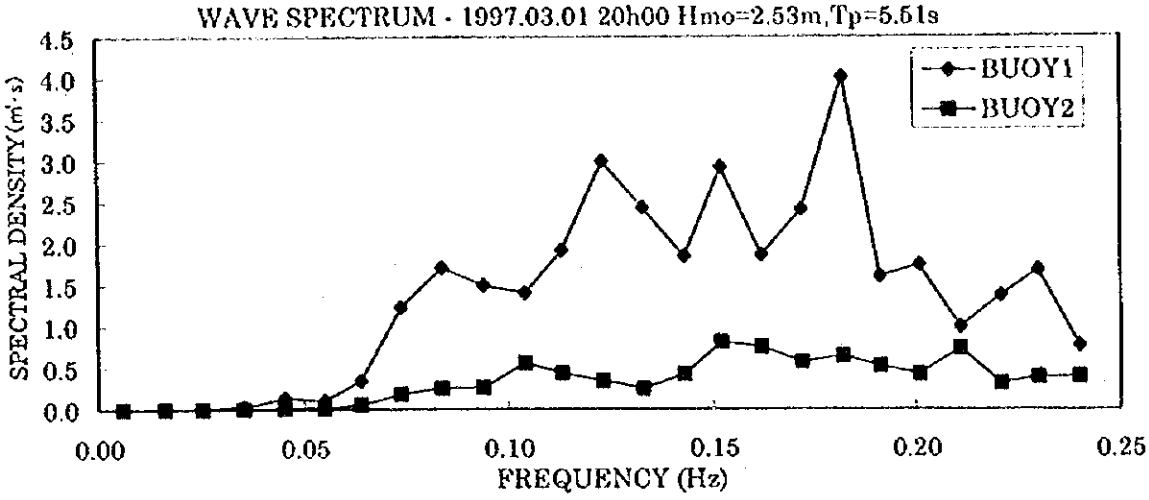

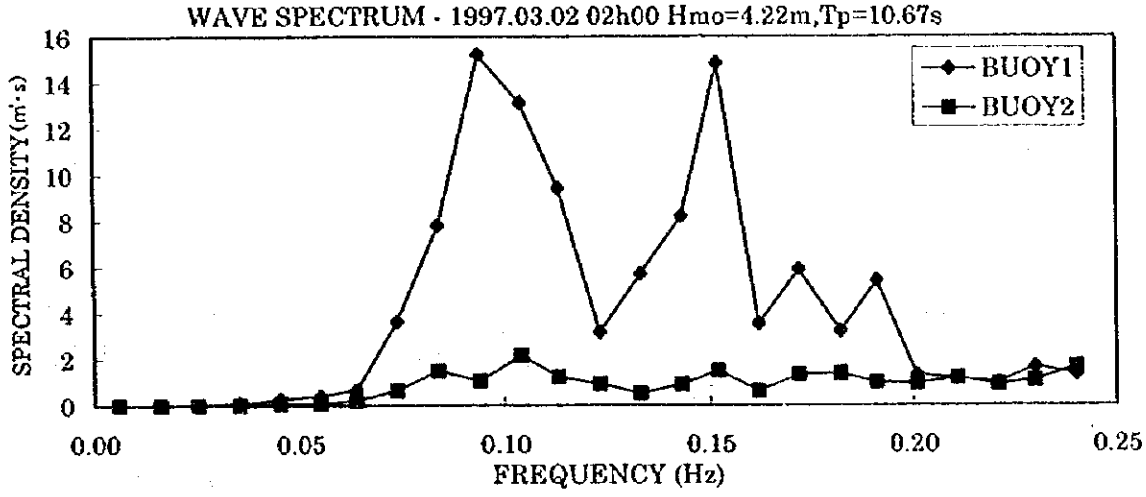

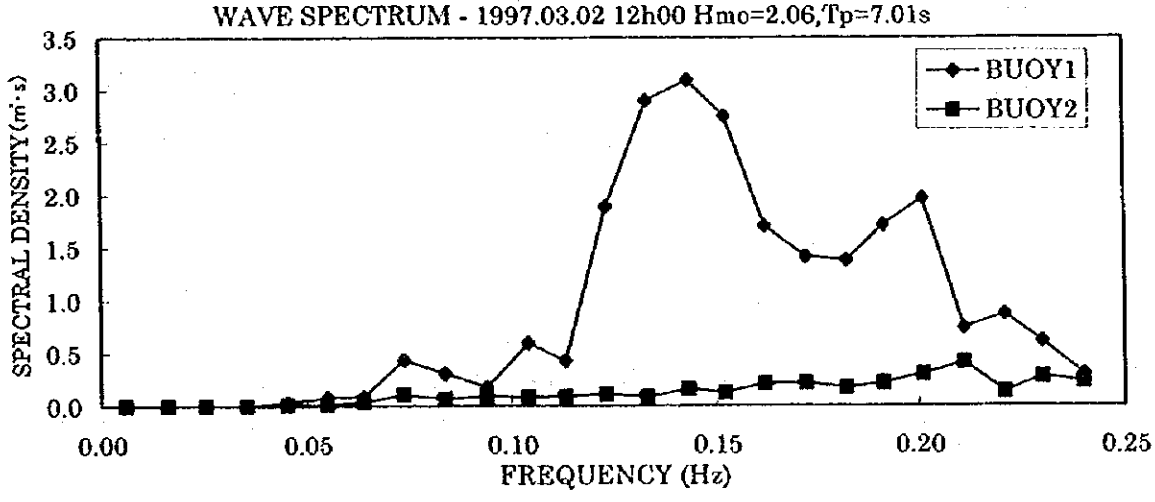

Figure 3.3.5-7 Wave Spectrum in Wet Season(2)

While, wave periods of 5.0 to 10.0 seconds are predominant at the both buoys except during stormy periods. These results can be considered as reflecting the location of each buoy. Buoy 1 has been installed at the offshore, whereas Buoy 2 is located near the coast.

Additionally, during the period of wave measurement, south eastern waves were predominant. Only in the first two weeks of March, eastern or east-north-eastern waves were frequently observed when cyclone "Lisette" affected at Sofala Province.

3.3.6 Current Measurement

Siltation of the Access Channel and the basin is caused by the interaction between wave and current. Therefore, the study team carried out the current observation and float tracking at spring and neap tides in both wet and dry seasons.

(1) Methodology

1) Current Measurement

After anchoring at each observation station, a survey of current velocity and direction was carried out at upper layer (-0.5 m below sea level), middle layer (half of sea depth) and bottom layer (+1.0 m above seabed) at flood and ebb tides during the period of spring and neap tides. At that time the sinker against strong current was attached on the current meter in order to hang down as vertically as possible.

2) Float Tracking

After dropping a drifting float at each observation point, a tracing of the position of the drifting float using the portable GPS was carried out every five minutes.

(2) Results of Field Survey

The results of current observation in the dry season are shown in Figures 3.3.6-1 to 3.3.6-6. Also the results of float tracking at station No.1 are shown in Figures 3.3.6-7 and 3.3.6-8. All figures of float tracking are presented in Appendix A-2.

The results of the analysis of these surveys are briefly described below.

1) Predominant Current in Upper Layer at Spring Tide

Predominant currents in upper layer are shown in Fig.3.3.6-1. Generally, current patterns during the spring tide reflected the change of tide level clearly.

The current patterns of the upper, middle and bottom layers at each station have similar trend. Especially from stations No. 7 to 13, which are situated off shore, the tendency is very clear. The current velocity of each station is of clear tendency that velocity is stronger from bottom to surface. At all the stations, the changing period from ebb current to flood current through the slack water is very short.

At the stations No. 1, 2, 3, 5, 6, 7 and 8, the north-northwesterly current is predominant during flood tide and the south-southwesterly current is predominant during ebb tide. At station No. 4, the northwesterly current at flood tide and the easterly current at ebb tide prevail along the coastal line.

At the stations No.10, 11, 12 and 13, which are situated in the east from the bending point, the westerly current is predominant at flood tide and the easterly current is predominant at ebb tide. These results show that the most of currents flow along the Access Channel

On the other hand, at station No.9 which is situated close to the bending point, the west-northwesterly current is predominant at flood tide and the south-southeasterly current is predominant at ebb tide. It seems that the flow regimes around No.9 are influenced by the sand bar which is located near and in the north of the Access Channel.

The strongest current was recorded at both flood and ebb tides at station No. 2. They were 2.50 m/sec northerly current at flood tide and 2.3 m/sec of south-southeasterly current at ebb tide.

The difference of current pattern in the wet and dry seasons is not clear. But it is clear that tidal flows in the vicinity of Beira play a dominant role in generating strong oscillation current along the Access Channel through all seasons.

2) Predominant Current at Upper Layer at Neap Tide

Predominant currents in the upper layer are shown in Figure 3.3.6-2. In general, the current pattern during the neap tide does not reflect the tide

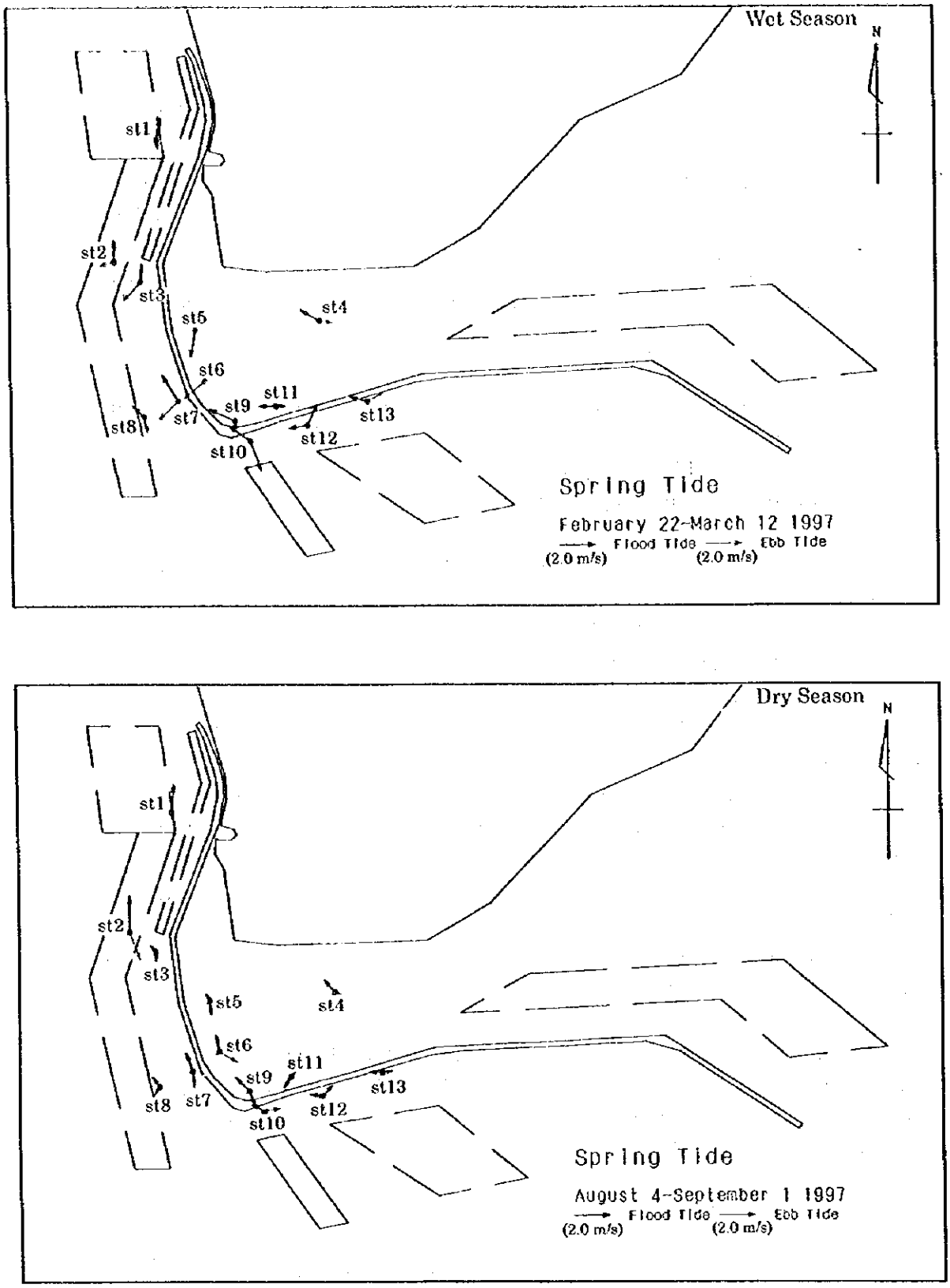

Figure 3.3.6-1 Strongest Current at Upper Layer on Spring Tide

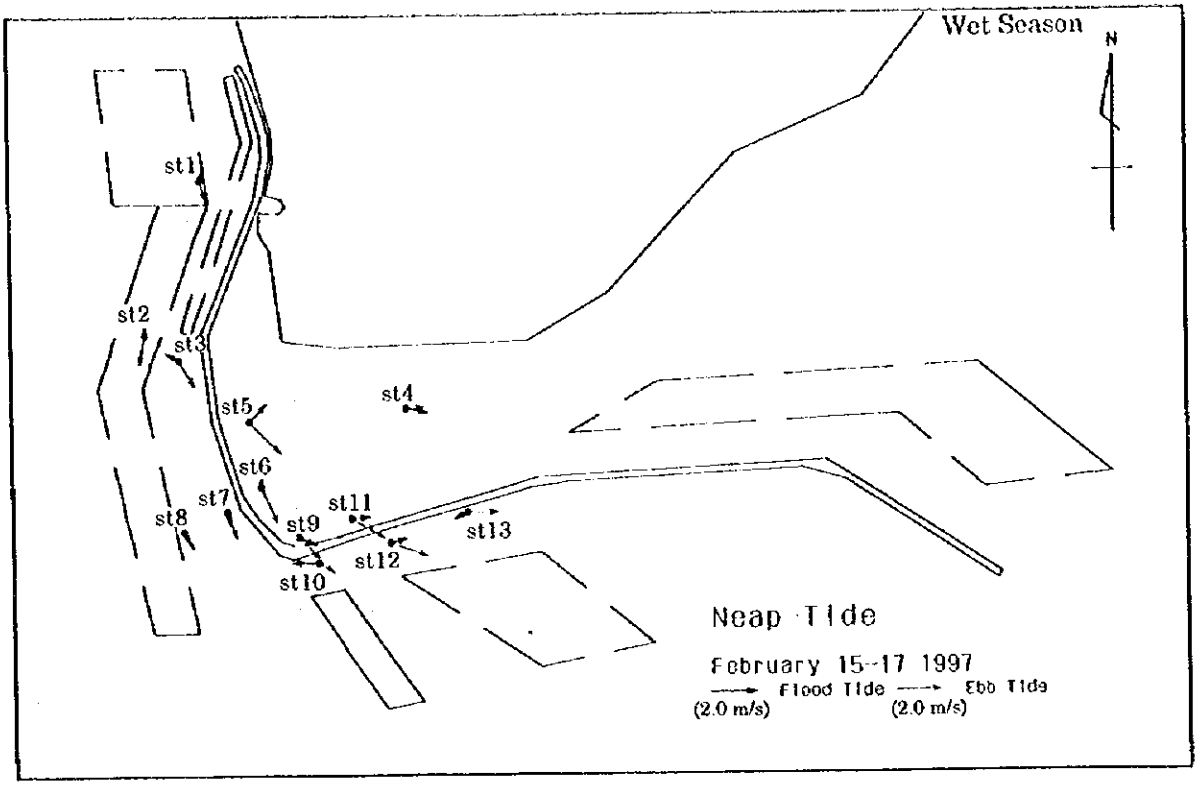

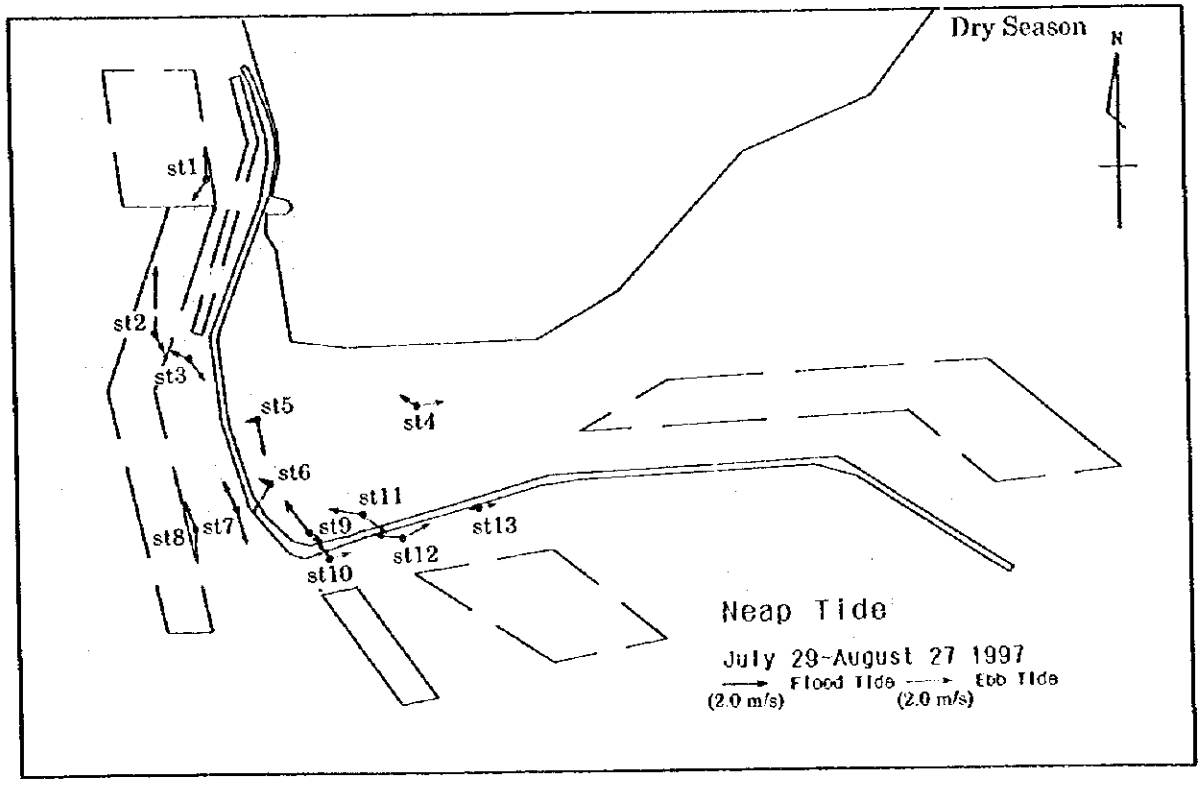

Figure 3.3.6-2 Strongest Current at Upper Layer on Neap Tide

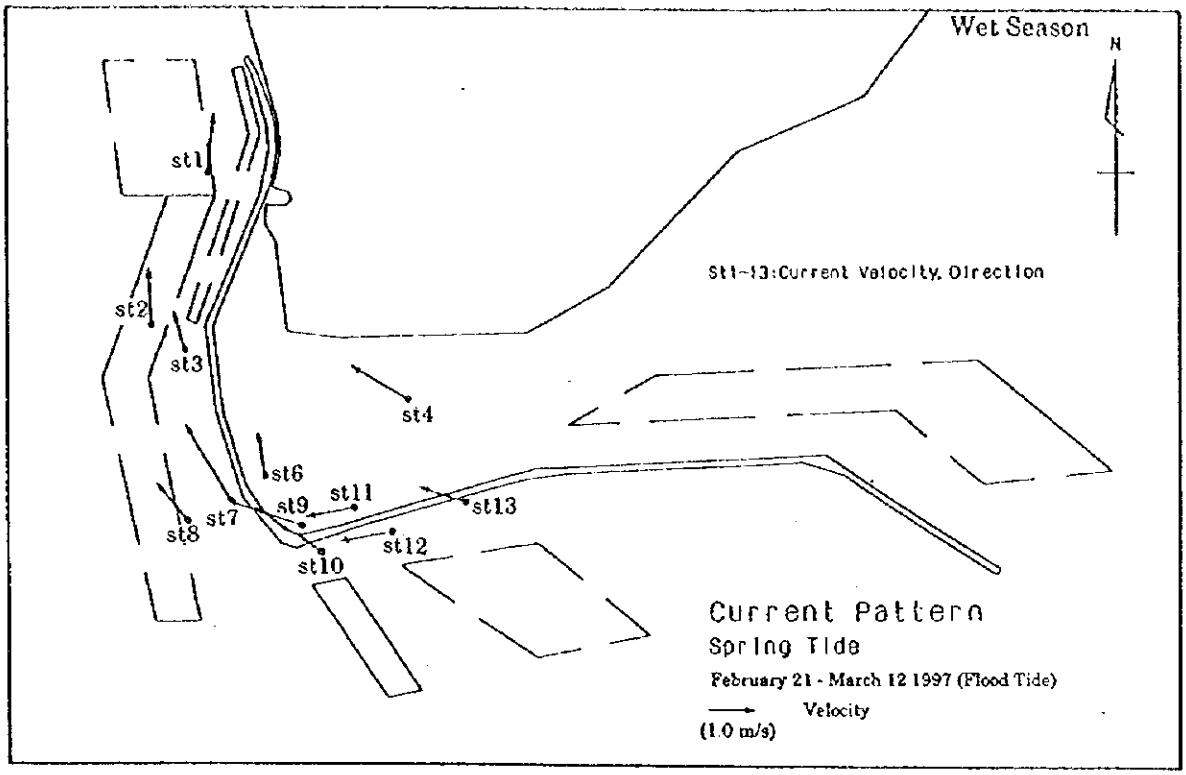

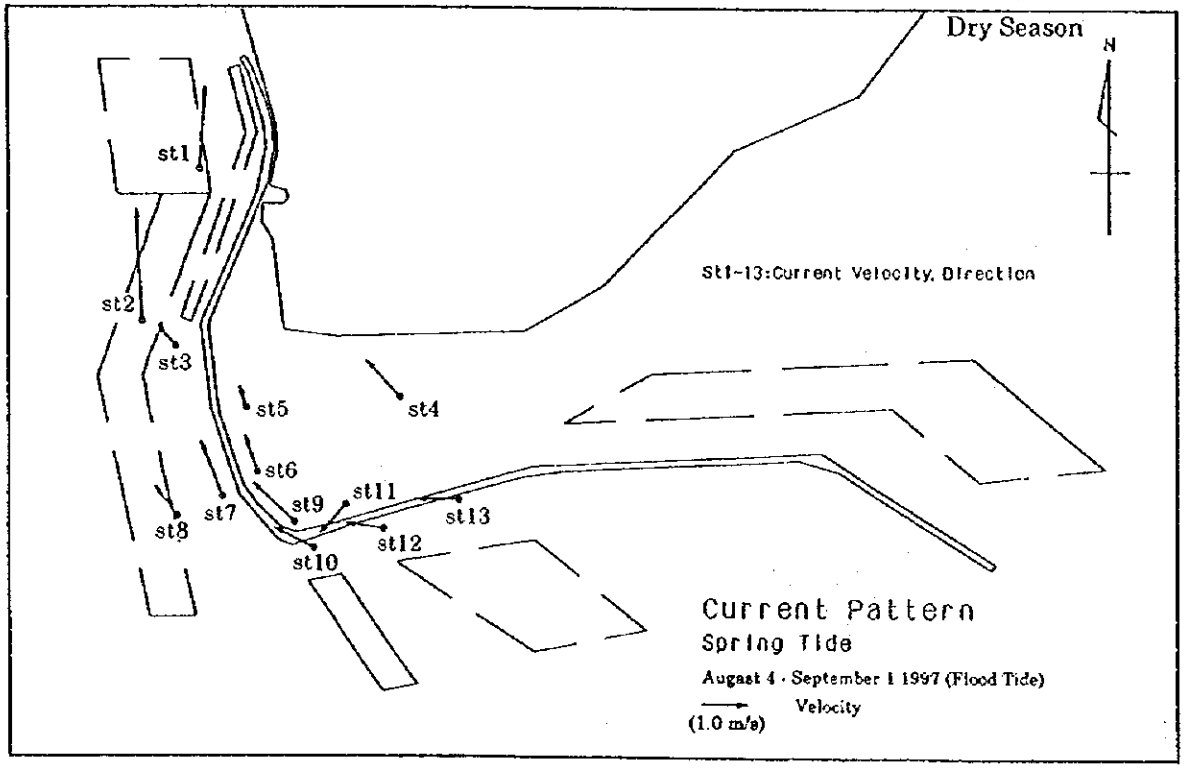

Figure 3.3.6-3 Current Pattern of Flood Tide on Spring Tide

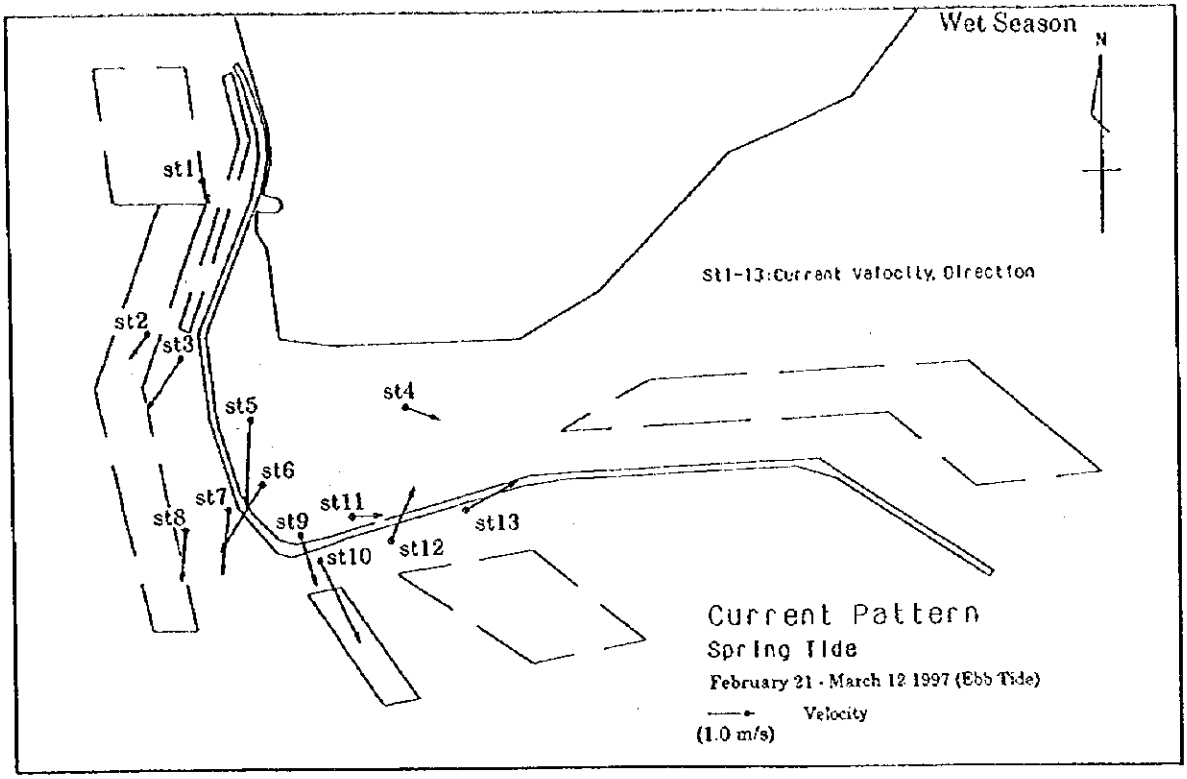

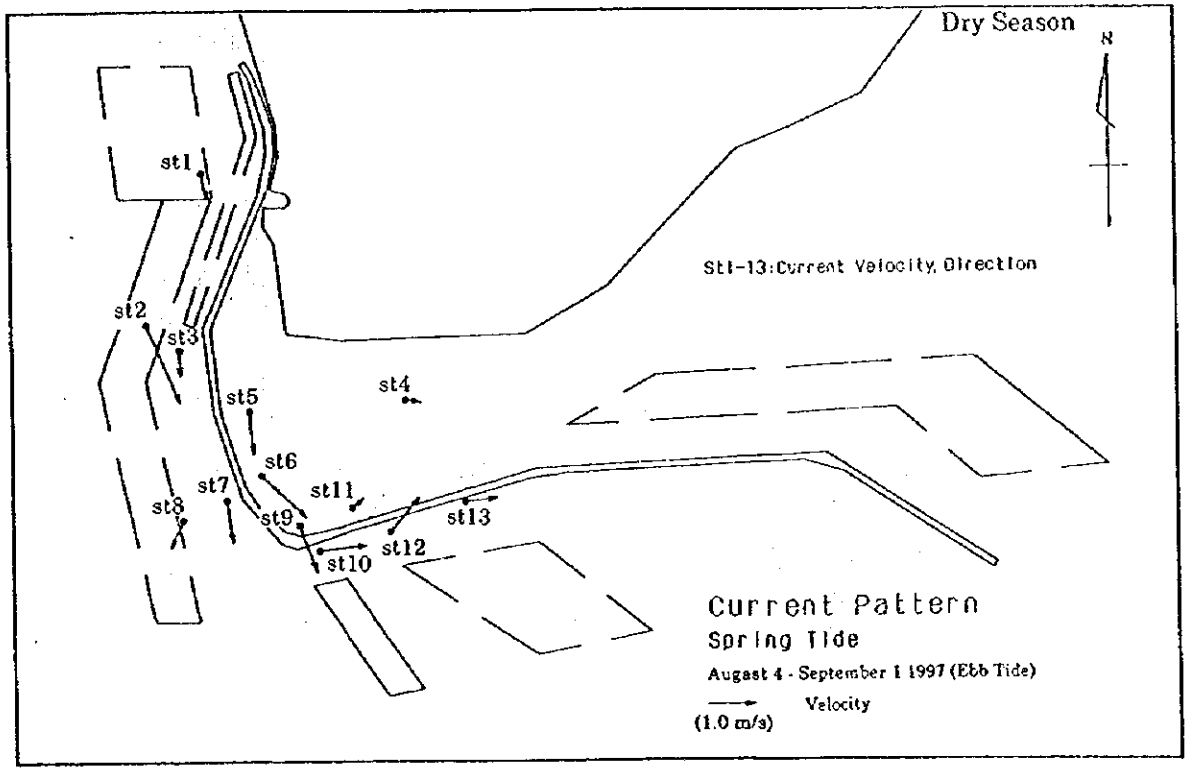

Figure 3.3.6-4 Current Pattern of Ebb Tide on Spring Tide

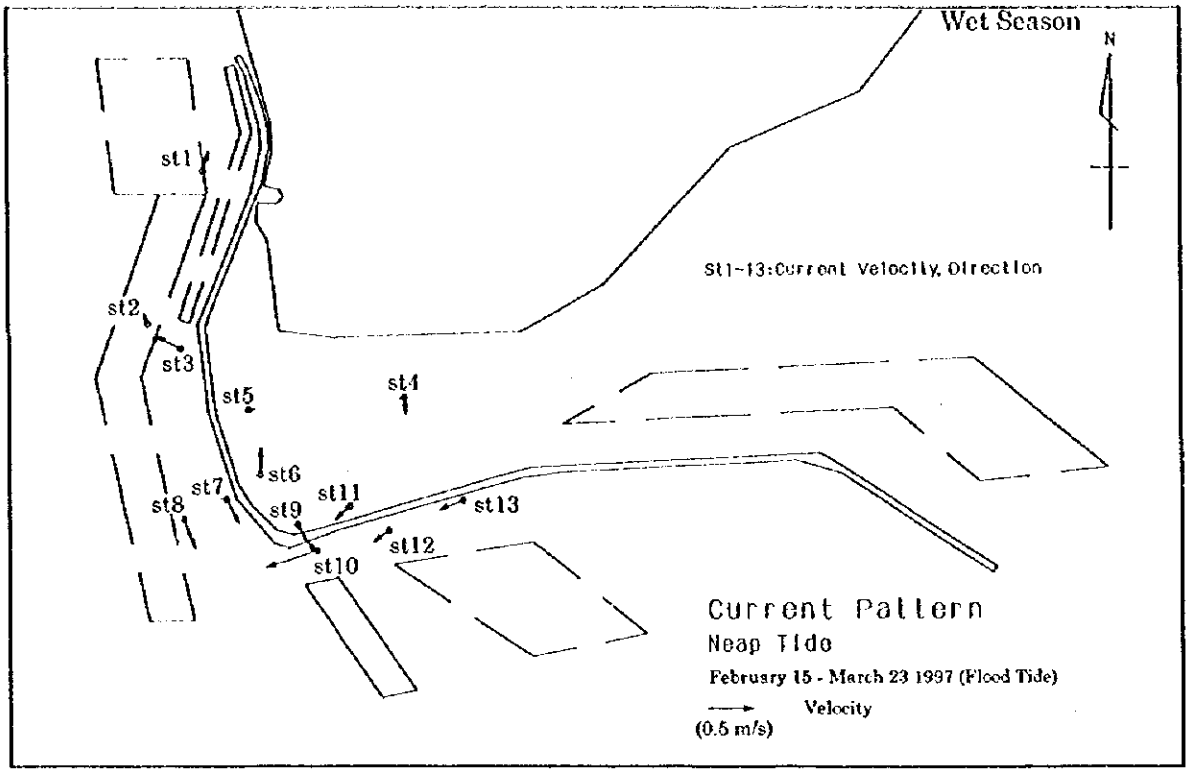

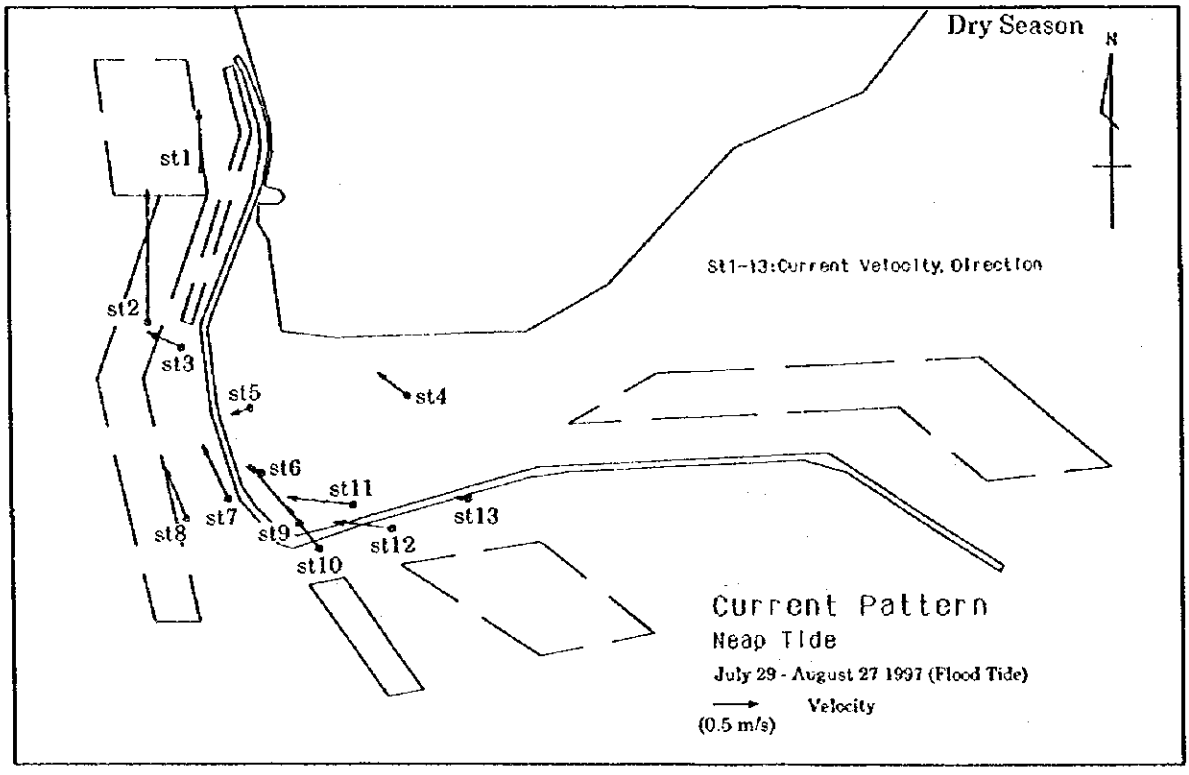

Figure 3.3.6-5 Current Pattern of Flood Tide on Neap Tide

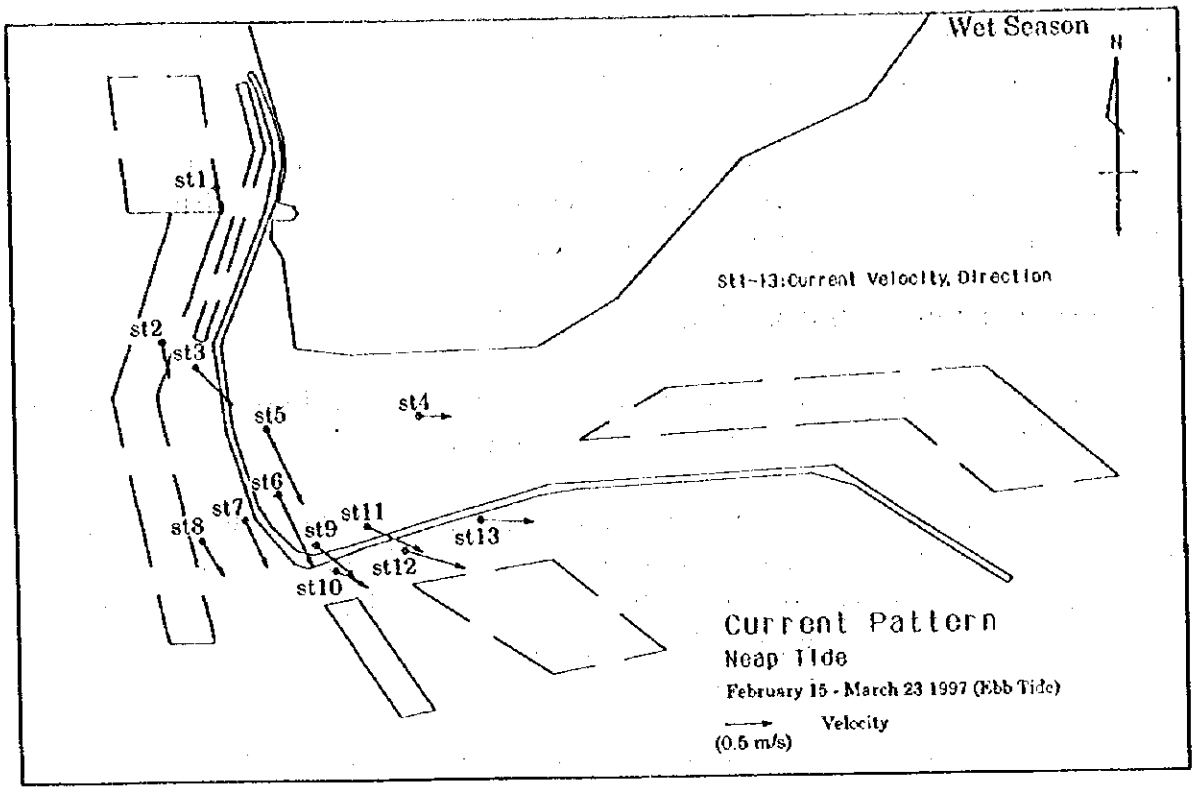

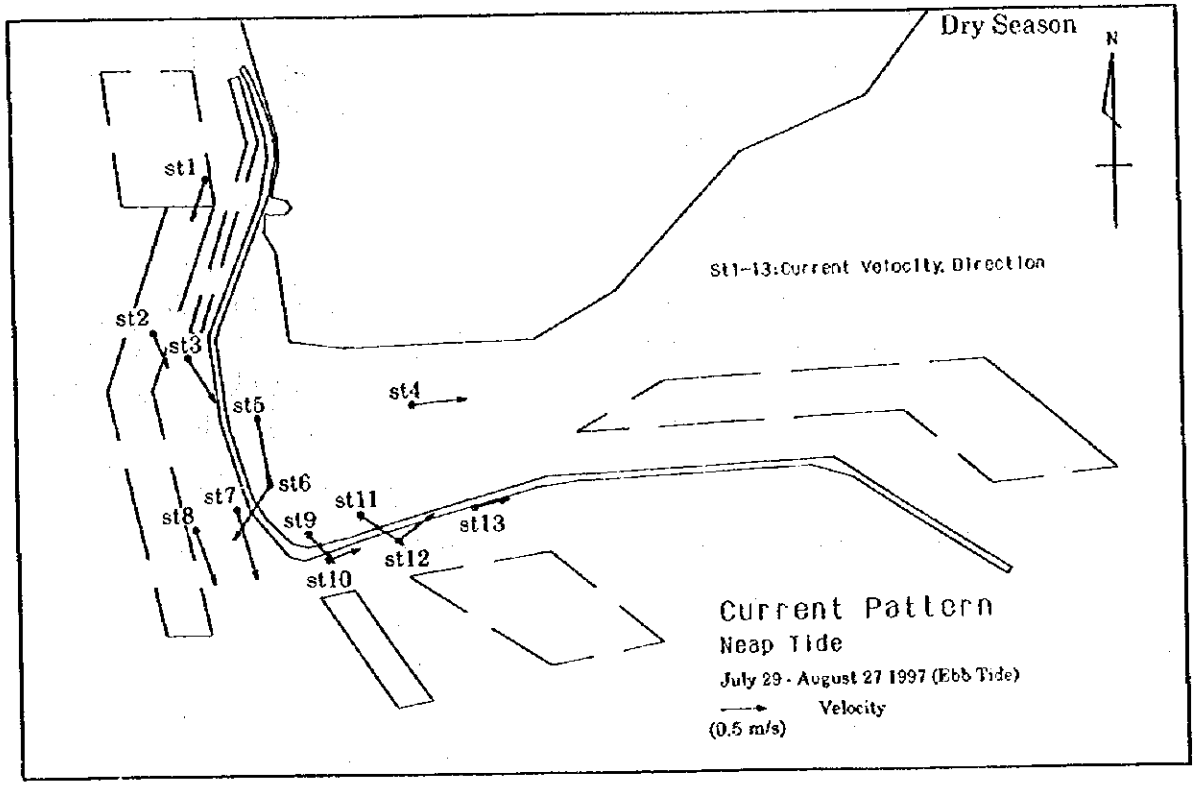

Figure 3.3.6-6 Current Pattern of Ebb Tide on Neap Tide

condition. The current directions at each station at both flood and ebb tides show a pattern which flow in to or along the channel.

The strongest current was recorded at station No.2 which is the northerly current with 1.45 m/sec at flood tide. Also at station No.5, the southerly current flows with 1.45 m/sec at ebb tide was recorded.

3) Float Tracking at Spring Tide

The representative currents in the upper layer at station No. Stf 1 by the float tracking in the dry season are shown in Figure 3.3.6-7.

At all the survey stations, the current patterns show that the similar oscillation current flow between easterly and westerly during the ebb tide until the slack water at the beginning of flood tide. After that, the swift flood water carries the float to the mouth of the Pungue river. The strongest current at each stations at flood and ebb tides are shown in the table below.

Table 3.3.6-1 Float Tracking Result at Spring Tide in Dry Season

Station	Velocity(F)*	Direction	Velocity(E)*	Direction
Stf 1	1.46m/sec	West	1.27m/sec	East
Stf 2	2.05m/sec	North	0.99m/sec	Northeast
Stf 3	1.85m/sec	North	1.41m/sec	Northeast

*(F)flood tide (E)ebb tide

4) Float Tracking at Neap Tide

The representative currents in the upper layer obtained at station No. Stf 1 by float tracking are shown in Figure 3.3.6-8. There is clear contrast between weak current to the west during flood tide and strong current to the east during ebb tide. The strongest current at each station at flood and ebb tides is shown in the table below.

Table 3.3.6-2 Float Tracking Result at Neap Tide in Dry Season

Station	Velocity(F)*	Direction	Velocity(E)*	Direction
Stf 1	0.19m/sec	West	0.88m/sec	East
Stf 2	0.31m/sec	North-northwest	0.88m/sec	East
Stf 3	0.31m/sec	West	0.83m/sec	East-northeast

*(F)flood tide (E)ebb tide

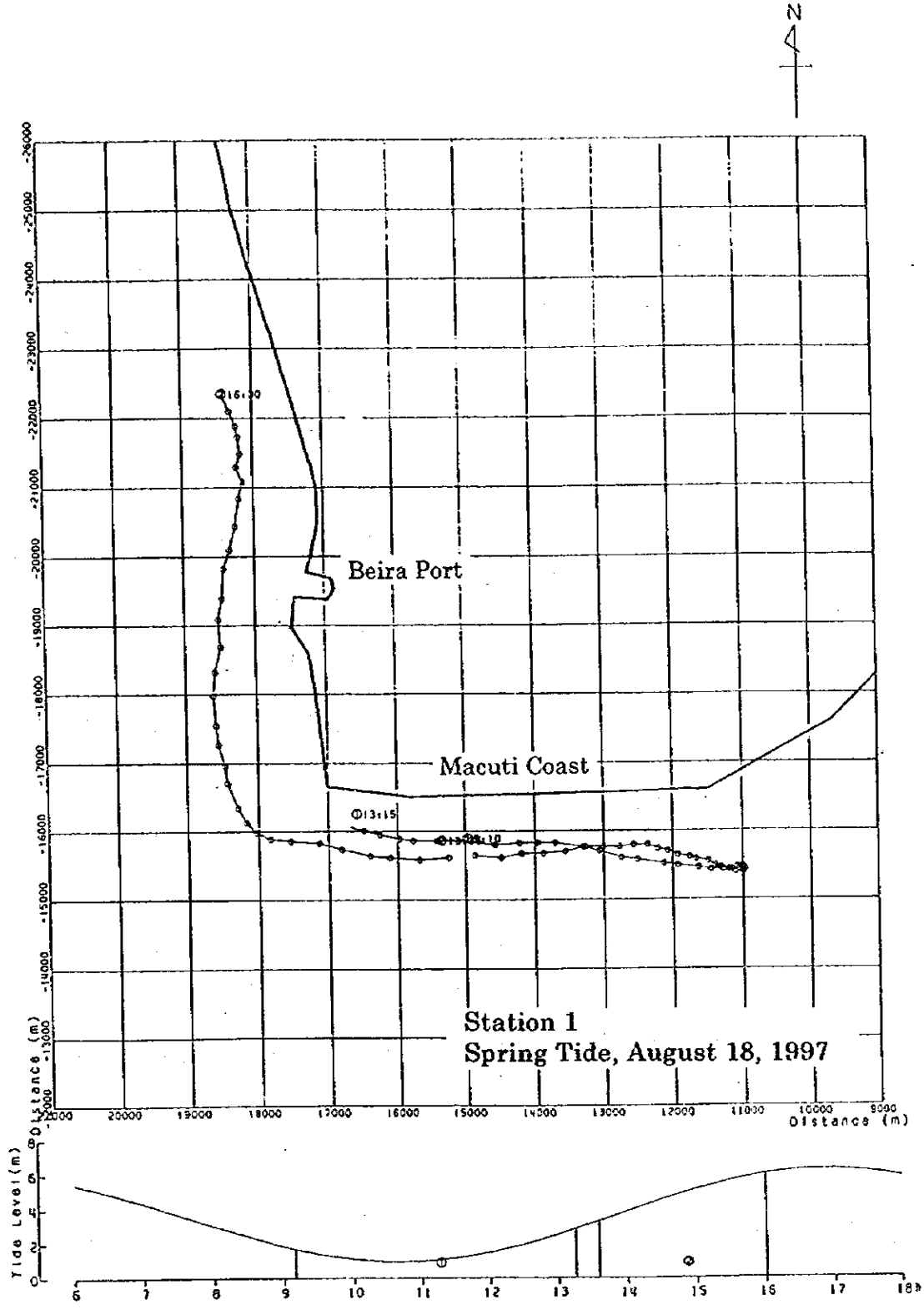

Figure 3.3.6-7 Float Tracking Result at Station 1 on Spring Tide in Dry Season

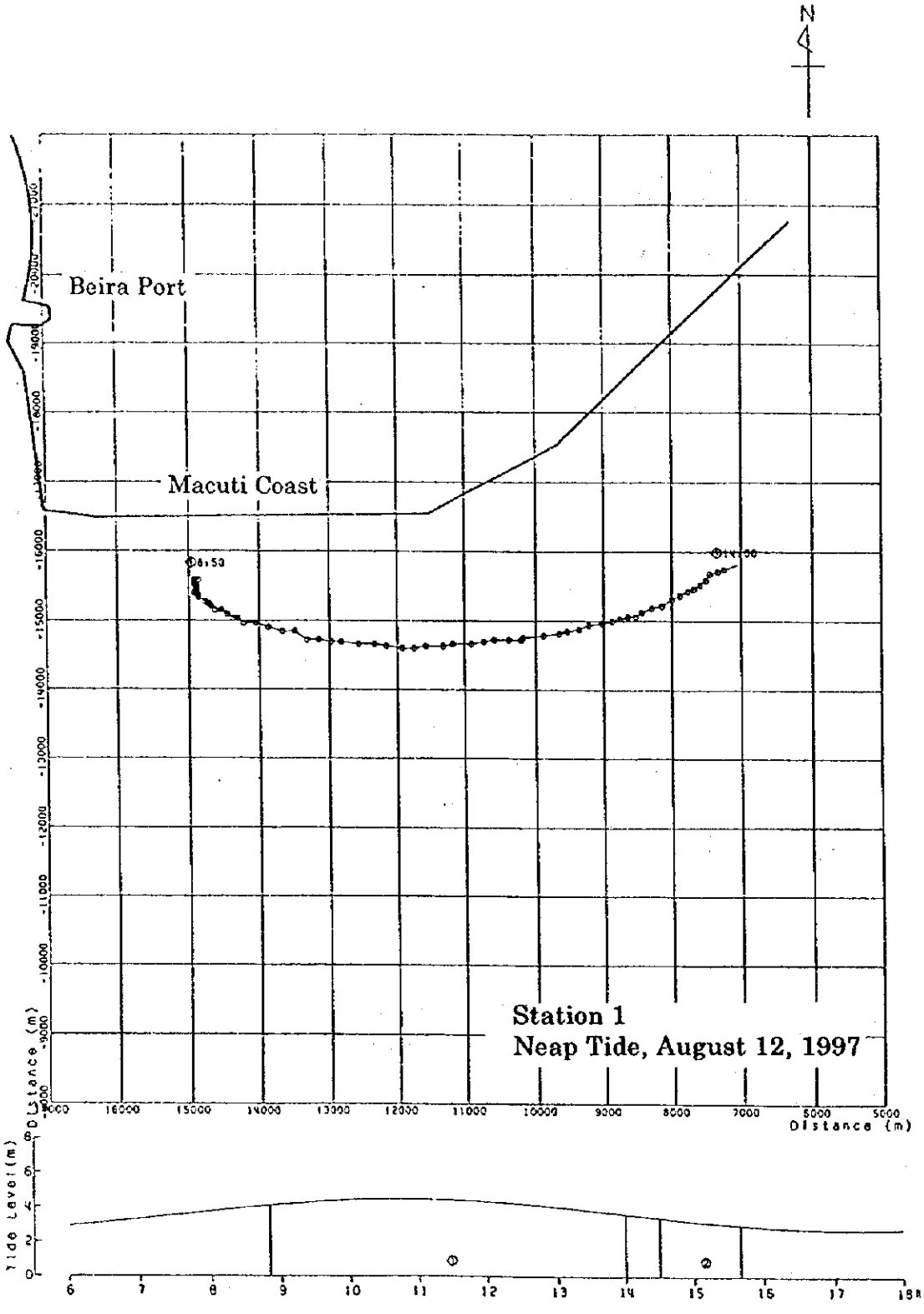

Figure 3.3.6-8 Float Tracking Result at Station 1 on Neap Tide in Dry Season

3.3.7 Turbidity Measurement

Observation of turbidity using a turbidity meter was carried out at the same stations as the current observation in the wet and dry seasons.

(1) Methodology

The turbidity measurement was carried out at the same layer and at the same time when the current observation survey was carried out.

(2) Results of Field Survey

The layout of each station for turbidity measurement is the same as current observation. The change of turbidity at No. 3, 9 and 13 the of the dry season are shown in Figures 3.3.7-1 to 3.3.7-3. All the results of turbidity measurements are presented in Appendix A-2. The results of these surveys are briefly described below.

1) Turbidity Measurements during Spring Tide

The maximum turbidity at flood and ebb tides and the slack water on each layer are described as follows:

The turbidity is influenced by the tide at the most of the stations. They show getting higher at all the layers of bottom, middle and upper when the tide changes from ebb tide to slack water. The turbidity during the flood tide is slightly smaller than the one during the ebb tide. As for the vertical change, the turbidity is higher from the surface to the bottom.

According to Table 3.3.7-1, the average maximum turbidity during the wet and dry seasons at spring and neap tides shows 7.1 times as high as that during the neap in the wet season and 8.5 times during the neap in the dry season. Therefore, it shows that the turbidity of the vicinity of Beira port is more affected by the spring tide than the ebb tide.

2) Turbidity Measurements during Neap Tide

It seems that the turbidity is not of close relation with tide oscillation because the reading of turbidity does not change clearly between flood and ebb tides. In the case of spring tide, for the vertical change, the turbidity is higher from the surface to the bottom.

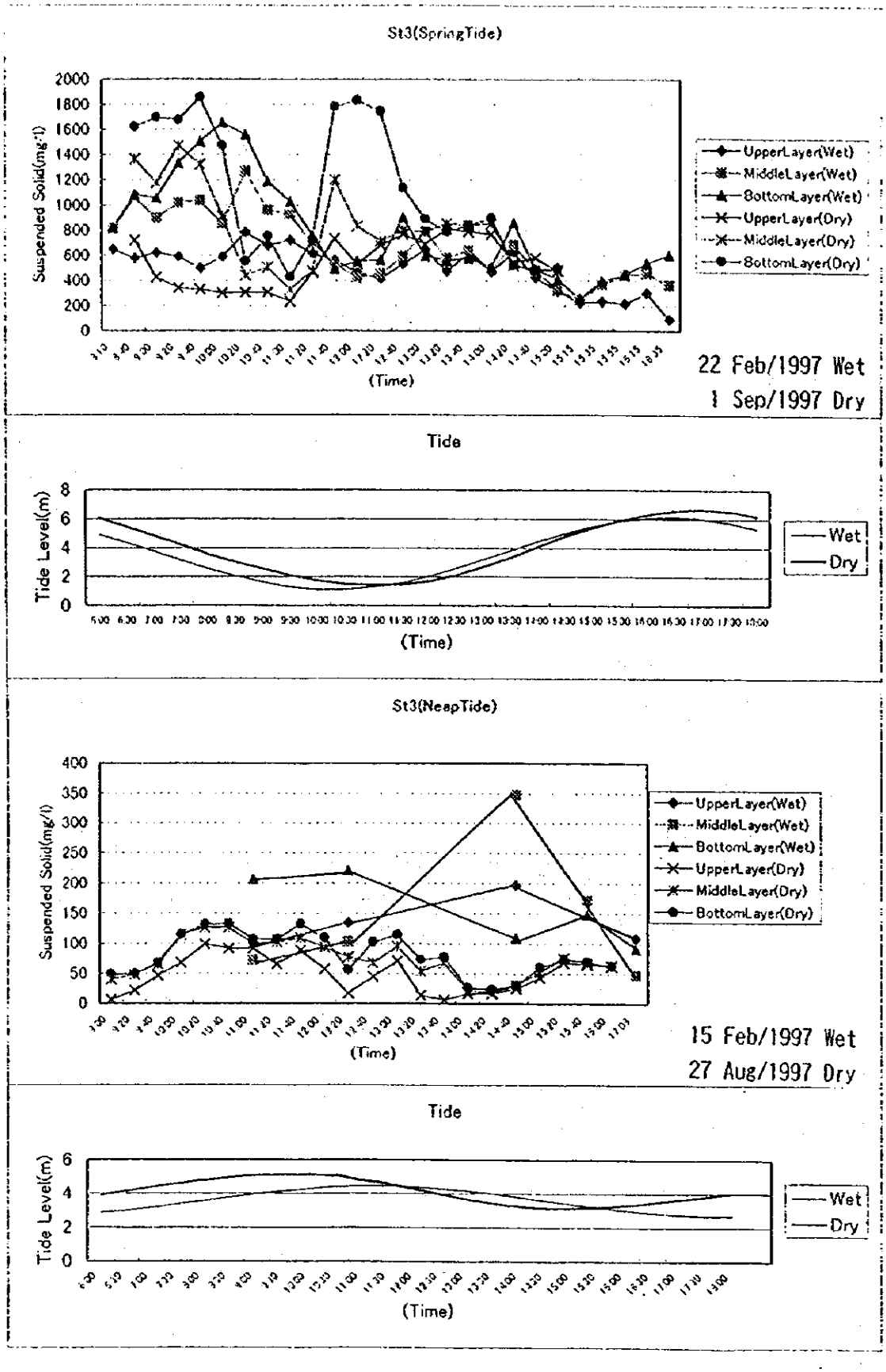

Figure 3.3.7-1 Turbidity at Ststion No.3

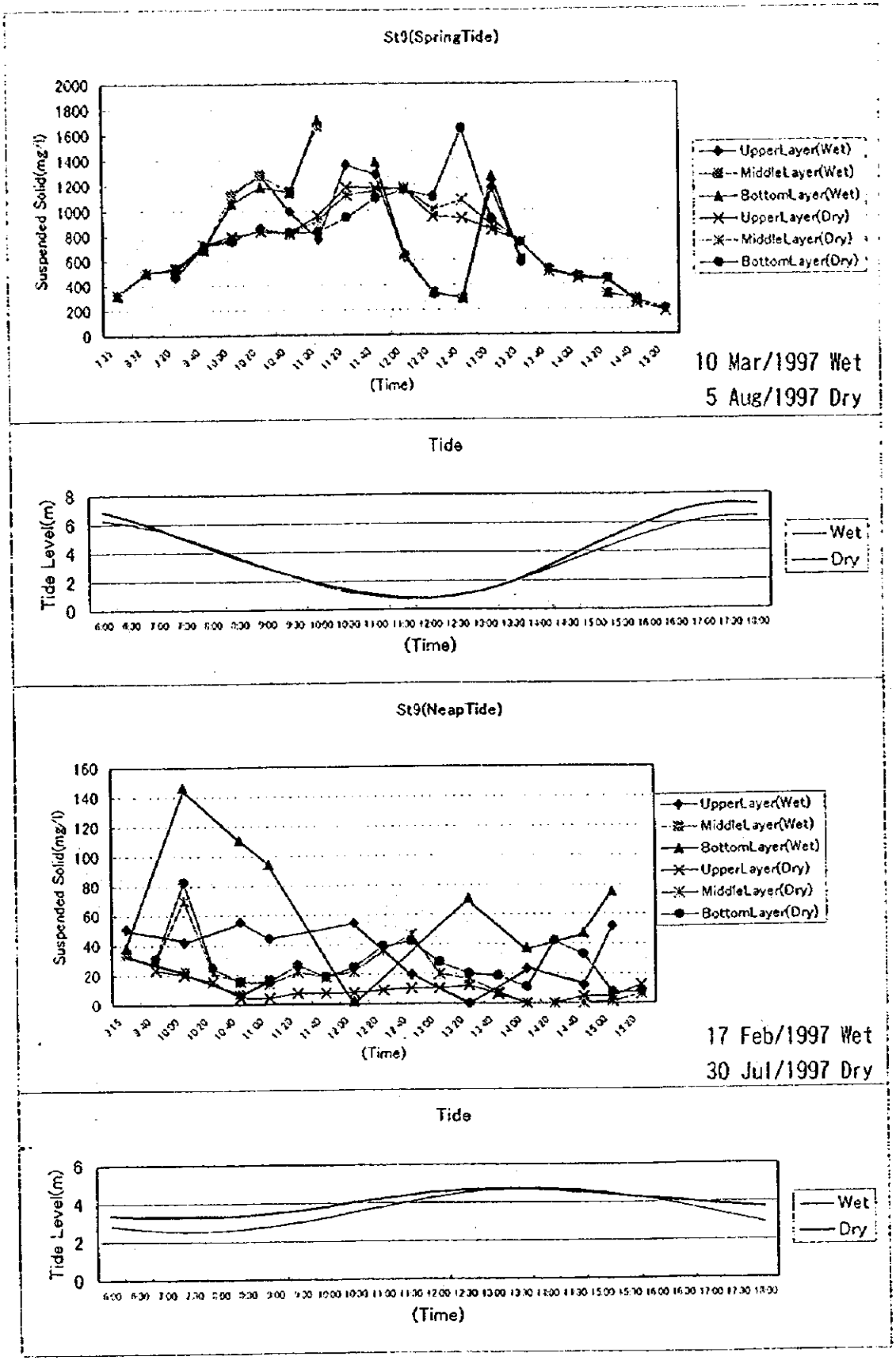

Figure 3.3.7-2 Turbidity at Ststion No.9

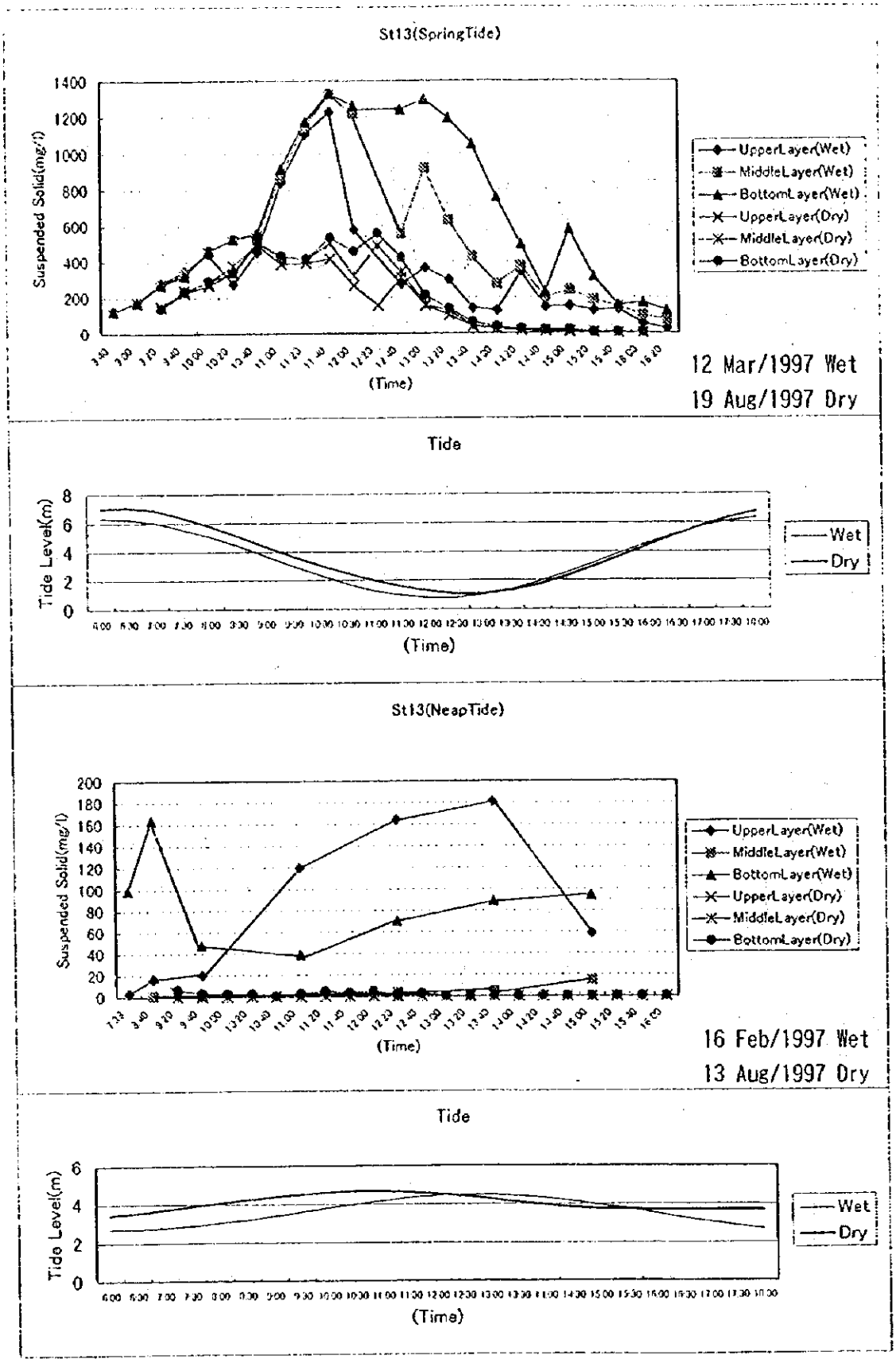

Figure 3.3.7-3 Turbidity at Ststion No.13

A comparison between the wet and dry seasons shows no clear indication except small deference between two seasons. It is slightly higher in the wet season than in the dry season, due to heavy rain fall in the up stream of the Pungue River in the wet season.

Table 3.3.7-1 Maximum Turbidities in Wet and Dry Seasons

Observation Station	Turbidity on Spring Tide (ppm)		Turbidity on Neap Tide (ppm)	
	Wet Season (maximum)	Dry Season (maximum)	Wet Season (maximum)	Dry Season (maximum)
1	1,020	1,719	225	84
2	1,250	1,726	230	105
3	1,512	1,692	335	142
4	764	739	190	80
5	1,665	1,651	305	336
6	1,443	1,220	332	561
7	1,624	1,132	65	73
8	1,420	802	103	166
9	1,523	1,089	154	96
10	1,220	1,247	90	74
11	1,284	1,158	278	173
12	1,382	669	202	146
13	1,220	524	185	28

*Turbidity at Nos.1 and 2 at Spring Tide in Dry Season was observed with Wave of 1.2m high.

3.4 Bottom Sediment Condition

In order to analyze bottom sediment conditions, seabed materials were sampled in Beira Port, the Access Channel and the offshore area in the wet and dry seasons.

3.4.1 Methodology

The Sampling of seabed materials was carried out to obtain the properties of silted material in the Access Channel and its surrounding area. The 33 sampling points of seabed materials are shown in Figure 3.4.1-1. Vessels Arrangement, Positioning System and Survey Equipment were prepared in the same manner as the sea condition survey.

Handy GPS and DGPS were used for positioning of each station. All the sediment samples were collected by using a small hand-operated Van-Veen grab sampler. The samples were put in 1-liter plastic bottles, sealed and labeled on-board. Before transporting to the laboratory in South Africa, the excess water

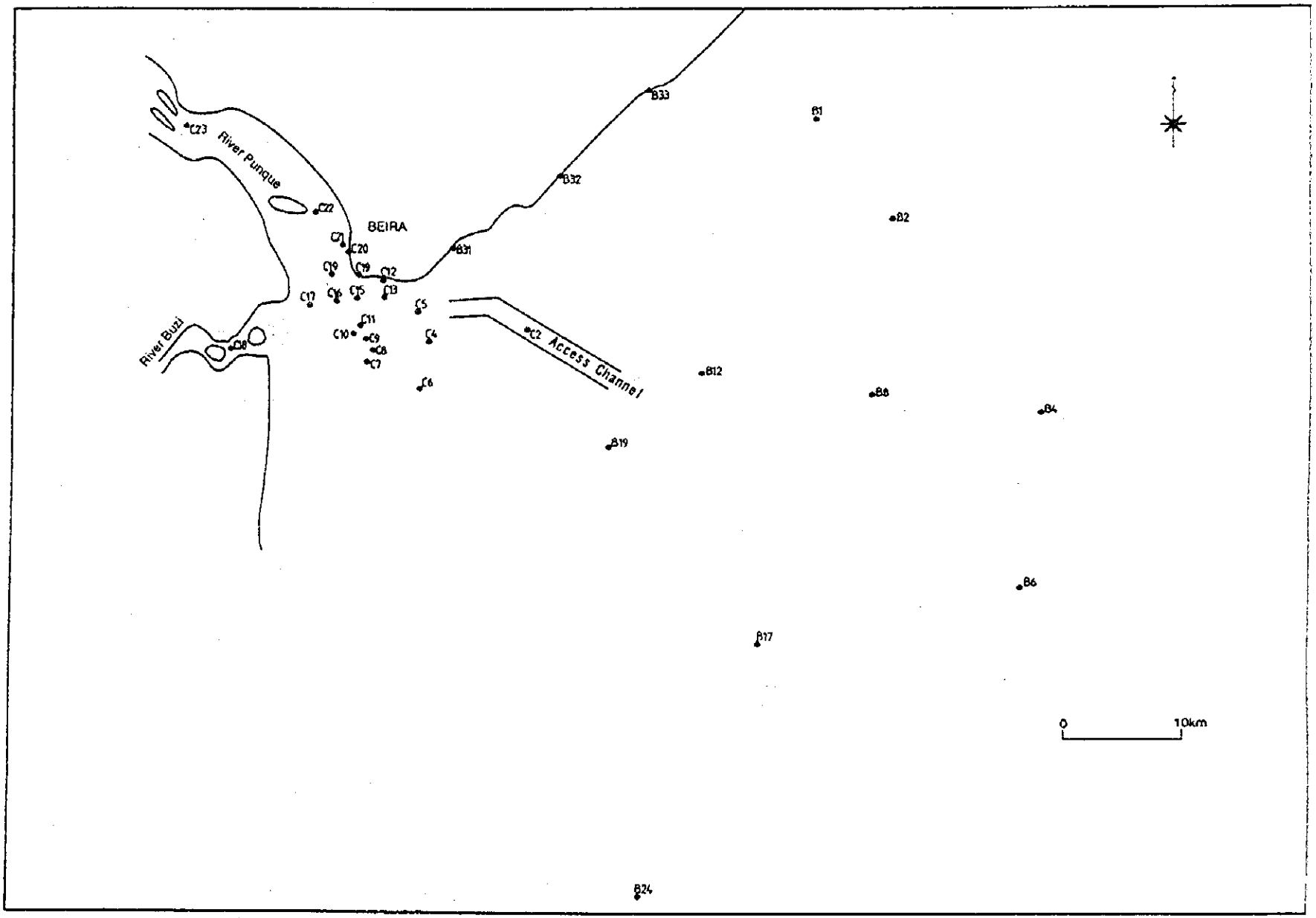

Figure 3.4.1-1 Location of Sampling Stations of Bottom Sediment

was drained from the bottles in order to reduce weight. All samples remained sealed until the start of the analysis in the laboratory. The soil mechanical analysis and the mineral component analyses were carried out at the laboratory.

3.4.2 Bottom Sediment Classification

The results of bottom sediment survey in the wet season are shown in Figures 3.4.2-1 and 3.4.2-2. The results of analysis for all samples in the wet season are presented in Table 3.4.2-1.

Concerning to the Access Channel, sand is predominant, but silt mainly exists at the south-east section in the port side of the bending corner and in the vicinity of Section E14 in the offshore. Coarse sand exists in the vicinity of the bending corner. While, in the offshore, fine sand is predominant, but silt exists more at the north side than at the south side of the Access Channel. As shown in Figure 3.4.2-2, the silty sand seabeds exist at the river and coastal area. On the other hand, the sandy seabeds predominantly exist at the Access Channel and the offshore area.

According to Table 3.4.2-1, the bulk density of sandy seabed is 1.6 to 1.9 g/cm^3 and silty seabed is 1.2 to 1.3 g/cm^3. The silty seabed which is more than 60 % in silt's ratio shows more than 4 of void ratio.

The results of sieve analysis for each sample along the Access Channel are shown in Figures 3.4.3-2 to 3.4.2-8.

All results of survey of bottom sediment, in dry season are presented in Appendix A-2. Seabed classification of those samples shows the same tendency mentioned above.

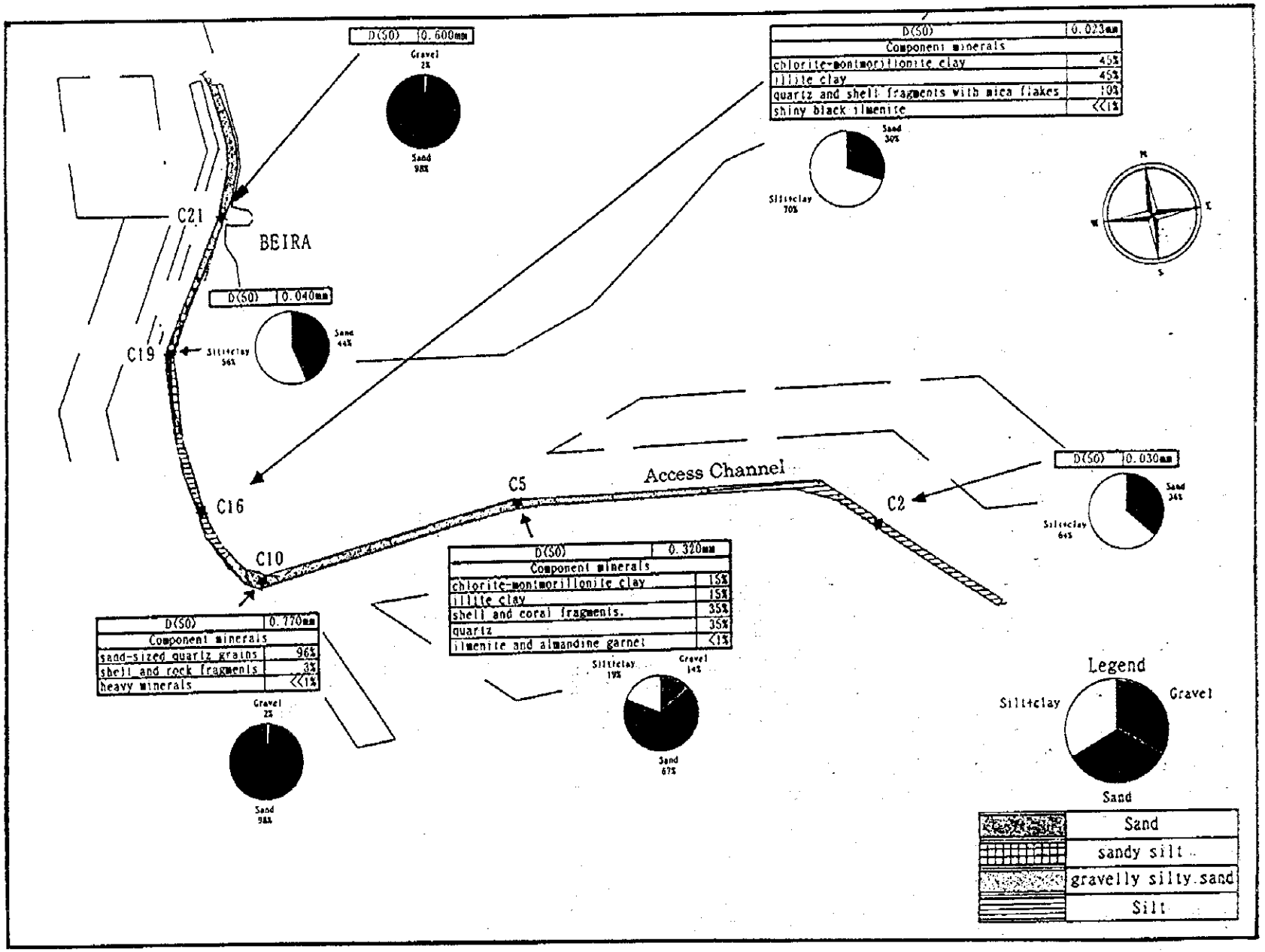

Figure 3.4.2-1 Bottom Sediment Classification along the Access Channel in Wet Season

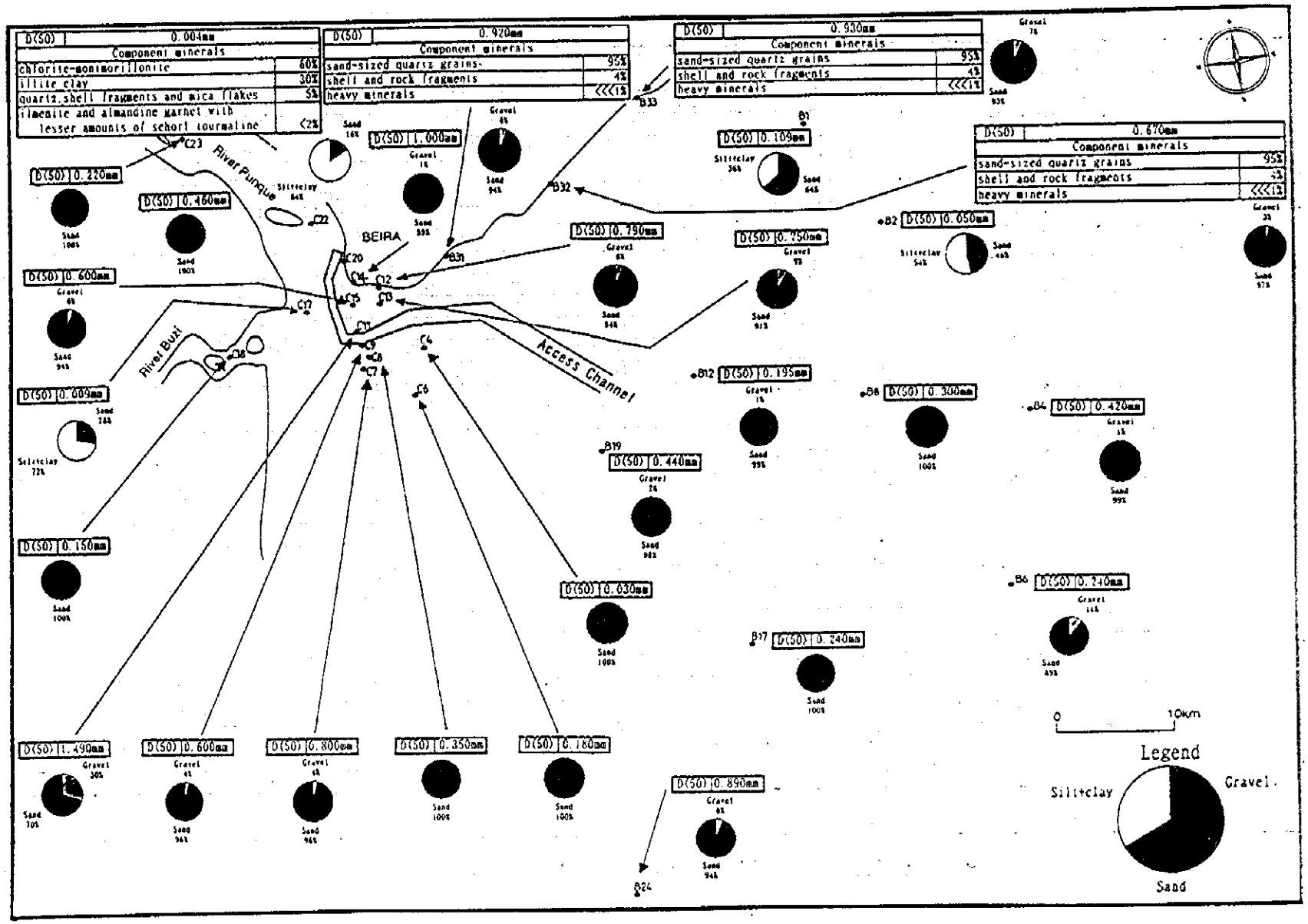

Figure 3.4.2-2 Bottom Sediment Classification at the Project Area in Wet Season

Table 3.4.2-1 Characteristics of Bottom Sediment in Wet Season

Sample No.	Gravel (%)	Sand (%)	Silt+clay (%)	Text. Class	D(50) (mm)	Moist. Cont.	Bulk Dens. (g/cm^3)	Dry dens. (g/cm^3)	Void ratio	S.G.	Component minerals
C2	0	36	63	sandy silt	0.030	197.7	1.270	0.431	5.08		
C4	0	100	0	Sand	0.420	16.9	1.901	1.626	0.63		
C5	14	67	19	gravelly silty sand	0.320	30.9	1.909	1.485	0.80	2.63	15%:chlorite-montmorillonite clay 15%:illite clay 35%:shell and coral fragments. 35%:quartz <1%:ilmenite and almandine garnet
C6	0	100	0	Sand	0.180	32.7	1.856	1.397	0.90		
C7	4	96	0	slightly gravelly sand	0.800	14.7	1.671	1.457	0.82		
C8	0	100	0	Sand	0.350	16.0	1.583	1.365	0.94		
C9	4	96	0	slightly gravelly sand	0.600	13.0	1.622	1.435	0.73		
C10	2	98	0	Sand	0.770	12.3	1.637	1.458	0.81	2.65	96%:sand-sized quartz grains 3%:shell and rock fragments <<1%:heavy minerals
C11	30	70	0	gravelly sand	1.490	9.8	1.686	1.536	0.73		
C12	6	94	0	slightly gravelly sand	0.790	10.9	1.585	1.429	0.85		
C13	9	91	0	slightly gravelly sand	0.750	13.4	1.719	1.516	0.75		
C14	1	99	0	Sand	1.000	5.5	1.531	1.451	0.83		
C15	6	94	0	slightly gravelly sand	0.600	16.9	1.741	1.489	0.78		
C16	0	33	77	sandy silt	0.023	179.0	1.282	0.458	4.72	2.61	45%:chlorite-montmorillonite clay 45%:illite clay 10%:quartz and shell fragments with mica flakes <<1%:shiny black ilmenite
C17	0	28	72	sandy silt	0.009	247.8	1.225	0.352	6.44		
C18	0	100	0	Sand	0.150	24.9	1.450	1.161	1.28		
C19	0	44	56	sandy silt	0.040	86.2	1.512	0.812	2.22		
C20	0	100	0	Sand	0.460	1.6	1.285	1.265	1.09		
C21	2	98	0	Sand	0.600	89.0	1.385	1.373	0.93		
C22	0	16	84	sandy silt	0.004	145.7	1.197	0.487	4.38	2.63	60%:chlorite-montmorillonite 30%:illite clay 5%:quartz, shell fragments and mica flakes <2%:ilmenite and almandine garnet with lesser amounts of schorl tourmaline
C23	0	100	0	Sand	0.220	31.4	1.871	1.424	1.86		
B1	0	64	36	silty sand	0.109	69.9	1.595	0.939	1.79		
B2	0	46	53	sandy silt	0.050	63.9	1.335	0.815	2.21		
B4	1	99	0	Sand	0.420	20.2	1.667	1.387	0.91		
B6	11	89	0	slightly gravelly sand	0.240	36.6	1.756	1.286	1.06		
B8	0	100	0	Sand	0.300	18.6	1.670	1.408	0.88		
B12	1	99	0	Sand	0.195	22.4	1.639	1.339	0.98		
B17	0	100	0	Sand	0.240	22.7	1.663	1.355	0.96		
B19	2	98	0	Sand	0.440	17.9	1.698	1.433	0.85		
B24	6	94	0	silty sand	0.890	18.4	1.629	1.376	0.93		Average 95%:sand-sized quartz grains Average 4%:shell and rock fragments <<<1%:heavy minerals
B31	6	94	0	silty sand	0.920	4.8	1.541	1.476	0.80	2.65	
B32	3	97	0	silty sand	0.670	12.0	1.641	1.465	0.81	2.65	
B33	7	93	0	silty sand	0.930	2.3	1.549	1.514	0.75	2.65	

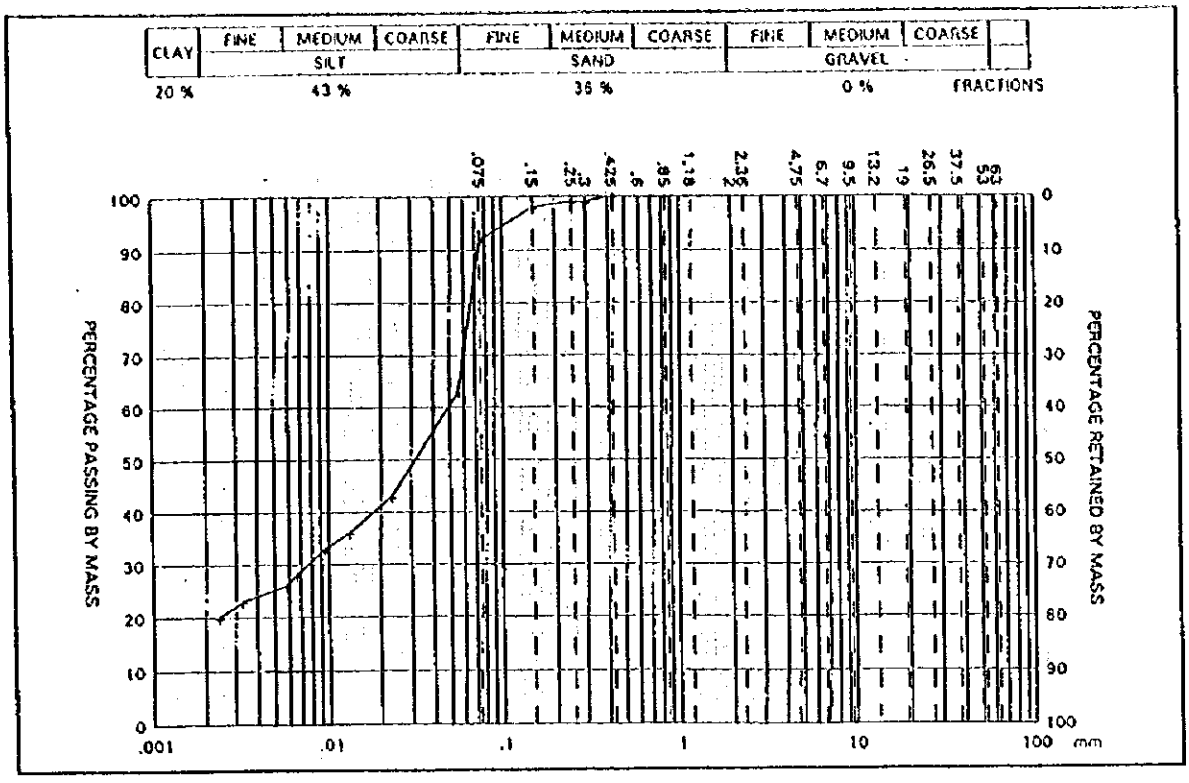

Figure 3.4.2-3 Grain-size Accumulation Curve of C2 in Wet Season

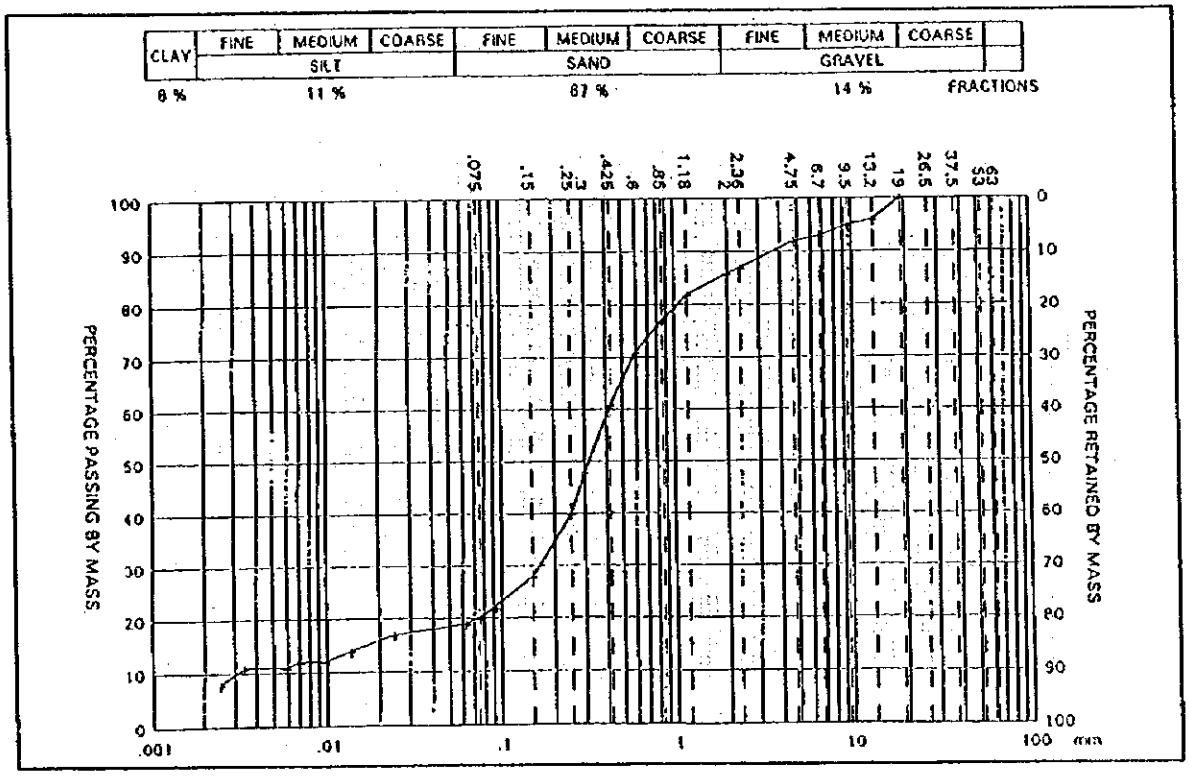

Figure 3.4.2-4 Grain-size Accumulation Curve of C5 in Wet Season

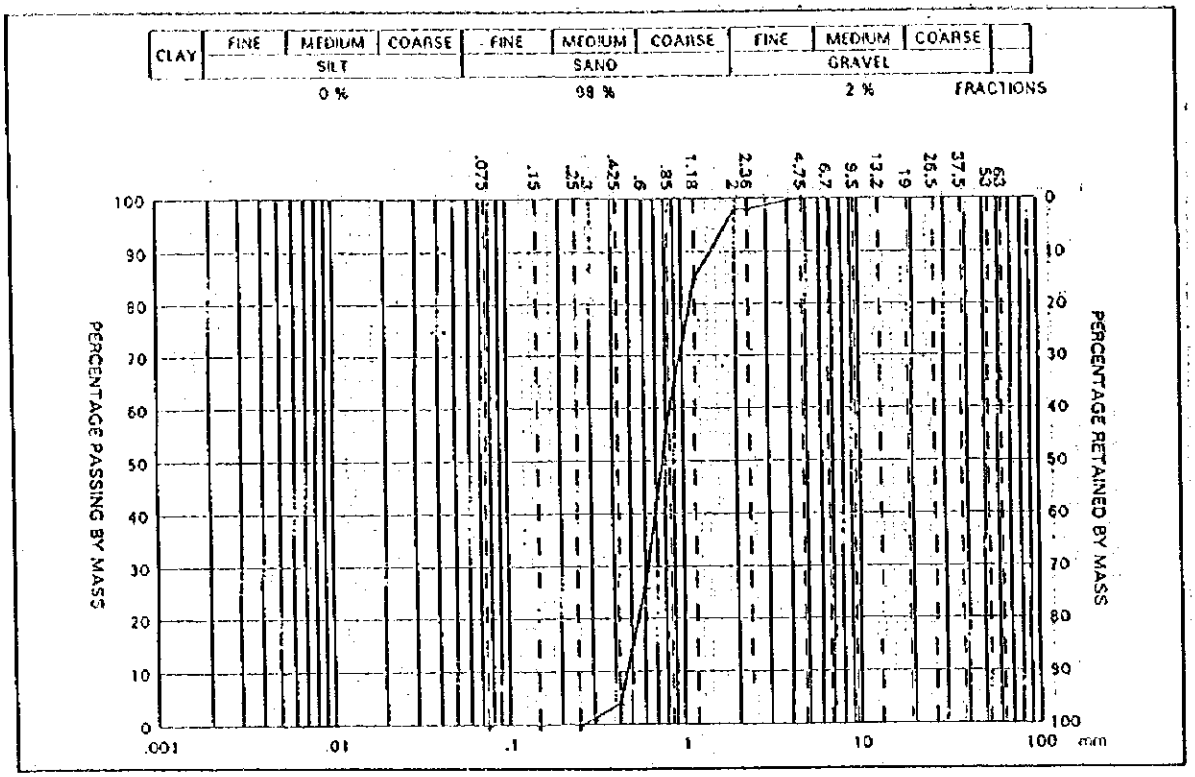

Figure 3.4.2-5 Grain-size Accumulation Curve of C10 in Wet Season

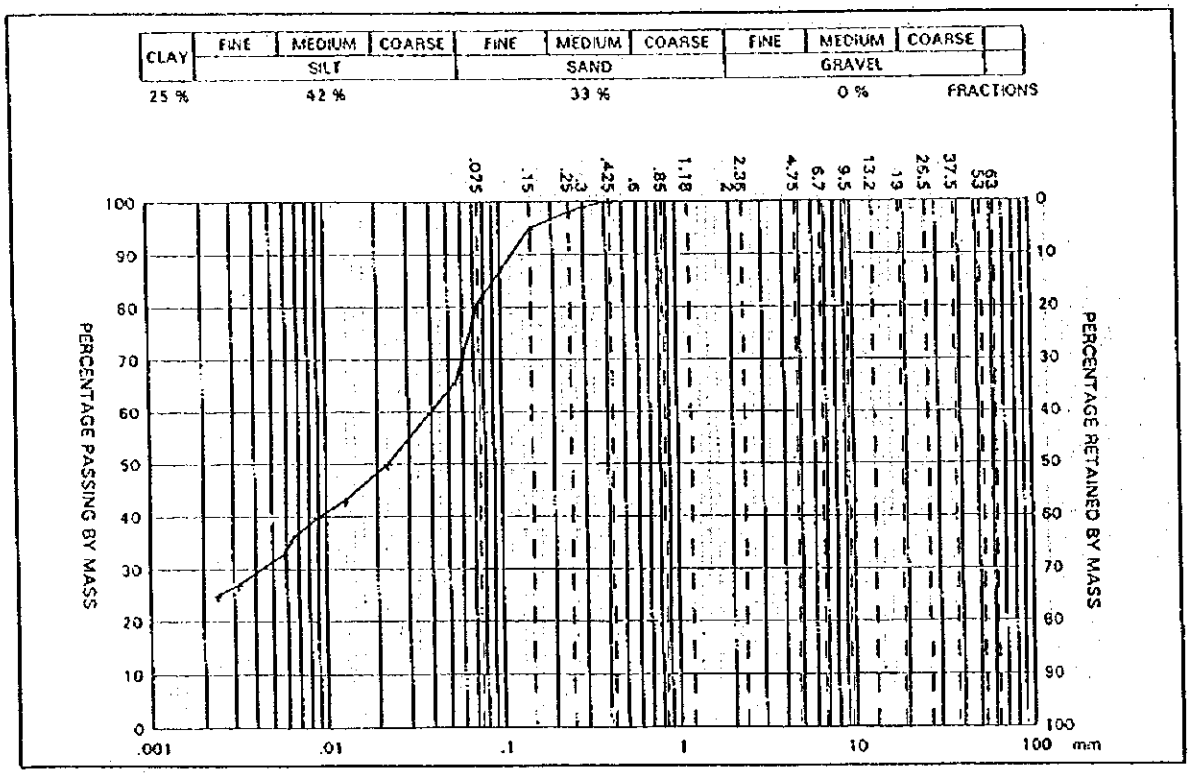

Figure 3.4.2-6 Grain-size Accumulation Curve of C16 in Wet Season

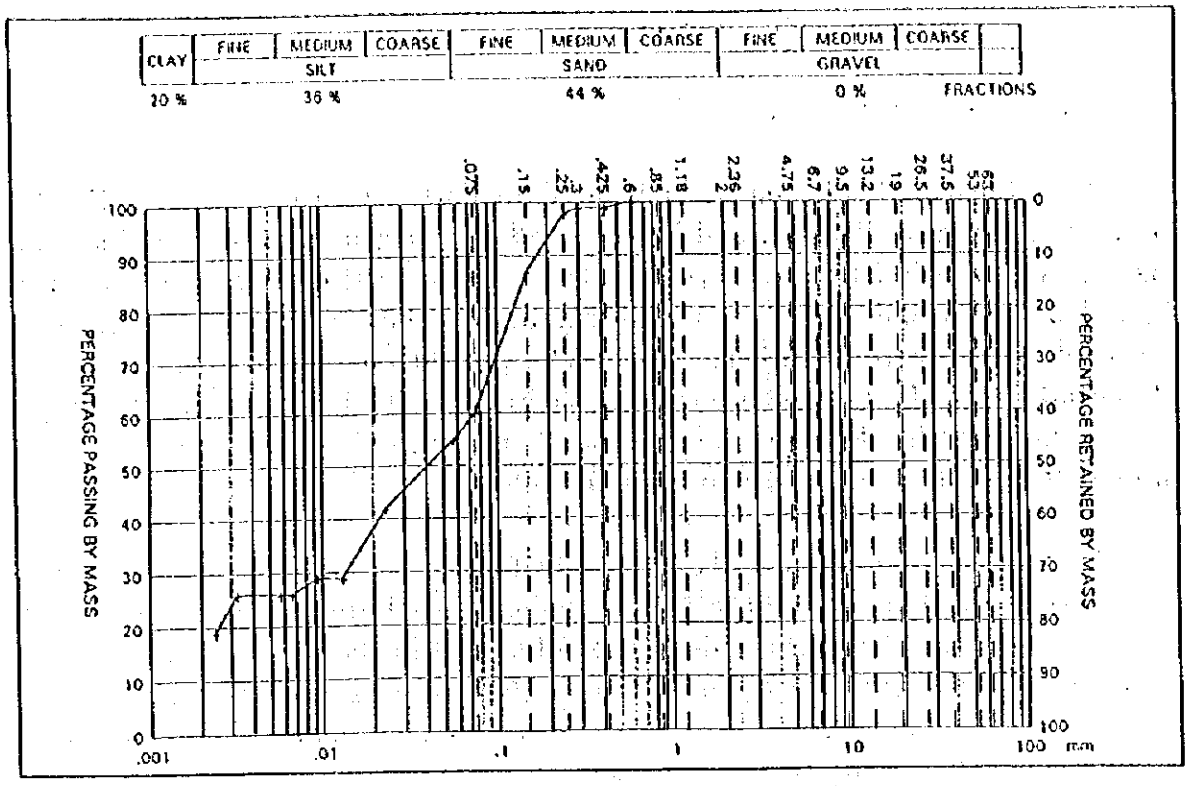

Figure 3.4.2-7 Grain-size Accumulation Curve of C19 in Wet Season

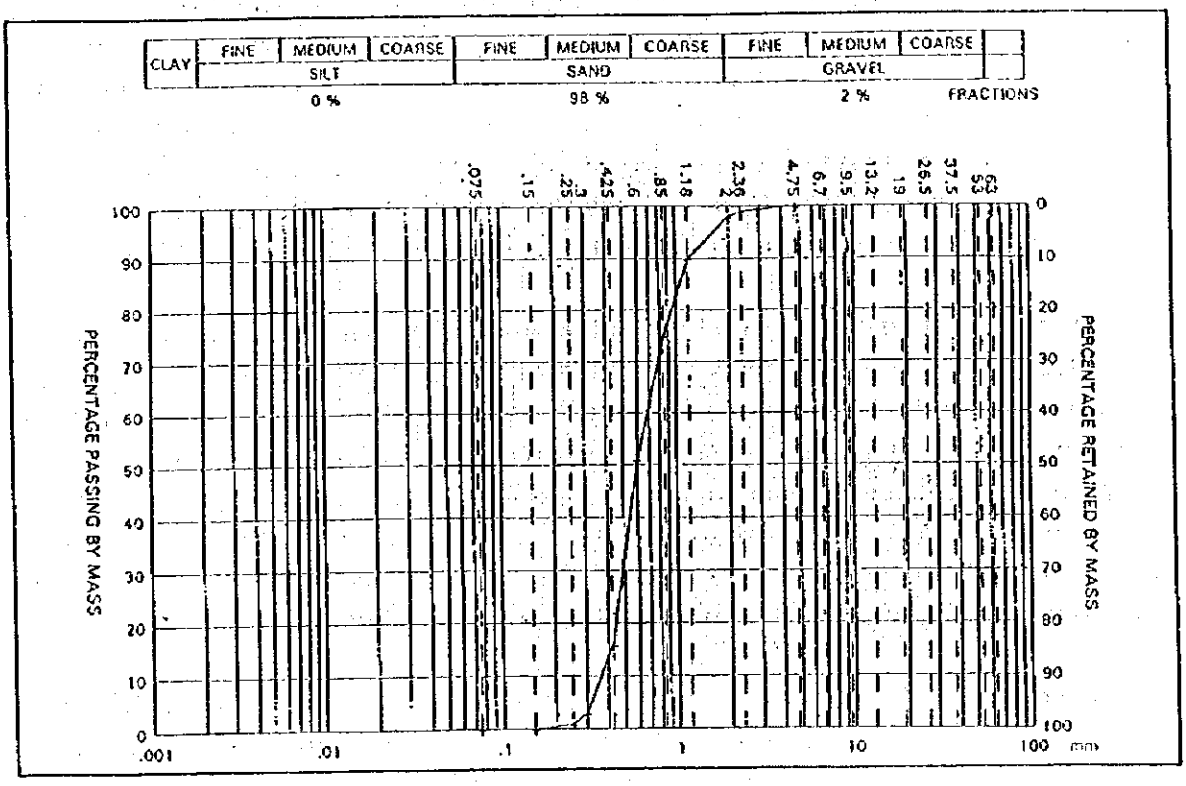

Figure 3.4.2-8 Grain-size Accumulation Curve of C21 in Wet Season

3.5 Littoral Drift and Sedimentation

3.5.1 General Aspect of Littoral Drift

The extensive shoal area in front of Beira Port, which is called the Sofala Bank, seems to have been formed by the sand discharged from the Pungue and Buzi Rivers, littoral drift transported southward along the coast from the mouth of Zambeze River and other rivers, and littoral drift moved northwards from the mouth of rivers in the southern area. The second one of these is the most influential, especially on the formation of the Macuti Shoal, because the drainage area of the Zambeze River is very extensive in comparison with the rivers of Pungue, Buzi and others as shown in Figure 3.5.1-1.

However, in recent years, the littoral drift propagating from the north has been decreasing on account of the decrease of sand discharged from the mouth of the Zambeze River due to the construction of a dam in the upper stream. As a result, the Macuti Beach located in the east of Beira Port is eroded as well as the further northern coast. As a result of the beach erosion, many groins for beach protection have been constructed along the Macuti Coast.

The rivers of Pungue and Buzi are not comparable with the Zambeze River in the scale of drainage area, but they play a very important role in the phenomena of sediment transport of the Sofala Bank. The Pungue and Buzi Rivers originate in the mountainous area close to the border with Zimbabwe. The Pungue River, playing an important role in the sedimentation condition of the Access Channel of Beira Port, reaches the coastal plain some 55 km upstream from Beira. The width of the estuary extends in some 5 km in front of Beira Port.

The tide is semi-diurnal and the tidal range at Beira Port is 5.6 m in mean spring tide and 1.5 m in mean neap tide. The tide of wide excursion range generates strong currents in the Pungue Estuary. These currents reach more than 2 m/s especially in the wet season as a results of their combination with the heavy river discharge as shown in the previous section. According to "Main Report on Beira Port Access Channel Study" by NEDECO (1982), the maximum river discharges in the Pungue and Buzi Rivers respectively are about 600 m^3/s and 300 m^3/s in the wet season, and 80 m^3/s and 50 m^3/s in the dry season.

However, sediments discharged from the estuary of the Pungue River in general seem to be fine sand and silt owing to their flat bottom slope except in major flood times. These fine sand and silt mostly seem to deposit westerly in the wide mouth area excluding the narrow area along the quays of Beira Port and in the south of the Macuti Channel. The sand transported from the Macuti Shoal

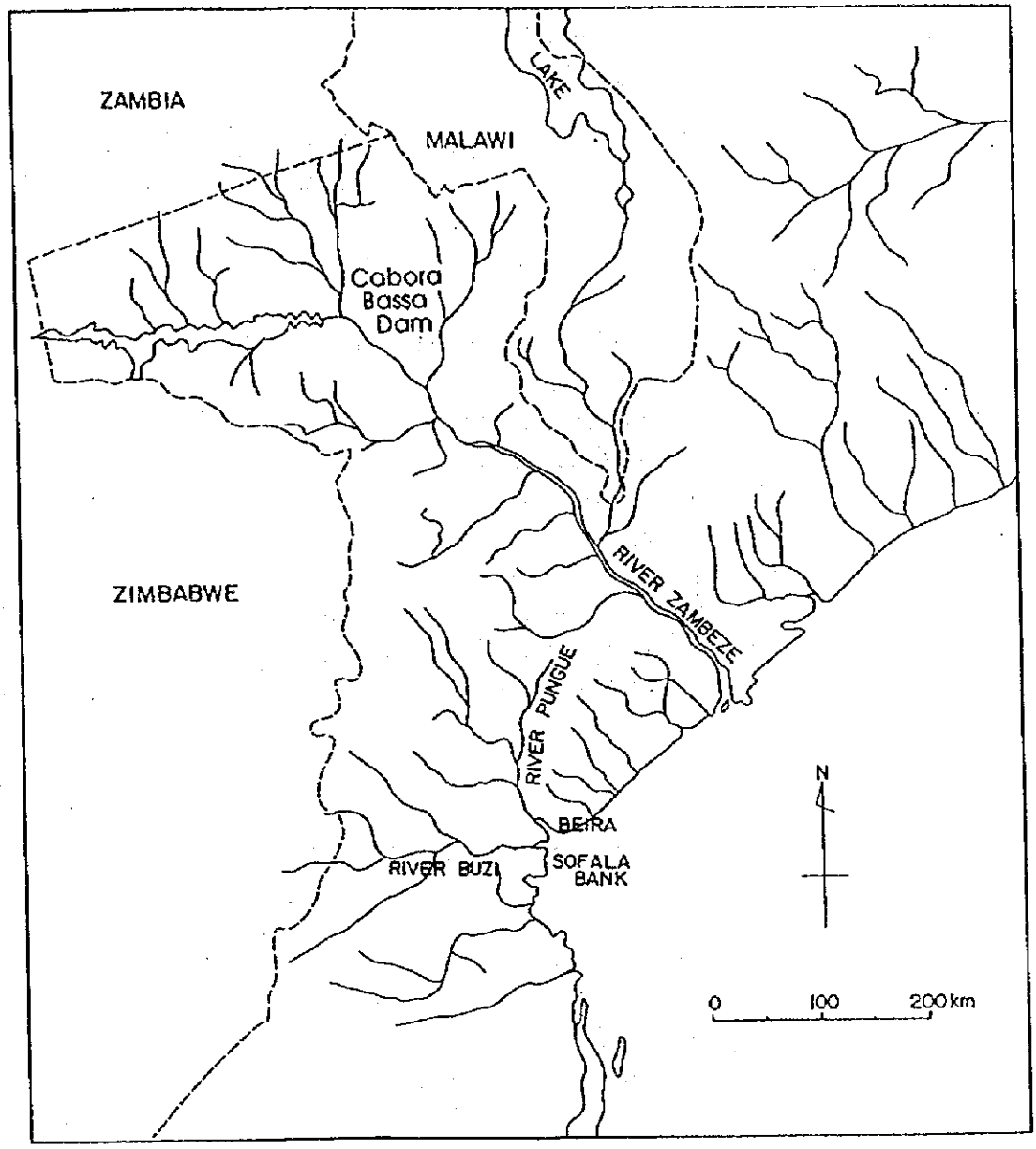

Figure 3.5.1-1 Situation of Sofala Bank and Zambeze, Pungue and Buzi Rivers

by strong tidal currents mostly enters into the Macuti Channel, which grows into large amount when the bottom sand is disturbed and suspended by storm waves.

As described in the previous sections, heavy rainfall and storm waves occur in the the wet season from December to March. Therefore, the sand transport in the Access Channel to Beira Port is more active in the wet season than in the dry season. Along the Macuti Coast, predominant waves propagate from the easterly direction against the perpendicular line to the coastal line, because the predominant offshore waves come from the direction of SE and E as shown in the preceeding sections, so that alongshore sand transport occurs towards Beira Port.

3.5.2 Sedimentation in the Access Channel

Figure 3.5.2-1 shows the shoal area near the Access Channel indicated on the marine chart published in 1991, where the value of water depth in the vicinity of the Access Channel is that before the capital dredging. According to the Main Report of Beira Port Study by NEDECO (1982), the shoals of Macuti, Pelican and Rambler have been rather stable since 1930, though some parts of their south sides have been changing slightly year by year. From the figure it seems that the bottom current in ebb tide from the Pungue River divides into two flows at the north tip of the Pelican Shoal, of which the western flow discharges joining with the ebb flow of the Buzi River and the eastern flow mainly discharges through the Macuti and Rambler Channels. The ebb flow from the Pungue River is strong along the left bank and the most part of it discharges toward the Macuti and Rambler Channels.

Figure 3.5.2-2 and following conclusions are presented based on the main report of Beira Port Study by NEDECO.

(a) The Macuti Cut seems to be rather stable and could be maintained at a depth of 6 m below CDL at cost of only modest maintenance dredging. Even a general tendency of erosion may be recognized considering the gradual increase of the total area with depth exceeding 8 m below CDL.

(b) Obviously, the sedimentation of the Macuti Cut and the adjacent approaches is caused by sand from the Macuti Shoals entering into the channel. From Figure 3.5.2-2, it can be recognized that the southern tip of the Macuti Shoals has slightly shifted towards the south during the period from 1968 through 1981 (0.0 meter contour lines), whereas the position of the channel (6.0 meter contour line) has remained rather stable.

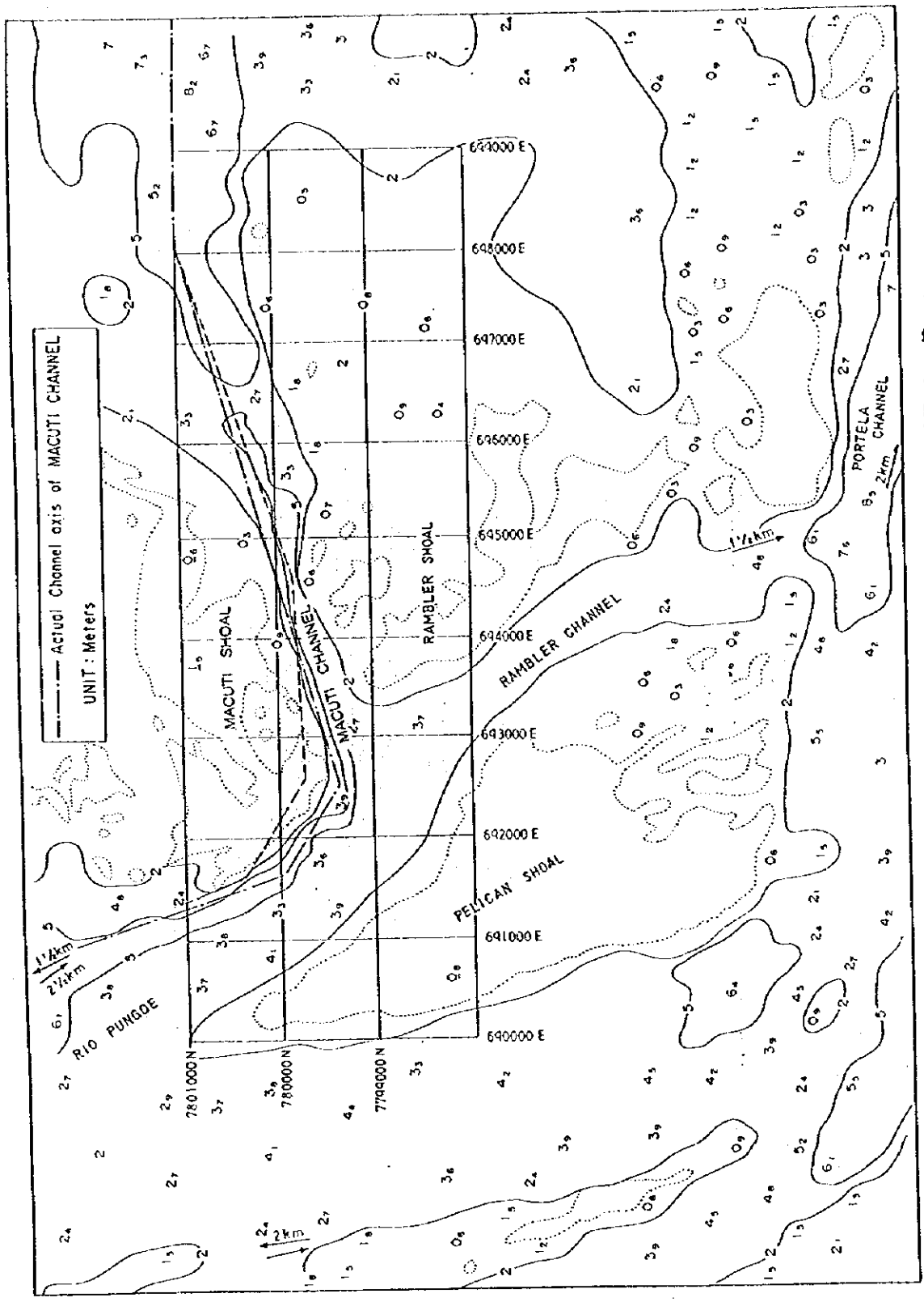

Figure 3.5.2-1 Shoal Area near the Access Channel of Beira Port

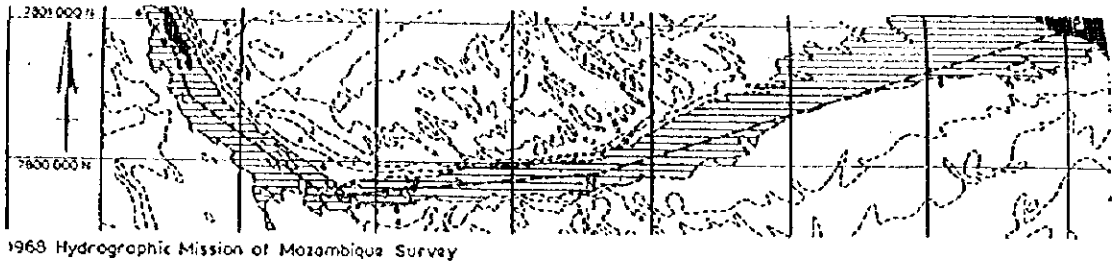

1968 Hydrographic Mission of Mozambique Survey

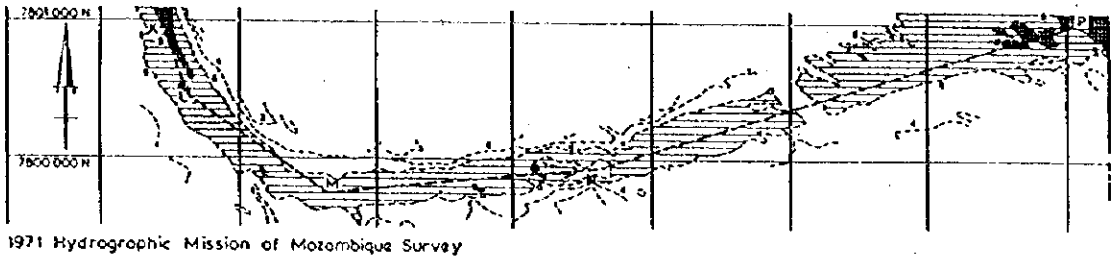

1971 Hydrographic Mission of Mozambique Survey

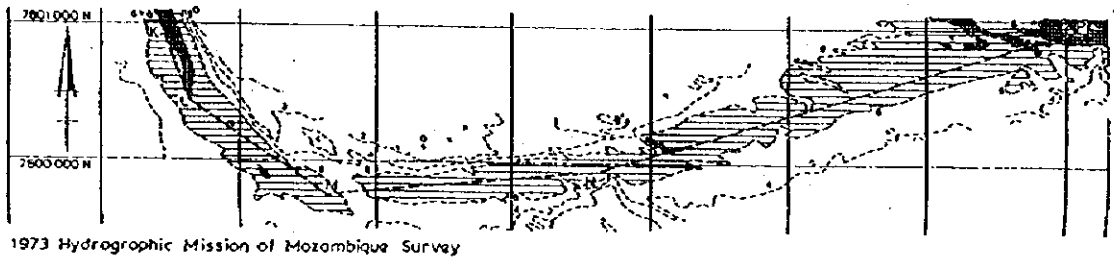

1973 Hydrographic Mission of Mozambique Survey

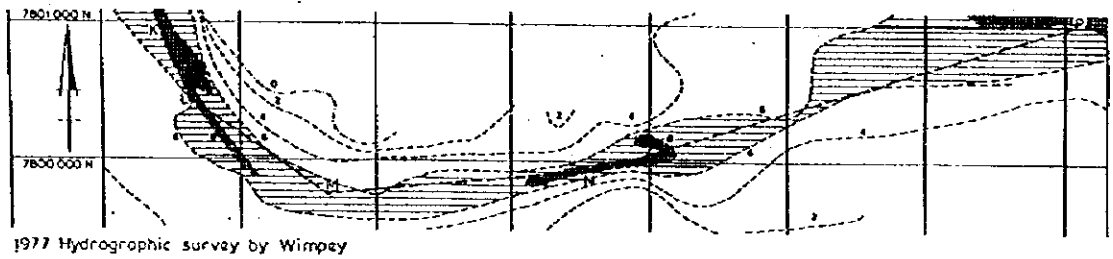

1977 Hydrographic survey by Wimpey

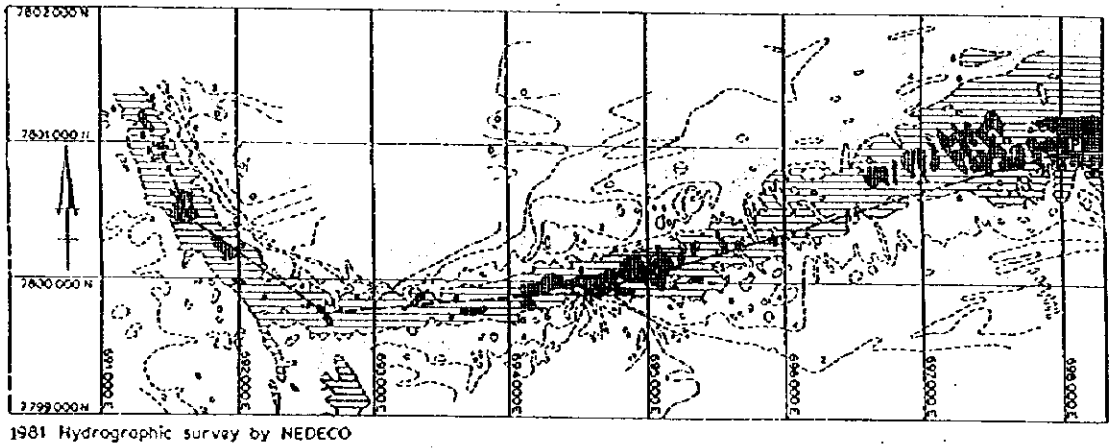

1981 Hydrographic survey by NEDECO

Figure 3.5.2-2 Hydraulic Surveys of Macuti Channel
(Source : Main Report, Beira Port Access Channel Study by NEDECO, September 1982)

(c) Since the suspension of the maintenance dredging, the permissible draft in the artificial channel has decreased somewhat. The minimum depth in 1981 appeared to be reduced to 4.9 m below CDL. This is caused by local depth reductions due to local sand penetration from the Macuti Shoals and the occurrence of sand waves which could develop since the suspension of the regular maintenance dredging.

Referring back to Figure 3.5.2-1, where the same dotted line as the one contained in Figure 3.5.2-2 is drawn, 0.0 m contour lines moreover shifts more southward than 1981 at the bending corner of the Macuti Channel. 0.0 m contour lines also shift towards the Access Channel in the vicinity of UTM Grid 694,500 E besides the bending corner and such a tendency also clearly appears in the map of 1973 of Figure 3.5.2-2. That is, if the dredging works are suspended for a long time, sand on the Macuti Shoals tends to cross towards the Rambler Shoal through the shallower part of the bending corner and sand on the Rambler Shoal tends to drop into the Macuti Channel in the vicinity of UTM Grid 694,500E to be transported towards the offshore through the Macuti Channel. Moreover, sand transported outside of the channel entrance would be moved towards the coast of Macuti by waves.

3.5.3 Sand Drift of Macuti Coast

Along the Macuti Coast, which is located in the east of Beira Port, sand transport toward the Pungue River is predominant, since most of waves come from an easterly direction against the perpendicular to the coast line and tidal currents also are prevailing in the direction toward the Pungue River. That is, most of sand floated-up by waves on the Macuti beach is moved toward the Pungue River by tidal currents and alongshore currents generated by breaking of waves. And some part of it moves toward the port along the left bank of the Pungue River and others deposit on the bottom of the sections from E6 to E8 of the Access Channel or flows inside of the channel by strong tidal currents.

Moreover, sand suspended-up by waves on the Macuti Shoal is also transported obliquely seaward by offshore-ward currents besides in parallel with the coastal line , the amount of which increases with the wave height. Some part of the sand can not reach the section from E6 to E8 by strong ebb-currents along the channel, forming sand banks toward the bending part of the channel and entering into the channel. Some sand also enters into the channel from the direction of the Pelican and Rambler Shoals by waves and tidal currents. Sand transported inside of the channel until the offshore end of the channel deposits widely in the vicinity , and a part of them is moved by waves toward the coast. However, this sand transported to the Macuti Beach is supposed to be a little in

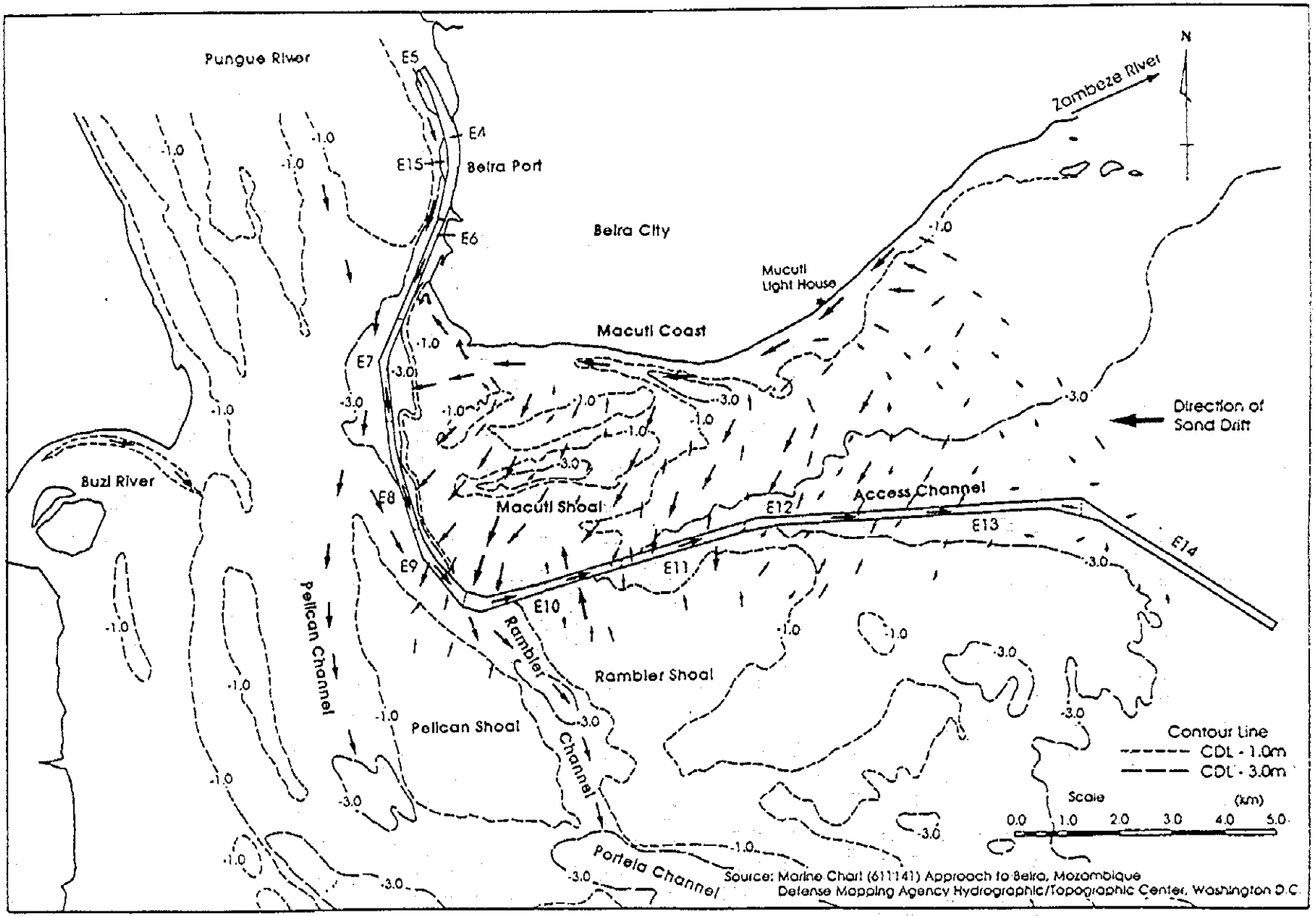

Figure 3.5.3-1 Overview of Littoral Drift in the Vicinity of Access Channel

volume as compared with the sand going out from the beach. These sand transport are schematized in Figure 3.5.3-1.

The sand drift transported from the mouth of the Zambeze River was compensating the sand going out from the Macuti Coast. But, the adjacent area of the river mouth of the Zambeze is very eroded currently by a decrease of discharged sand supposedly due to the dam construction in the upstream, so that whole of the coast from the Zambeze to the Macuti Coast shows a trend of beach erosion. That is, the main factor of the erosion along the Macuti Coast is a decrease of sand drift propagating from the north.

The above mentioned characteristics of sand transport are also confirmed by the results of chemical element analysis of sand. Figure 3.5.3-2 shows the sampling points of analyzed sand, where Pts. 2 to 10 were sampled in February 1997 and other Pts. in August 1997. 10 grams of each sampled sand were dried and pulverized, and pressed to make a cylindrical sample of 5 cm in diameter and 3 mm in thickness. The cylindrical sample was investigated by a fluorescent X-ray apparatus in order to get the content density of the following elements:

Si, Al, K, Ca, Fe, Pb, As, Ti, Mg, Mn, Zn, Cu, Sb, Ni, Co, and Cr

Table 3.5.3-1 Correlation Coefficient Matrix of Chemical Element Composition of Sand

Pt.	1	2	3	4	5	6	7	8	9	10	11	12	13	14	15	16
1	1.00	0.37	0.37	0.37	0.37	0.36	0.34	0.34	0.36	0.34	0.43	0.82	0.87	0.54	0.63	0.68
2	0.37	1.00	1.00	1.00	1.00	1.00	0.92	0.98	1.00	0.93	0.68	0.31	0.35	0.48	0.34	0.35
3	0.37	1.00	1.00	1.00	1.00	1.00	1.00	1.00	0.98	1.00	0.80	0.37	0.32	0.47	0.32	0.32
4	0.37	1.00	1.00	1.00	1.00	1.00	1.00	1.00	1.00	0.93	0.69	0.34	0.35	0.44	0.32	0.33
5	0.37	1.00	1.00	1.00	1.00	1.00	1.00	1.00	1.00	1.00	0.69	0.34	0.37	0.44	0.33	0.33
6	0.36	1.00	1.00	1.00	1.00	1.00	1.00	1.00	1.00	1.00	0.72	0.35	0.36	0.49	0.32	0.32
7	0.34	0.92	1.00	1.00	1.00	1.00	1.00	1.00	1.00	1.00	0.68	0.33	0.34	0.41	0.32	0.32
8	0.34	0.97	1.00	1.00	1.00	1.00	1.00	1.00	1.00	1.00	0.72	0.33	0.35	0.44	0.33	0.33
9	0.36	1.00	0.98	1.00	1.00	1.00	1.00	1.00	1.00	0.96	0.68	0.32	0.32	0.41	0.32	0.34
10	0.34	0.93	0.93	1.00	1.00	1.00	1.00	0.96	1.00	1.00	0.56	0.32	0.33	0.39	0.32	0.33
11	0.43	0.68	0.80	0.69	0.69	0.72	0.68	0.72	0.68	0.56	1.00	0.44	0.46	0.69	0.42	0.38
12	0.82	0.31	0.37	0.34	0.34	0.35	0.33	0.33	0.32	0.32	0.44	1.00	0.98	0.46	0.62	0.61
13	0.87	0.35	0.35	0.37	0.36	0.34	0.35	0.32	0.33	0.34	0.46	0.98	1.00	0.55	0.72	0.63
14	0.54	0.48	0.47	0.44	0.44	0.49	0.41	0.44	0.41	0.39	0.69	0.46	0.55	1.00	0.48	0.47
15	0.63	0.34	0.32	0.32	0.33	0.32	0.32	0.33	0.32	0.32	0.42	0.42	0.72	0.48	1.00	0.99
16	0.68	0.35	0.32	0.33	0.33	0.32	0.32	0.33	0.34	0.33	0.38	0.62	0.63	0.47	0.99	1.00

From the investigation, the element composition of each sample was calculated, and then the correlation coefficients among them were calculated as shown in Table 3.5.3-1.

From the table, the followings are seen:

(a) Pts. from 2 to 10 are more than 0.92 in correlation coefficient among them, namely have the same element composition.
(b) Pt. 11 at Savane Coast has high correlation from 0.56 to 0.80 with Pts. 2 to 10. Namely, sand on Macuti Coast is supposed to be that transported from the north along the coast.
(c) Pts. 12 and 13 have high correlation coefficient from 0.82 to 0.87 with Pt. 1 at the upper stream of the Pungue River and less than 0.37 with Pts. 2 to 10 on the beach of Macuti. Namely, sand at Pts. 12 to 13 seems to come from the Pungue and Buzi Rivers, not coming from the Macuti Beach.
(d) Pt. 14 is low in correlation with other points, but the correlation with Pt. 11 is higher than Pt. 1. Namely, sand at this point comes more from the north than from the River Pungue.
(e) Pts. 15 and 16 are also low in correlation with other points, but it with Pt. 1 is higher than Pt. 11. Namely, sand there has a tendency to come more from the River Pungue than from the north.

These characteristics of sand transport coincide with Figure 3.5.3-1.

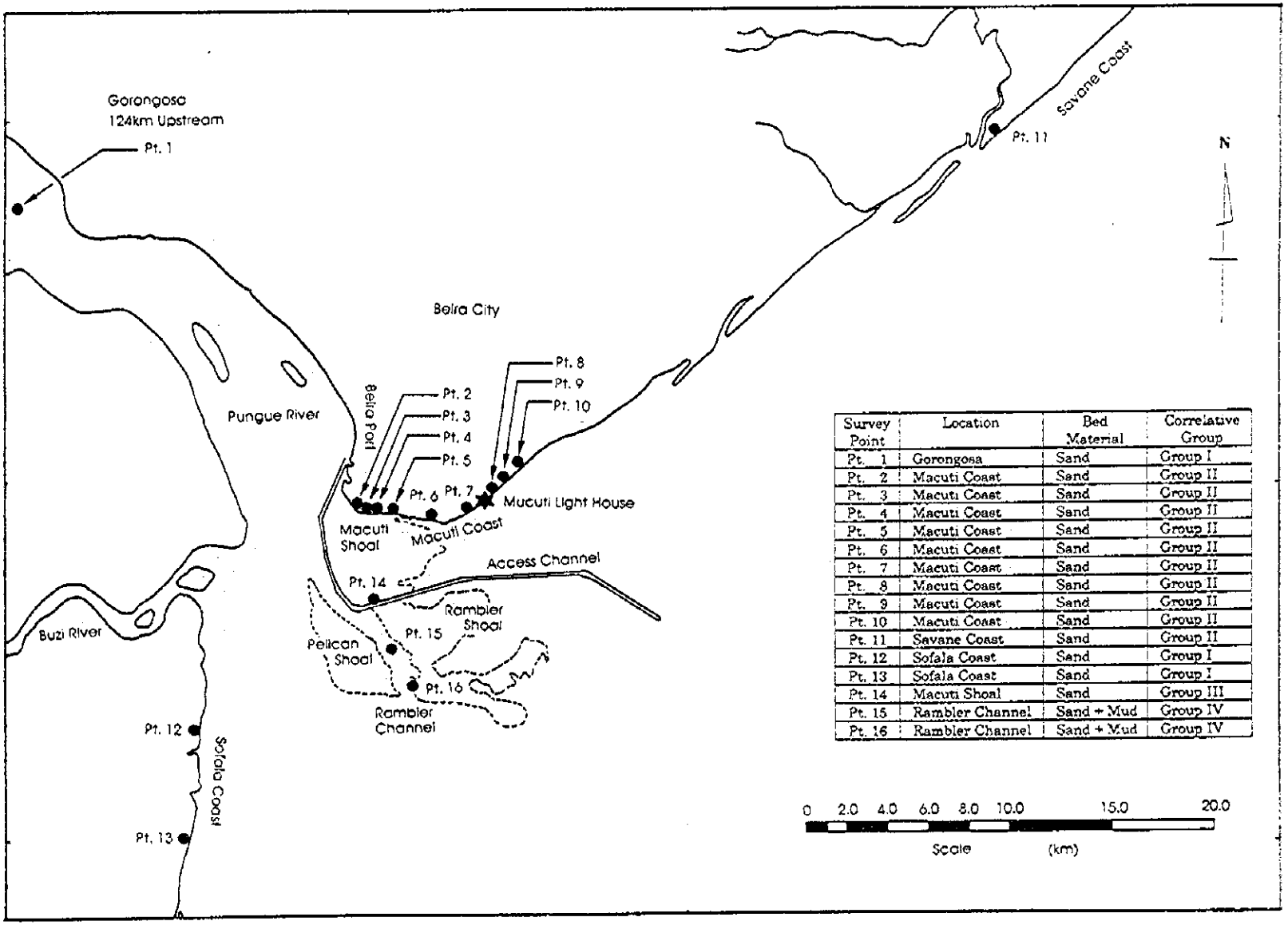

Survey Point	Location	Bed Material	Correlative Group
Pt. 1	Gorongosa	Sand	Group I
Pt. 2	Macuti Coast	Sand	Group II
Pt. 3	Macuti Coast	Sand	Group II
Pt. 4	Macuti Coast	Sand	Group II
Pt. 5	Macuti Coast	Sand	Group II
Pt. 6	Macuti Coast	Sand	Group II
Pt. 7	Macuti Coast	Sand	Group II
Pt. 8	Macuti Coast	Sand	Group II
Pt. 9	Macuti Coast	Sand	Group II
Pt. 10	Macuti Coast	Sand	Group II
Pt. 11	Savane Coast	Sand	Group II
Pt. 12	Sofala Coast	Sand	Group I
Pt. 13	Sofala Coast	Sand	Group I
Pt. 14	Macuti Shoal	Sand	Group III
Pt. 15	Rambler Channel	Sand + Mud	Group IV
Pt. 16	Rambler Channel	Sand + Mud	Group IV

Figure 3.5.3-2 Sampling Points for Chemical Element Analysis of Sand